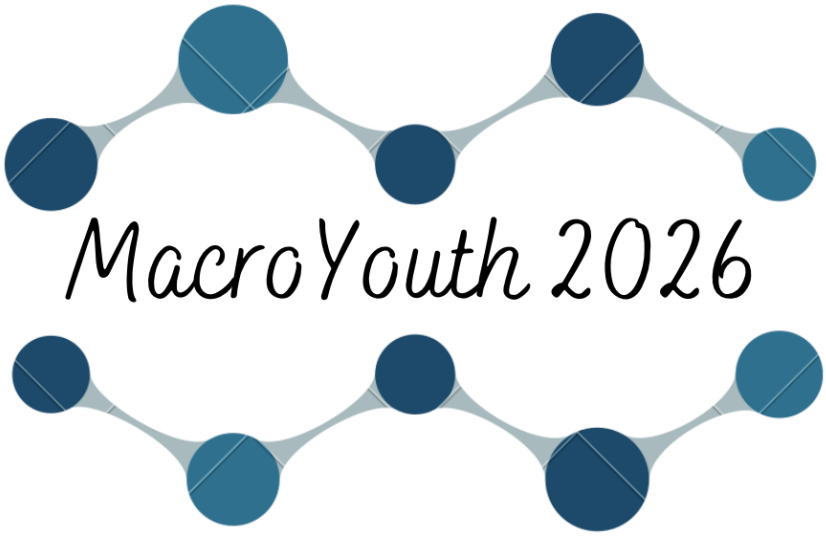


OPEN DOOR TO THE FUTURE
SCIENTIFIC COMMUNICATIONS OF YOUNG RESEARCHERS

7th Edition

Marking the Romanian Researcher's Day

Program & Book of Abstracts

ICMPP – Petru Poni Institute of Macromolecular Chemistry
Iasi | Romania | November 19, 2026
https://icmpp.ro/macroyouth2026

Edited by
Marcela MIHAI
Marius-Mihai ZAHARIA
Larisa-Maria PETRILA

Cover by
Diana SCHWAB

Copyright © 2026

All rights reserved. Except as permitted under current legislation no part of this publication may be photocopied, reproduced or distributed in any form or by any means or stored in a database or retrieval system, without the prior permission from the copyright holders.

This book contains information obtained from authentic and highly regarded sources. Reprinted material is quoted with permission as signed by authors, and sources are indicated. Copyright for individual articles remains with the authors as indicated. A wide variety of references are listed. Reasonable efforts have been made to publish reliable data and information, but the authors, editors, and the publisher cannot assume responsibility for the validity of all materials or the consequences of their use.

Welcome to the

OPEN DOOR TO THE FUTURE

Scientific Communications of Young Researchers with international participation,

MacroYouth 2026

It is a great pleasure to welcome you in Iasi, on 19.11.2026, on the occasion of the 7th Edition OPEN DOOR TO THE FUTURE Scientific Communications of Young Researchers with international participation, MacroYouth 2026. The scientific communications event with international participation is organized by the Doctoral School of Chemical Sciences of the School of Advanced Studies of Romanian Academy, through Petru Poni Institute of Macromolecular Chemistry - ICMPP, and the Romanian Chemical Society, to mark the Romanian Researcher's Day, and offers the opportunity for the doctoral students and young scientists (maximum 3 years from thesis defense) to present the results of their studies. The scientific program includes various topics in organic and macromolecular chemistry and physics.

Best wishes for a professionally rewarding scientific meeting!

Dr. Valeria HARABAGIU and Dr. Marcela MIHAI

Chairpersons of MacroYouth 2026

CHAIRPERSONS of MacroYouth 2026

Dr. Valeria HARABAGIU and Dr. Marcela MIHAI

SCIENTIFIC BOARD

- Acad. Maria ZAHARESCU (Romanian Academy)
- Acad. Marius ANDRUH (Romanian Academy)
- Dr. Maria CAZACU (ICMPP Iasi)
- Dr. Liliana CSEH (ICCD Timisoara)
- Dr. Sergiu COSERI (ICMPP Iasi)
- Dr. Mariana Dana DAMACEANU (ICMPP Iasi)
- Dr. Gheorghe FUNDUEANU (ICMPP Iasi)
- Dr. Gabriela IONITA (ICFIM Bucharest)
- Dr. Luminita MARIN (ICMPP Iasi)
- Dr. Mariana PINTEALA (ICMPP Iasi)

ORGANIZING BOARD

Program

- Dr. Petrisor SAMOILA
- Dr. Florin BUCATARIU
- Dr. Corneliu COJOCARU

Editorial

- Dr. Marius-Mihai ZAHARIA
- Dr. Larisa-Maria PETRILA

Executive

- Dr. Narcisa Laura MARANGOCI
- Dr. Florica DOROFTEI
- Dr. Andra-Cristina ENACHE
- Dr. Daniela PAMFIL
- Dr. Bogdan-Constantin CONDURACHE
- Dr. Dumitru POPOVICI
- Catalin BUZDUGAN – IT support

CONTENT

SHORT PROGRAM 11

PROGRAM 12

INVITED LECTURE

Sergejs Gaidukovs – short CV 21

ORAL COMUNICATIONS

A CATIONIC CURDLAN DERIVATIVE AS A FLOCCULANT FOR WASTEWATER TREATMENT
Maria-Magdalena Nafureanu, Dana Mihaela Suflet, Marieta Constantin 23

HYDROTHERMAL SYNTHESIS OF $BaTiO_3$-BASED HIGH ENTROPY PEROVSKITE OXIDES
Mihail-Calin Licu, Florentina Maxim, Florina Teodorescu, Daniela Berger, Elena Maria Anghel, Ancuta Sofronia, Cristian Matei, Speranta Tanasescu 25

DUAL-CROSSLINKED COLMA/GELMA/HAMA BIOINKS FOR EXTRUSION-BASED 3D BIOPRINTING OF ARTIFICIAL SKIN CONSTRUCTS
Zechuan Wang, Maria Butnaru, Maria Valentina Dinu, Liliana Verestiuc 27

HUMAN SERUM ALBUMIN AS A MOLECULAR HOST FOR HYBRID CHIMERIC DERIVATIVES WITH PYRROLO-QUINOLINE STRUCTURE
Camelia-Georgiana Marandis, Dorina Amăriucăi-Mantu, Vasilichia Antoci, Violeta Mangalagiu, Ionel I. Mangalagiu, Marcela Mihai..... 29

THE SELECTIVE COMPLEXATION MECHANISM OF AN ORGANIC SALT BASED DRUG WITH β-CYCLODEXTRIN FOR THE TREATMENT OF ALOPECIA
Petru Tirnovan, Dragos-Lucian Isac, Narcisa-Laura Marangoci, Alina Nicolescu, Adina Coroaba, Andrei Neamtu, Aatto Laaksonen, Mariana Pinteala..... 31

EVALUATION OF THE CHEMICAL COMPOSITION AND BIOLOGICAL ACTIVITIES OF *SIDERITIS SYRIACA*
Alexandra-Mariana Ionescu, Andreea Veronica Botezatu, Ana-Maria Mocanu, Anna Busuioc, Bianca Furdui, Alina Viorica Iancu, Marques Fernanda Marujo, Costel Vinatoru, Geanina Negosanu, Rodica Mihaela Dinica 33

LINKER-DEPENDENT CONFORMATIONAL DYNAMICS OF BIS-ACRIDINE ORANGE DYES: INSIGHTS FROM MOLECULAR DYNAMICS AND ENHANCED SAMPLING
Razvan Puf, Aatto Laaksonen 35

POLYMERIC THIN FILMS FOR RASPBERRY PRESERVATION
Paula Cucu, Irina Apostol, Iuliana Spiridon, Mihai Mares 37

HYBRID COMPOSITE AMYLOPECTIN-*g*-POLY(*N*-ISOPROPYLACRYLAMIDE) /MAGNETITE AND ITS POTENTIAL FOR CONGO RED REMOVAL
Melinda-Maria Bazarghideanu, Florin Bucatariu, Marius-Mihai Zaharia, Stergios Pispas, Marcela Mihai 39

MODULATING CYCLODEXTRIN-NITROXIDE HOST-GUEST INTERACTIONS THROUGH STEREOCHEMISTRY, FUNCTIONALIZATION, AND IONIC STRENGTH
Alexandru G. Bucur, Jean P. Joly, Mihaela Banica, Sylvain R. A. Marque, Florența D. Savonea, Gabriela Ionita 41

MODULATING THE THERMORESPONSIVENESS OF INTELLIGENT HYDROGELS FOR BIOMEDICAL APPLICATION
Adina Ferariu, Marieta Constantin, Sanda Bucatariu, Gheorghe Fundueanu 43

FLAME-RETARDANT PHOSPHORUS-FUNCTIONALIZED CELLULOSE OBTAINED THROUGH RADICAL GRAFTING OF PHOSPHONATE MONOMERS IN IONIC LIQUID MEDIA
Ayoub Abarkan, Ridouan El Yousfi, Brahim Elmekaoui, Nafea Achalhi, Abderrahman El Idrissi 45

OPTIMIZATION OF DYE ADSORPTION PROCESS FROM SINGLE- AND MULTICOMPONENT AQUEOUS SYSTEMS USING MAGNETIC NANOCOMPOSITES
Maria Andreea Nistor, Liliana Halip, Simona Gabriela Muntean 47

***IN SILICO* EVALUATION OF ADME/TOX PROFILES USING MULTIPLE ONLINE PREDICTION TOOLS**
Lucia Gradinaru, Alina Bora, Luminita Crisan 49

BORONATE-GUANOSINE-ASSISTED GROWTH OF INTERCONNECTED GOLD NANOASSEMBLIES ON DEXTRAN-COATED IRON OXIDE NANOPARTICLES FOR MAGNETICALLY RECOVERABLE SERS
Tecla Dulgheriu, Elena-Laura Ursu, Alexandru Rotaru 51

CYANOBACTERIA SPIRULINA MEDIATED BIOSYNTHESIS OF COPPER-BASED HYBRID MATERIALS AND PHOTOCATALYTIC DEGRADATION OF DYE INDIGO CARMINE
Cristina Bostaca, Larisa-Maria Petrila, Marcela Mihai 53

HYDROPHOBIC NATURAL DEEP EUTECTIC SOLVENT-BASED MATERIALS AS SOLUBILIZING AND DELIVERY VEHICLES FOR FERULIC ACID
Catalin Chersan, Raluca Nicoleta Darie-Nita, Oana Ursache, Marin-Aurel Trofin, Sergiu Coseri 55

RIM-SELECTIVE OLIGOCAPROLACTONE SUBSTITUTION OF β-CYCLODEXTRIN AS A STRATEGY FOR TAILORING NANOSPONGE PROPERTIES
Marius Prodan, Valeria Harabagiu, Diana-Andreea Blaj, Cristian Peptu 57

HYDROGELS BASED ON POLYSACCHARIDES, AMINO ACIDS AND EUTECTIC SOLVENTS
Lorena-Elena Grigoriu, Alexandra Vieru, Diana Elena Ciolacu, Alexandru-Mihail Serban, Alina Gabriela Rusu, Loredana-Elena Nita 59

POSTERS

EFFECT OF A CARBON NANOPARTICLE DISPERSION ON THE STRUCTURE AND PHOTOLUMINESCENCE OF ELECTROSPUN POLY(VINYL ALCOHOL) NANOFIBRES
Sebastian-Marian Alupoaie, Bogdan-George Rusu, Iuliana Stoica, Magdalena Aflori..... 63

EPR SPECTROSCOPIC INVESTIGATION OF SPIN-LABELLED BOVINE SERUM ALBUMIN IN ALGINATE-BASED HYDROGELS
Elena-Erika Antonia, Elena-Gabriela Ionita 65

OPTIMIZATION OF THE UGI REACTION FOR ALGINATE FUNCTIONALIZATION: CHARACTERIZATION AND ANTIMICROBIAL ACTIVITY
Raluca-Elena Avram, Gabriela Liliana Ailiesei, Maria Marinela Lazar, Maria Valentina Dinu..... 67

INFLUENCE OF DEEP EUTECTIC SOLVENT PRETREATMENT ON PRODUCTION AND PROPERTIES OF CELLULOSE NANOFIBERS
Mădălina-Roxana Birtea, Gabriela Biliuta, Raluca-Ioana Baron, Raluca Nicoleta Darie-Nita, Sergiu Coseri..... 69

SYNTHESIS AND STRUCTURAL CHARACTERIZATION OF PYRIDINE SCHIFF BASES WITH ALIPHATIC AND SILOXANE UNITS
Alexandra Bîrzu, Mihaela Dascălu, Sergiu Shova, Maria Cazacu..... 71

CARBON QUANTUM DOT-LOADED SODIUM ALGINATE/K-CARRAGEENAN HYDROGELS
Cosmina-Maria Bogza, Carmen-Mihaela Popescu, Maria-Cristina Popescu 73

EXTENDED π-CONJUGATED SCHIFF BASE COMPLEXES OF TRANSITION AND RARE-EARTH METALS
Robert I. Botea, Augustin Madalan..... 75

EXPLORING LIGNIN MODEL DIMER INTERACTIONS IN IMIDAZOLIUM-BASED IONIC LIQUIDS THROUGH MOLECULAR DYNAMICS SIMULATIONS
Narcis Cibotariu, Aatto Laaksonen 77

MOLECULARLY IMPRINTED POLYMER-BASED ELECTROCHEMICAL SENSORS FOR BIOGENIC AMINES DETECTION – A REVIEW
Andreea-Loredana Comănescu, Andra-Georgiana Trifan, Constantin Apetrei 79

POTENTIAL APPLICATIONS OF PHYTOCHEMICAL AND SYNTHETIC ANTI-INFLAMMATORY COMPOUNDS
Manuela Elena Coviț, Denis Ionut Defta, Fanica Balanescu, Anna Busuioc, Andreea Veronica Botezatu, Rodica Mihaela Dinica 81

ELECTROCHEMICAL DETECTION OF POLYPHENOLIC COMPOUNDS OF INTEREST IN WINES – A REVIEW –
Andrei-Daniel Geman, Constantin Apetrei 83

DNA CONDENSATION BY 4-ARM PEG–HISTIDINE/LYSINE PEPTIDE POLYPLEXES: TUNING TRANSFECTION AND BIOCOMPATIBILITY
Razvan Ghiarasim, Dragos Peptanariu, Mihaela Silion, Alina Nicolescu, Lucian Bahrin, Mariana Pinteala 85

Mn-DOPED ALUMINIUM IRON OXIDES AS ADVANCED MATERIALS FOR WASTEWATER REMEDIATION
Ionela Grecu, Maria Emiliana Fortuna, Alexandra Lapusneanu, Ioan-Andrei Dascalu, Andra-Cristina Enache, Corneliu Cojocaru, Petrisor Samoila 87

SORBTION OF NITRONYL NITROXIDE BENZALDEHIDE IN POLY(ETHYLENE GLYCOL)/B-CD HYDROGELS HYBRID AuNPs
Alexandra Ana-Maria Iancu, Alexandru Gabriel Bucur, Mihaela Banica, Gabriela Ionita 89

RHENIUM TRICARBONYL COMPLEXES-LOADED POLYESTER NANOPARTICLES FOR POTENTIAL BIOMEDICAL APPLICATIONS
Andrei-Alexandru Ivu, Alina Gabriela Rusu, Alexandru Mihail Serban, Isabella Nacu, Fabio Zobi, Liliana Verestiuc, Loredana Elena Nita 91

FROM COUMARIN-CONTAINING QUATERNARY SALTS TO CYCLOADDUCTS: A COMPARATIVE UV–VIS STUDY
Florentina-Gabriela Lazar, Cristina AL-Matarneh, Dorina Amariucai-Mantu, Ashraf AL-Matarneh, Mariana Pinteala 93

PREPARATION OF THE COPPER ALGINATE COMPLEXES USING ION EXCHANGER COLUMN METHOD
Alina-Petronela Moraru, Marius-Mihai Zaharia, Marcela Mihai 95

HYDROPHOBISED SILICA-BASED NANOCOMPOSITE FORMULATIONS FOR SUPERHYDROPHOBIC WOOD SURFACES
Monica-Georgiana Musteata, Maria-Cristina Popescu, Carmen-Mihaela Popescu 97

SCAFFOLD ARCHITECTURE AS A DESIGN PARAMETER IN 3D-PRINTED SCAFFOLDS FOR TISSUE REGENERATION
Isabella Nacu, Anca Toma, Liliana Verestiuc 99

VOLATILE ORGANIC COMPOUNDS FROM COFFEE AS POTENTIAL BIOACTIVE AGENTS IN CHITOSAN BASED MATERIALS
Andrei-Razvan Pana, Grigore Ungureanu, Cristopher Anel Boya, Mihai Brebu, Elena Stoleru 101

BIOACTIVE HYBRID HYDROGEL FOR CONTROLLED DELIVERY IN BIOMEDICAL APPLICATIONS
Ana Rebeca Pintilii, Anca Mihaela Mocanu, Margareta Gabriela Ciobanu 103

CHROMATOGRAPHIC IDENTIFICATION OF BIOLOGICALLY ACTIVE COMPOUNDS FROM DIFFERENT PLANT SPECIES
Raluca-Nicoleta Răileanu, Anna Busuioc, Alexandra-Mariana Ionescu, Costel Vinatoru, Geanina Negosanu, Andreea Veronica Botezatu, Bianca Furdui, Rodica Mihaela Dinica 105

PHENANTHRIDINIUM YLIDES IN [3+2] CYCLOADDITIONS: DIPOLAROPHILE EFFECTS AND NMR CHARACTERIZATION
Claudiu Ticaleac, Costel Moldoveanu, Cătălina Ciobanu, Ionel Mangalagiu, Gheorghita Zbancioc 107

SENSORS FOR MELATONIN DETECTION: RECENT ADVANCES, ANALYTICAL PERFORMANCE, AND FUTURE PERSPECTIVES
Andra-Georgiana Trifan, Andreea-Loredana Comanescu, Constantin Apetrei 109

VOLATILE ORGANIC COMPOUND FROM HONEY TO INDUCE A CASEIN BAZED MATERIALS
Grigore Ungureanu, Marius Niculaua, Alin-Constantin Dirtu, Elena Stoleru, Mihai Brebu..... 111

SPONSORS

INTEGRATED ANALYTICAL INSTRUMENTATION - PRO ANALYSIS SYSTEMS PORTFOLIO AND MICROPLASTICS DETERMINATION BY MILD PYROLISYS-GC-MS
Gheorghita Cretu-**Pro Analysis Systems** 115

SC EKY-SAM SRL 117

CARL ZEISS INSTRUMENTS 119


MacroYouth 2026

PROGRAM

Petru Poni Institute of Macromolecular Chemistry, Conference Hall		
Thursday 19.11.2026		
https://us06web.zoom.us/j/84755005648?pwd=7vW5uaq3FIMAauTPxWvaocWafBDHxw.1		
	8:30-9:00	Registration of Participants
S1	9:00-9:15	Opening Ceremony
	9:15-10:00	**IL** Sergejs GAIDUKOVS
	10:00-10:15	Coffee break
S2	10:15-10:30	**OC1**: Maria-Magdalena NAFUREANU
	10:30-10:45	**OC2**: Mihail Calin LICU
	10:45-11:00	**OC3**: Zechuan WANG
	11:00-11:15	**OC4**: Camelia-Georgiana MARANDIS
	11:15-11:30	**OC5**: Petru TIRNOVAN
	11:30-11:45	**OC6**: Alexandra-Mariana IONESCU
	11:45-12:15	Coffee break & Poster session
S3	12:15-12:30	**OC7**: Razvan PUF
	12:30-12:45	**OC8**: Paula CUCU
	12:45-13:00	**OC9**: Melinda-Maria BAZARGHIDEANU
	13:00-13:15	**OC10**: Alexandru-Gabriel BUCUR
	13:15-13:30	**OC11**: Adina FERARIU
	13:30-14:30	Lunch break - ICMPP Library
S4	14:30-15:15	**SL** Gheorghita CRETU
	15:15-15:30	**OC12**: Ayoub ABARKAN
	15:30-15:45	**OC13**: Maria-Andreea NISTOR
	15:45-16:00	**OC14**: Lucia GRADINARU
	16:00-16:30	Coffee break & Poster session
S5	16:30-16:45	**OC15**: Tecla DULGHERIU
	16:45-17:00	**OC16**: Cristina BOSTACA
	17:00-17:15	**OC17**: Catalin CHERSAN
	17:15-17:30	**OC18**: Marius PRODAN
	17:30-17:45	**OC19**: Lorena-Elena GRIGORIU
	17:45-18:00	Coffee break
	18:00-18:30	Analysis, Awarding and Closing Ceremony

ICMPP Conference Hall	
https://us06web.zoom.us/j/84755005648?pwd=7vW5uaq3FIMAauTPxWvaocWafBDHxw.1	
$08^{30} – 09^{00}$	**Registration of Participants**
	$09^{00} – 10^{00}$ **Session 1** Chairs: Dr. Petrisor SAMOILA and Dr. Florin BUCATARIU
$09^{00} – 09^{15}$	**Opening Ceremony** Dr. Valeria HARABAGIU and Dr. Marcela MIHAI *Petru Poni Institute of Macromolecular Chemistry, Iasi, Romanian Academy, Romania*
$09^{15} – 10^{00}$	**IL. Bio-Based Polymers with Linear Tunability and Multi-Stimuli Actuation for Sustainable Soft Robotics and Energy Materials Applications** **INVITED LECTURE** Sergejs GAIDUKOVS *Riga Technical University, Riga, Latvia*
$10^{00} – 10^{15}$	**Coffee break & POSTER SESSION**
	$10^{15} – 11^{45}$ **Session 2** Chairs: Dr. Larisa-Maria PETRILA and Dr. Madalin DAMOC
$10^{15} – 10^{30}$	**OC1. A cationic curdlan derivative as a flocculant for wastewater treatment** Maria-Magdalena NAFUREANU, Dana Mihaela SUFLET, Marieta CONSTANTIN *Petru Poni Institute of Macromolecular Chemistry, Romanian Academy, Iasi, Romania*
$10^{30} – 10^{45}$	**OC2. Radiation-mediated synthesis of silver nanoparticles in silica-based drug delivery systems with antimicrobial properties** Mihail-Calin LICU[1], Florentina MAXIM[1], Florina TEODORESCU[1], Daniela BERGER[2], Elena Maria ANGHEL[1], Ancuta SOFRONIA[1], Cristian MATEI[2], Speranta TANASESCU[1] [1]*Institute of Physical Chemistry-Ilie Murgulescu, Romanian Academy, Bucharest, Romania* [2]*Faculty of Chemical Engineering and Biotechnology, Polytechnic University of Bucharest, Bucharest,Romania*
$10^{45} – 11^{00}$	**OC3. Dual-crosslinked colma/gelma/hama bioinks for extrusion-based 3d bioprinting of artificial skin constructs** Zechuan WANG[1,2], Maria BUTNARU[2], Maria Valentina DINU[1], Liliana VERESTIUC[2] [1]*Petru Poni Institute of Macromolecular Chemistry, Romanian Academy, Iasi, Romania* [2]*Faculty of Medical Bioengineering, "Grigore T. Popa" University of Medicine and Pharmacy, Iasi, Romania*

11^{00}– 11^{15}	**OC4. Human serum albumin as a molecular host for hybrid chimeric derivatives with pyrrolo-quinoline structure**
	Camelia-Georgiana MARANDIS[1,2], Dorina AMARIUCAI-MANTU[1], Vasilichia ANTOCI[1], Violeta MANGALAGIU[3,4], Ionel I. MANGALAGIU[1], Marcela MIHAI[5] [1]*Faculty of Chemistry, "Alexandru Ioan Cuza" University of Iasi, Iasi, Romania* [2]*RECENT AIR, "Alexandru Ioan Cuza" University of Iasi, Iasi, Romania* [3]*CERNESIM, "Alexandru Ioan Cuza" University of Iasi, Iasi, Romania* [4]*Faculty of Food Engineering, "Stefan cel Mare" University of Suceava, , Suceava, Romania* [5]*Petru Poni Institute of Macromolecular Chemistry, Romanian Academy, Iasi, Romania*
11^{15}– 11^{30}	**OC5. The selective complexation mechanism of an organic salt based drug with β-cyclodextrin for the treatment of Alopecia**
	Petru TIRNOVAN[1], Dragos-Lucian ISAC[1], Narcisa-Laura MARANGOCI[1], Alina NICOLESCU[1], Adina COROABA[1], Andrei NEAMTU[1,2], Aatto LAAKSONEN[1,3], Mariana PINTEALA[1] [1]*Petru Poni Institute of Macromolecular Chemistry, Romanian Academy, Iasi, Romania* [2]*Department of Physiology, Faculty of Medicine, Grigore T. Popa University of Medicine and Pharmacy, Iasi, Romania* [3]*Department of Materials and Environmental Chemistry, Division of Physical Chemistry, Arrhenius Laboratory, Stockholm University, Stockholm, Sweden*
11^{30}– 11^{45}	**OC6. Evaluation of the chemical composition and biological activities of *Sideritis Syriaca***
	Alexandra-Mariana IONESCU[1], Andreea Veronica BOTEZATU[1], Ana-Maria MOCANU[1], Anna BUSUIOC[1], Bianca FURDUI[1], Alina Viorica IANCU[2], Marques Fernanda MARUJO[3], Costel VINATORU[4], Geanina NEGOSANU[4], Rodica Mihaela DINICA[1] [1]*Faculty of Sciences and Environment, "Dunarea de Jos" University of Galati, Galati, Romania* [2]*Faculty of Medicine and Pharmacy, "Dunarea de Jos" University of Galati, Galati, Romania* [3]*Instituto Superior Técnico, Universidade de Lisboa, Campus Tecnológico e Nuclear, Bobadela, Lisbon, Portugal* [4]*Genetic and Vegetal Resources Bank (GVRB), Buzau, Romania*
11^{45}– 12^{15}	**Coffee break & POSTER SESSION**

	12^{15} – 13^{30} **Session 3** Chairs: Dr. Sabina TRIFAN and Dr. Bogdan Florin CRĂCIUN
12^{15}– 12^{30}	**OC7. Linker-dependent conformational dynamics of bis-acridine orange dyes: insights from molecular dynamics and enhanced sampling**
	Răzvan PUF[1], Aatto LAAKSONEN[1,2] [1]*Petru Poni Institute of Macromolecular Chemistry, Romanian Academy, Iasi, Romania* [2]*Department of Materials and Environmental Chemistry, Division of Physical Chemistry, Arrhenius Laboratory, Stockholm University, Stockholm, Sweden*
12^{30}– 12^{45}	**OC8. Polymeric thin films for raspberry preservation**
	Paula CUCU[1,2], Irina APOSTOL[2], Iuliana SPIRIDON[2], Mihai MARES[1] [1]*Faculty of Veterinary Medicine, "Ion Ionescu de la Brad" University of Life Sciences, Iasi, Romania* [2]*Petru Poni Institute of Macromolecular Chemistry, Romanian Academy, Iasi, Romania*
12^{45}– 13^{00}	**OC9. Hybrid composite Amylopectin-*g*-Poly(*N*-isopropylacrylamide) /magnetite and its potential for Congo red removal**
	Melinda-Maria BAZARGHIDEANU[1], Florin BUCATARIU[1], Marius-Mihai ZAHARIA[1], Stergios PISPAS[1,2], Marcela MIHAI[1] [1]*Petru Poni Institute of Macromolecular Chemistry, Romanian Academy, Iasi, Romania* [2]*Theoretical and Physical Chemistry Institute, National Hellenic Research Foundation, Athens, Greece*
13^{00}– 13^{15}	**OC10. Modulating cyclodextrin-nitroxide host-guest interactions through stereochemistry, functionalization, and ionic strength**
	Alexandru G. BUCUR[1], Jean P. JOLY[2], Mihaela BANICA[1], Sylvain R. A. MARQUE[2], Florența D. SAVONEA[1], Gabriela IONITA[1] [1]*Institute of Physical Chemistry - Ilie Murgulescu, Romanian Academy, Bucharest, Romania* [2]*Aix Marseille Univ., CNRS, ICR, UMR 7273, Marseille, France*
13^{15}– 13^{30}	**OC11. Modulating the thermoresponsiveness of intelligent hydrogels for biomedical applications**
	Adina FERARIU, Marieta CONSTANTIN, Sanda BUCATARIU, Gheorghe FUNDUEANU *Petru Poni Institute of Macromolecular Chemistry, Romanian Academy, Iasi, Romania*
13^{30}– 14^{30}	**Lunch break - ICMPP Library**

	14^{30} – 16^{00} **Session 4** Chairs: Dr. Irina APOSTOL and Dr. Bogdan-George RUSU
14^{30}– 15^{15}	**SL. Integrated analytical instrumentation - Pro Analysis Systems portfolio and microplastics determination by mild pyrolisys-GC-MS**
	Gheorghița CRETU *Pro Analysis Systems, Bucharest, Romania*
15^{15}– 15^{30}	**OC12. Flame-retardant phosphorus-functionalized cellulose obtained through radical grafting of phosphonate monomers in ionic liquid media**
	Ayoub ABARKAN[1], Ridouan El YOUSFI[1], Brahim ELMEKAOUI[2], Nafea ACHALHI[1], Abderrahman EL IDRISSI[1] [1]*Laboratory of Applied Chemistry and Environment, Faculty of Sciences, Mohamed first University, Oujda, Morocco* [2]*Materials Science, Energy and Nanoengineering (MSN) Department, Mohammed VI Polytechnic University, Benguerir, Morocco*
15^{30}– 15^{45}	**OC13. Optimization of dye adsorption process from single- and multicomponent aqueous systems using magnetic nanocomposites**
	Maria Andreea NISTOR, Liliana HALIP, Simona Gabriela MUNTEAN *"Coriolan Drăgulescu" Institute of Chemistry, Romanian Academy, Timisoara, Romania*
15^{45}– 16^{00}	**OC14. *In silico* evaluation of ADME/TOX profiles using multiple online prediction tools**
	Lucia GRADINARU*, Alina BORA, Luminita CRISAN *"Coriolan Drăgulescu" Institute of Chemistry, Romanian Academy, Timisoara, Romania*
16^{00}– 16^{30}	**Coffee break & POSTER SESSION**
	16^{30}– 18^{00} **Session 5** Chairs: Dr. Vera PLATON and Dr. Catalin-Paul CONSTANTIN
16^{30}– 16^{45}	**OC15. Boronate-guanosine-assisted growth of interconnected gold nanoassemblies on dextran-coated iron oxide nanoparticles for magnetically recoverable sers**
	Tecla DULGHERIU, Elena-Laura URSU, Alexandru ROTARU *Petru Poni Institute of Macromolecular Chemistry, Romanian Academy, Iasi, Romania*
16^{45}– 17^{00}	**OC16. Cyanobacteria Spirulina mediated biosynthesis of copper-based hybrid materials and photocatalytic degradation of dye Indigo Carmine**
	Cristina BOSTACA, Larisa-Maria PETRILA, Marcela MIHAI *Petru Poni Institute of Macromolecular Chemistry, Romanian Academy, Iasi, Romania*

17^{00}– 17^{15}	**OC17. Hydrophobic natural deep eutectic solvent-based materials as solubilizing and delivery vehicles for ferulic acid** Catalin CHERSAN, Raluca Nicoleta DARIE-NITA, Oana URSACHE, Marin-Aurel TROFIN, Sergiu COSERI *Petru Poni Institute of Macromolecular Chemistry, Romanian Academy, Iasi, Romania*
17^{15}– 17^{30}	**OC18. RIM-selective oligocaprolactone substitution of β-cyclodextrin as a strategy for tailoring nanosponge properties** Marius PRODAN, Valeria HARABAGIU, Diana-Andreea BLAJ, Cristian PEPTU *Petru Poni Institute of Macromolecular Chemistry, Romanian Academy, Iasi, Romania*
17^{30}– 17^{45}	**OC19. Hydrogels based on polysaccharides, amino acids and eutectic solvents** Lorena-Elena GRIGORIU, Alexandra VIERU, Diana Elena CIOLACU, Alexandru-Mihail SERBAN, Alina Gabriela RUSU, Loredana-Elena NITA *Petru Poni Institute of Macromolecular Chemistry, Romanian Academy, Iasi Romania*
17^{45}– 18^{00}	**Coffee break**
18^{00}– 18^{30}	**ANALYSIS, AWARDING AND CLOSING CEREMONY**

IL – Invited lecture, **SL** – Seminar, **OC** – Oral communication

POSTERS LIST

Chairs: Dr. Daniela PAMFIL and Dr. Marius-Mihai ZAHARIA

PP1 **Effect of a carbon nanoparticle dispersion on the structure and photoluminescence of electrospun poly(vinyl alcohol) nanofibres**
Sebastian-Marian ALUPOAIE, Bogdan-George RUSU, Iuliana STOICA, Magdalena AFLORI
Petru Poni Institute of Macromolecular Chemistry, Romanian Academy, Iasi, Romania

PP2 **EPR spectroscopic investigation of spin-labelled bovine serum albumin in alginate-based hydrogels**
Elena-Erika ANTONIA, Elena-Gabriela IONITA
Institute of Physical Chemistry - Ilie Murgulescu, Romanian Academy, Bucharest, Romania

PP3 **Optimization of the ugi reaction for alginate functionalization: characterization and antimicrobial activity**
Raluca-Elena AVRAM, Gabriela Liliana AILIESEI, Maria Marinela LAZAR, Maria Valentina DINU
Petru Poni Institute of Macromolecular Chemistry, Romanian Academy, Iasi, Romania

PP4 **Influence of deep eutectic solvent pretreatment on production and properties of cellulose nanofibers**
Mădălina-Roxana BIRTEA, Gabriela BILIUTA, Raluca-Ioana BARON, Raluca Nicoleta DARIE-NITA, Sergiu COSERI
Petru Poni Institute of Macromolecular Chemistry, Romanian Academy, Iasi, Romania

PP5 **Synthesis and structural characterization of pyridine Schiff bases with aliphatic and siloxane units**
Alexandra BIRZU, Mihaela DASCALU, Sergiu SHOVA, Maria CAZACU
Petru Poni Institute of Macromolecular Chemistry, Romanian Academy, Iasi, Romania

PP6 **Carbon quantum dot-loaded sodium alginate/κ-carrageenan hydrogels**
Cosmina-Maria BOGZA, Carmen-Mihaela POPESCU, Maria-Cristina POPESCU
Petru Poni Institute of Macromolecular Chemistry, Romanian Academy, Iasi, Romania

PP7 **Extended π-conjugated Schiff base complexes of transition and rare-earth metals**
Robert I. BOTEA, Augustin MADALAN
Faculty of Chemistry, University of Bucharest, Bucharest, Romania

PP8 **Exploring lignin model dimer interactions in imidazolium-based ionic liquids through molecular dynamics simulations**
Narcis CIBOTARIU[1], Aatto LAAKSONEN[1,2]
[1]*Petru Poni Institute of Macromolecular Chemistry, Romanian Academy, Iasi, Romania*
[2]*Department of Materials and Environmental Chemistry, Division of Physical Chemistry, Arrhenius Laboratory, Stockholm University, Stockholm, Sweden*

PP9 **Molecularly imprinted polymer-based electrochemical sensors for biogenic amines detection – A review**
Andreea-Loredana COMANESCU, Andra-Georgiana TRIFAN, Constantin APETREI
Faculty of Sciences and Environment, "Dunarea de Jos" University of Galati, Galati, Romania

PP10 **Potential applications of phytochemical and synthetic anti-inflammatory compounds**
Manuela Elena COVIT[1], Denis Ionut DEFTA[1], Fănică BALANESCU[2], Anna BUSUIOC[1], Andreea Veronica BOTEZATU[1], Rodica Mihaela DINICA[1]
[1]*Faculty of Science and Environment, "Dunarea de Jos" University of Galati, Romania*
[2]*Faculty of Medicine and Pharmacy, "Dunarea de Jos" University of Galati, Galati, Romania*

PP11 **Electrochemical detection of polyphenolic compounds of interest in wines – A Review –**
Andrei-Daniel GEMAN, Constantin APETREI
Faculty of Science and Environment, "Dunarea de Jos" University of Galati, Galati, Romania

PP12 **DNA condensation by 4-ARM PEG–histidine/lysine peptide polyplexes: tuning transfection and biocompatibility**
Razvan GHIARASIM, Dragos PEPTANARIU, Mihaela SILION, Alina NICOLESCU, Lucian BAHRIN, Mariana PINTEALA
Petru Poni Institute of Macromolecular Chemistry, Romanian Academy, Iasi, Romania

PP13 **Mn-doped aluminium iron oxides as advanced materials for wastewater remediation**
Ionela GRECU[1], Maria Emiliana FORTUNA[1], Alexandra LAPUSNEANU[2], Ioan-Andrei DASCALU[1], Andra-Cristina ENACHE[1], Corneliu COJOCARU[1], Petrisor SAMOILA[1]
[1]*Petru Poni Institute of Macromolecular Chemistry, Romanian Academy, Iasi, Romania*
[2]*"Costache Negruzzi" National College, Iasi, Romania*

PP14 **Sorbtion of nitronyl nitroxide benzaldehyde in poly(ethylene glycol)/β-CD hydrogels hybrid AuNPs**
Alexandra Ana-Maria IANCU, Alexandru Gabriel BUCUR, Mihaela BANICA, Gabriela IONITA
Institute of Physical Chemistry – Ilie Murgulescu, Romanian Academy, Bucharest, Romania Country

PP15 **Rhenium tricarbonyl complexes-loaded polyester nanoparticles for potential biomedical applications**
Andrei-Alexandru IVU[1], Alina Gabriela RUSU[1], Alexandru Mihail SERBAN[1], Isabella NACU[2], Fabio ZOBI[3], Liliana VERESTIUC[2], Loredana Elena NITA[1]
[1]*Petru Poni Institute of Macromolecular Chemistry, Romanian Academy, Iasi, Romania*
[2]*Department of Biomedical Sciences, Faculty of Medical Bioengineering, Grigore T. Popa University of Medicine and Pharmacy Iasi, Iasi, Romania*
[3]*Department of Chemistry, Fribourg University, Fribourg, Switzerland*

PP16 **From coumarin-containing quaternary salts to cycloadducts: a comparative UV–Vis study**
Florentina-Gabriela LAZAR[1], Cristina AL-MATARNEH[1], Dorina AMARIUCAI-MANTU[2], Ashraf AL-MATARNEH[1,2], Mariana PINTEALA[1]
[1]*Petru Poni Institute of Macromolecular Chemistry, Romanian Academy, Iasi, Romania*
[2]*Faculty of Chemistry, "Alexandru Ioan Cuza" University of Iasi, Iasi, Romania*

PP17 **Preparation of the copper alginate complexes using ion exchanger column method**
Alina-Petronela MORARU, Marius-Mihai ZAHARIA, Marcela MIHAI
Petru Poni Institute of Macromolecular Chemistry, Romanian Academy, Iasi, Romania

PP18 **Hydrophobized silica-based nanocomposite formulations for superhydrophobic wood surfaces**

Monica-Georgiana MUSTEATA, Maria-Cristina POPESCU, Carmen-Mihaela POPESCU
Petru Poni" Institute of Macromolecular Chemistry, Romanian Academy, Iasi, Romania

PP19 **Scaffold architecture as a design parameter in 3d-printed scaffolds for tissue regeneration**

Isabella NACU, Anca TOMA, Liliana VERESTIUC
Department Biomedical Sciences, Faculty of Medical Bioengineering, "Grigore T. Popa" University of Medicine and Pharmacy, Iasi, Romania

PP20 **Volatile organic compounds from coffee as potential bioactive agents in chitosan based materials**

Andrei-Razvan PANA[1], Grigore UNGUREANU[1], Cristopher Anel BOYA[2], Mihai BREBU[1], Elena STOLERU[1]
[1]*Petru Poni Institute of Macromolecular Chemistry, Romanian Academy, Iasi, Romania*
[2]*Center for Biodiversity and Drug Discovery, Institute for Scientific Research and High Technology Services (INDICASAT AIP), Panama City, Panama*

PP21 **Bioactive hybrid hydrogel for controlled delivery in biomedical applications**

Ana Rebeca PINTILII, Anca Mihaela MOCANU, Margareta Gabriela CIOBANU
Cristofor Simionescu Faculty of Chemical Engineering and Environmental Protection, Gheorghe Asachi Technical University of Iasi, Iasi, Romania

PP22 **Chromatographic identification of biologically active compounds from different plant species**

Raluca-Nicoleta RAILEANU[1], Anna BUSUIOC[1], Alexandra-Mariana IONESCU[1], Costel VINATORU[2], Geanina NEGOSANU[2], Andreea Veronica BOTEZATU[1], Bianca FURDUI[1], Rodica Mihaela DINICA[1]
[1]*Faculty of Sciences and Environment, "Dunarea de Jos" University of Galati, Galati, Romania*
[2]*Genetic and Vegetal Resources Bank (GVRB), Buzau, Romania*

PP23 **Phenanthridinium ylides in [3+2] cycloadditions: dipolarophile effects and NMR characterization**

Claudiu TICALEAC[1], Costel MOLDOVEANU[1], Catalina CIOBANU[2], Ionel MANGALAGIU[1], Gheorghita ZBANCIOC[1]
[1]*Faculty of Chemistry, "Alexandru Ioan Cuza" University of Iasi, Iasi, Romania*
[2]*CERNESIM Centre, "Alexandru Ioan Cuza" University of Iasi, Iasi, Romania*

PP24 **Sensors for melatonin detection: recent advances, analytical performance, and future perspectives**

Andra-Georgiana TRIFAN, Andreea-Loredana COMANESCU, Constantin APETREI
Faculty of Science and Environment, "Dunarea de Jos" University of Galati, Galati, Romania

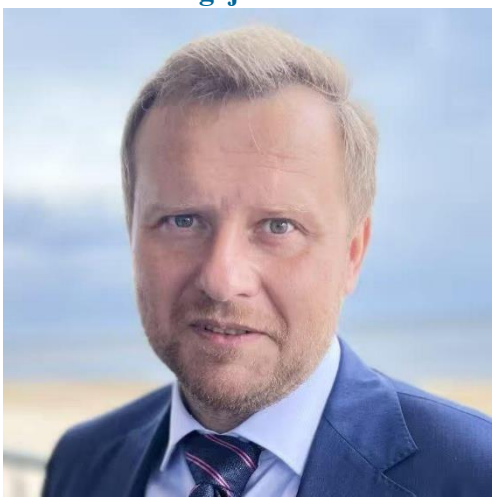
PP25 **Volatile organic compound from honey to induce a casein bazed materials**

Grigore UNGUREANU[1], Marius NICULAUA[2], Alin-Constantin DÎRȚU[3], Elena STOLERU[1], Mihai BREBU[1]
[1]*Petru Poni Institute of Macromolecular Chemistry, Romanian Academy, Iasi, Romania*
[2]*Center for Oenological Research - Romanian Academy, Iași, Romania*
[3]*Faculty of Chemistry, "Alexandru Ioan Cuza" University of Iași, Iași, Romania*

Invited lecture

INVITED LECTURE

Prof. Dr. Sergejs GAIDUKOVS is a distinguished expert in Polymer Chemistry and Technology with over 25 years of experience at Riga Technical University (RTU), Latvia. He currently serves as a Professor and Leading Researcher, contributing significantly to advancements in polymer science.



Throughout his academic career, Prof. Gaidukovs has held key positions at RTU, including Associate Professor (2017–2021) before his promotion to Professor in 2021. His research focuses on cutting-edge developments in polymer chemistry, material science, and sustainable technologies.

With extensive experience in research and industry, Prof. Gaidukovs continues to drive innovation in polymer technology and applied materials, bridging academia with industrial applications.

Oral Communications

OC1. A CATIONIC CURDLAN DERIVATIVE AS A FLOCCULANT FOR WASTEWATER TREATMENT

Maria-Magdalena Nafureanu*, Dana Mihaela Suflet, Marieta Constantin
Petru Poni Institute of Macromolecular Chemistry, Romanian Academy, Iasi, Romania
**nafureanu.magda@icmpp.ro*

The increasing demand for wastewater treatment represents a major global challenge, requiring continued scientific efforts to protect water resources from pollution arising from diverse anthropogenic activities, including industrial, domestic, agricultural, and commercial, as well as natural processes [1, 2]. Among the available wastewater treatment methods, flocculation is widely used due to its operational simplicity, potential cost-effectiveness, and ability to remove suspended solids and colloidal particles [3]. In this context, polysaccharide-based derivatives have attracted interest as alternatives to conventional synthetic flocculants, owing to their renewable origin and low toxicity. The incorporation of ionogenic groups into polymer chains can enhance polymer-particle interactions, thereby promoting destabilization and aggregation [4]. However, sludge is an unavoidable by-product of flocculation processes, and improper disposal may lead to soil and groundwater contamination. The reuse of this sludge as an adsorbent for various pollutants provides an environmentally friendly strategy within a circular approach to wastewater treatment [5].

In this study, a cationic curdlan derivative ($TMAC_{0.4}$-C) bearing quaternary ammonium groups ([*N*-(3-chloro-2-hydroxypropyl)-trimethylammonium] chloride) was synthesized according to a previously reported method [6]. The polymer exhibited a degree of substitution (DS) of 0.4, corresponding to a cationic charge density of 1.09 meq/g. Its flocculation performance was investigated using individual metal oxide dispersions (FeO, Cr_2O_3, and TiO_2) (Figure 1a) and multicomponent systems containing metal oxides, mono- and divalent salts, and kaolin. The flocs recovered after the separation of FeO and kaolin particles were subsequently evaluated as adsorbents for Bordeaux Mixture (BM) fungicide removal (Figure 1b), exploring their potential for sludge valorization.

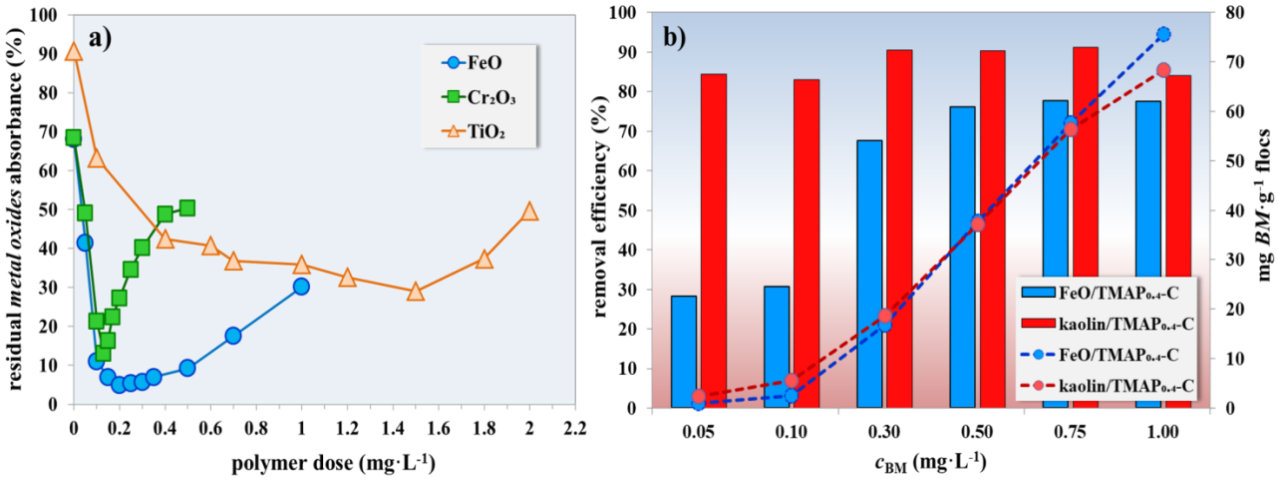


Figure 1. Effect of $TMAP_{0.4}$-C dose ($mg \cdot L^{-1}$) on the residual *metal oxides* absorbance (%) (a), and effect of Bordeaux Mixture dispersion concentration on the removal efficiency (%) and adsorption capacity ($mg \cdot g^{-1}$) of the recovered flocs (b).

As shown in Figure 1a, increasing the $TMAP_{0.4}$-C dose progressively enhanced metal oxide removal, reaching maximum efficiencies of 95%, 87%, and 71% for FeO, Cr_2O_3, and TiO_2, respectively, at optimum polymer doses (OPDs) of 0.2, 0.13, and 1.5 $mg \cdot L^{-1}$. Further polymer addition led to dispersion restabilization, possibly due to electrostatic repulsion between excess adsorbed cationic chains. The negative zeta potential (ζ) values of the initial metal oxide suspensions (-32.7 mV for FeO, -40.5 mV for Cr_2O_3, and -38.1 mV for TiO_2), suggest that electrostatic attraction between the quaternary ammonium groups of $TMAP_{0.4}$-C and the negatively charged particle surfaces contributes to flocculation. To obtain information regarding the separation mechanism, zeta potential measurements were performed on supernatant samples. At the OPDs, the ζ values remained negative (-14 mV for FeO, -17.7 mV for Cr_2O_3, and -22 mV for TiO_2), indicating that maximum removal occurred without complete charge neutralization [7] and that the charge-patch mechanism may have been involved in particle separation. To reinforce this interpretation, particle size distribution analyses were conducted on both untreated particles and the flocs formed after addition of the curdlan derivative. The narrow size distribution of the metal oxide/$TMAP_{0.4}$-C aggregates and their slightly increased average size ($D50_{Cr2O3}$ = 4.64 µm; $D50_{FeO}$ = 10.29 µm; $D50_{TiO2}$ = 1.95 µm) compared to the initial particles, supports that mechanism based on electrostatic attractions between oppositely charged regions (patches) on the particles has a significant role in the separation process. The presence of salts and kaolin did not prevent effective metal oxide removal from multicomponent dispersions. Removal efficiencies exceeding 95% were achieved at low OPDs ranging from 0.01 to 1 $mg \cdot L^{-1}$. Increasing salt concentrations reduced the magnitude of the zeta potential, consistent with electrical double layer compression and enhanced particle aggregation [8]. However, at concentrations above $5 \cdot 10^{-2}$ M, the dispersions became unstable even before polymer addition, indicating a substantial salt-induced coagulation effect.

The FeO/$TMAP_{0.4}$-C and kaolin/$TMAP_{0.4}$-C flocs exhibited different BM removal performances, as illustrated in Figure1b. The kaolin-based flocs achieved consistently high removal efficiencies of 84-90%, whereas those containing FeO reached up to 76%. Adsorption capacities increased with the initial fungicide concentration, reaching 75.6 $mg \cdot g^{-1}$ for FeO-based flocs and 68.2 $mg \cdot g^{-1}$ for kaolin-based flocs. The pseudo-second-order model best described the adsorption kinetics, while the Elovich model also fitted the experimental data well, suggesting contributions from surface interactions and heterogeneous adsorption processes.

In conclusion, $TMAP_{0.4}$-C effectively removed metal oxides from both single-component and multicomponent dispersions, while the recovered flocs proved suitable for subsequent Bordeaux Mixture fungicide removal, highlighting the potential for their reuse in wastewater treatment.

References

[1] S. Pandey, A. Kumar, K. Kumar, S. Krishnamoorthi, K. Tungala, *Bioresour. Technol. Rep.* 2025, 29, 102023.
[2] A. Fatima, M. Naz, A. Haider, I. Shahzadi, A. Ul-Hamid, H. Ullah, G. Ali, S. Moeen, S.M. El-Bahy, M. Ikram, *Surf.Interfaces* 2025, 58, 105907.
[3] S.B. Kurniawan, M.F. Imron, C.E.N.C.E. Chik, A.A. Owodunni, A. Ahmad, M.M. Alnawajha, N.F.M. Rahim, N.S.M. Said, S.R.S. Abdullah, N.A. Kasan, S. Ismail, A.R. Othman, H.A. Hasan, *Sci.Total Environ.* 2022, 806, 150902.
[4] S. Leonhartsberger, P. Carmona, B. Seidl, K.J. Mann, M. Kozich, I. Sulaeva, C. Stanetty, M.D. Mihovilovic, *Carbohydr.Polym.* 2025, 358, 123527.
[5] Y. Bian, Q. Yuan, G. Zhu, B. Ren, A. Hursthouse, P. Zhang, *Int.J.Polym.Sci.* 2018, 2018, 8320609.
[6] D.M. Suflet, I. Popescu, I.M. Pelin, A. Nicolescu, G. Hitruc, *Carbohydr.Polym.* 2015, 123, 396-405.
[7] J. Kleimann, C. Gehin-Delval, H. Auweter, M. Borkovec, *Langmuir* 2005, 21, 3688-3698.
[8] M.S. Lucas, A.R. Teixeira, N. Jorge, J.A. Peres, *Water* 2025, 17, 1934.

OC2. HYDROTHERMAL SYNTHESIS OF $BaTiO_3$-BASED HIGH ENTROPY PEROVSKITE OXIDES

Mihail-Calin Licu[1]*, Florentina Maxim[1], Florina Teodorescu[1], Daniela Berger[2], Elena Maria Anghel[1], Ancuta Sofronia[1], Cristian Matei[2], Speranta Tanasescu[1]
[1]*Institute of Physical Chemistry - Ilie Murgulescu, Romanian Academy, Bucharest, Romania*
[2]*Faculty of Chemical Engineering and Biotechnology, Polytechnic University of Bucharest, Bucharest, Romania*
**mlicu@icf.ro*

High entropy perovskite oxides (HEPOs) are a class of materials in which several different cations, usually five or more in near-equimolar proportions, share one or more crystallographic sites of the ABO_3 perovskite lattice [1,2]. The stability of the single phase is attributed to the high configurational entropy of mixing, which for an ideal solid solution of a perovskite is the sum of the contributions of the A, B and oxygen sublattices. Systems with configurational entropy higher than 1.5R are conventionally considered "high entropy" [3], as depicted in Figure 1a. The large differences in ionic radius and valence among the cations cause lattice distortion and random electric and stress fields, which are the origin of the specific properties of these materials. In titanate HEPOs, this disorder breaks the long-range ferroelectric order and produces polar nanoregions, leading to relaxor ferroelectric behaviour with high permittivity and slim polarisation–electric field loops [2,4]. Other reported properties emphasize reduced thermal conductivity, enhanced catalytic activity, high thermal and chemical stability, and improved proton conductivity and oxygen permeability making them promising candidates for dielectric energy storage capacitors, piezoelectric materials, solid oxide fuel cells, lithium-ion batteries, thermoelectrics, catalysts and supercapacitors [1,2]. HEPOs are mostly prepared by solid-state reaction. Because diffusion in high entropy materials is sluggish, this route needs prolonged high-temperature annealing, which leads porous ceramics with defects, and the loss of volatile elements [1]. Hydrothermal synthesis is an alternative that gives fine crystalline oxide powders directly at low temperatures, up to about 300 °C, and avoids the high-temperature calcination step. Being a wet chemical route, all the metal ions are dissolved, which favours a uniform composition distribution at the molecular level [4].

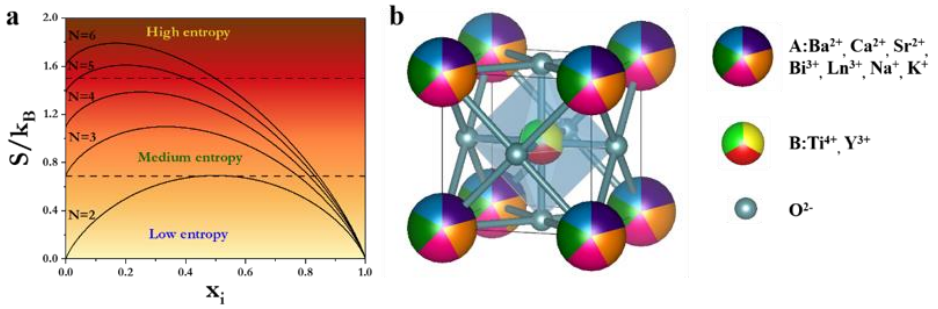


Figure 1. a. Configurational entropy evolution with number of components and their stoichiometry; b. $BaTiO_3$-derived HEPOs structure with the cations used in the present work.

In the present work, a stable aqueous TiO_2 sol was prepared and used as Ti^{4+} source. The sol was characterised by dynamic light scattering (DLS) showing a narrow, monomodal size distribution and UV-Vis absorption spectroscopy, confirming the formation of the anatase phase. Several

$BaTiO_3$-derived HEPOs (Figure 1b) were synthesised hydrothermally using a Berghof BR100 high pressure reactor (https://eertis.eu/ereq-2300-008t-1559). The salts of the cations were dissolved in the aqueous TiO_2 sol, and this solution was added dropwise to a KOH or NaOH mineralizer solution in which barium acetate had been previously dissolved. The obtained compositions were $(BaBiCaNaSr)_{0.2}TiO_3$, $(BaBiCaKSr)_{0.2}TiO_3$ and $(BaCaKLnSr)_{0.2}TiO_3$, where Ln = La, Nd, Sm. $BaTiO_3$ was synthesised under the same conditions and was used as a reference material. Working parameters such as temperature (150-200 °C), pressure (autogenous, or with applied 6.0 purity N_2 overpressure up to 25 bar), mixing conditions (stirring/no stirring) and reaction time (4-24 h) were systematically varied in order to find the conditions favouring single-phase formation. The samples were characterised by X-ray diffraction (XRD) for phase identification, crystal structure, and confirmation of single-phase formation (Figure 2), Raman spectroscopy for local structure and symmetry, scanning electron microscopy with energy-dispersive X-ray analysis (SEM/EDX) for morphology and elemental distribution, and differential scanning calorimetry (DSC) for thermal behaviour and phase transitions.

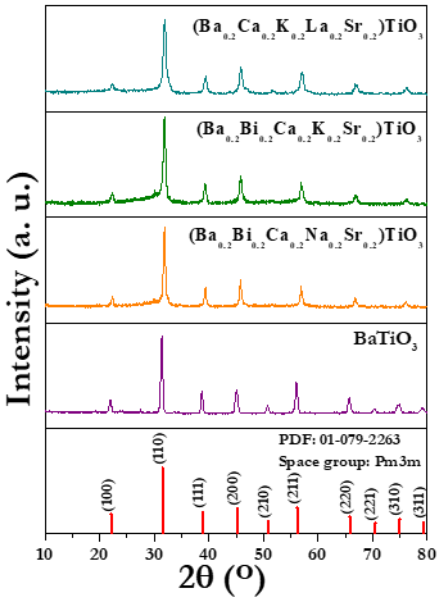


Figure 2. X-ray diffraction patterns of synthesised HEPOs, showing single-phase formation.

This study shows that hydrothermal synthesis is a viable route to single-phase $BaTiO_3$-based HEPOs at moderate temperatures. Future work will extend this approach to supercritical hydrothermal synthesis, and will include the thermodynamic analysis in order to evidence the relevant functions suitable for evaluation of thermodynamic stability of the new synthesized high entropy oxides.

References

[1] J. Ma, T. Liu, W. Ye, Q. He, K. Chen, *J. Energy Storage* 2024, 90, 111890.
[2] K. Bunpang, S. Singkammo, D. P. Cann, N. Raengthon, *Sci. Rep*. 2024, 14, 6017.
[3] C. M. Rost et al., *Nat. Commun.* 2015, 6, 8485.
[4] W. Sun, F. Zhang, X. Zhang, T. Shi, J. Li, Y. Bai, C. Wang, Z. Wang, *Ceram. Int.* 2022, 48, 19492-19500.

Acknowledgment: The work reported in this study was mainly carried out within the framework of Research Program: "*Thermodynamics and Quantum Chemistry*" implemented at the Institute of Physical Chemistry - Ilie Murgulescu of the Romanian Academy.

OC3. DUAL-CROSSLINKED COLMA/GELMA/HAMA BIOINKS FOR EXTRUSION-BASED 3D BIOPRINTING OF ARTIFICIAL SKIN CONSTRUCTS

Zechuan Wang[1,2*], Maria Butnaru[2], Maria Valentina Dinu[1], Liliana Verestiuc[2]
[1]*Petru Poni Institute of Macromolecular Chemistry, Romanian Academy, Iasi, Romania*
[2]*Faculty of Medical Bioengineering, "Grigore T. Popa" University of Medicine and Pharmacy, Iasi, Romania*
**wang.zechuan@icmpp.ro*

Introduction

There is a pressing clinical need for effective strategies to achieve durable closure of large, non-healing skin wounds. Methacrylated natural polymers are among the most attractive bioink materials for skin because of their biological relevance and controllable crosslinking chemistry. However, photocrosslinking alone tends to form a soft network, which swells up and degrades fast. This is solved by a second chemical crosslinking step with genipin, which creates more crosslinks between polymer chains.

Aim

We report the development and characterization of a dual-crosslinked bioink for extrusion-based skin engineering made of three methacrylated natural polymers, ColMA, GelMA and HAMA. The printability, pore structure, swelling, compressive behavior and cytocompatibility of the four inks were compared to identify the composition that gives the best compromise between these properties for a dermal substitute.

Materials and Methods

Four formulations (G1–G4) were designed based on a 2×2 factorial design, changing the bulk protein (GelMA or unmodified gelatin) and the low concentration methacrylated component (ColMA or GelMA) (Table 1).

Table 1. Bioink formulation

Group	Low-concentration position	High-concentration position	HAMA (mg)	LAP (mg)	Genipin (mg)
G1	GelMA	GelMA	29.17	10	2
G2	ColMA	GelMA	29.17	10	2
G3	ColMA	Gelatin	29.17	10	2
G4	GelMA	Gelatin	29.17	10	2

The cytocompatibility of each group was evaluated by MTT assay after the indirect extract method based on ISO 10993-5 using primary normal human dermal fibroblasts (NHDF) as the cell type [1].

Results and Discussion

When GelMA was used as the bulk protein, G1 and G2 extruded as discrete droplets that collapsed into an amorphous mass and were unable to maintain a grid structure. G3 and G4 were bulk gelatin,

which extruded as continuous filaments and retained stable square-grid architectures, due to the fact that gelatin retains thermally induced physical gelation at room temperature, while GelMA loses this property by methacrylation (Figure 1).

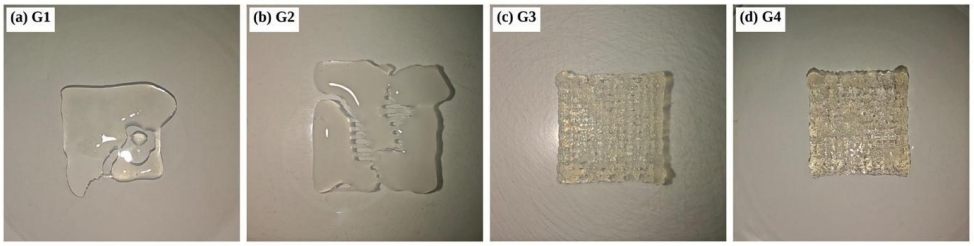


Figure 1. Printed constructs of the four bioinks. (a) G1 and (b) G2 failed to form a defined shape; (c) G3 and (d) G4 printed as continuous filaments into a stable square grid.

G3 and G4 produced thick-walled honeycomb-like open-cell foams with G4 having the largest pores (253 ± 92 µm) and the most secondary microporosity. G3 swelled much more than the other formulations in PBS, consistent with charge-screening effects from its more hydrated, less dense network. The increased ionic strength in DMEM screened these electrostatic effects and swelling converged for all groups. G3 showed a nearly linear stress-strain response and failed at ~33% strain with a compressive modulus of ~6.6 kPa. G4 exhibited significant strain stiffening, higher stress at break (~5.0 kPa), failure (~57% strain) and lower modulus (~4.1 kPa). All four formulations were citocompatibility with primary dermal fibroblast cells. To test the epidermal compatibility under more difficult conditions, HaCaT keratinocytes were seeded directly on the surface of the scaffold and followed for nine days with calcein-AM staining (Figure 2). G1 and G4 lost structural integrity during this prolonged culture period and were unavailable for evaluation beyond early time points; only G2 and G3 were available for analysis through day 9. In G3, keratinocytes adhered, were viable and formed a more dense, more confluent fluorescent population on day 9 versus day 5.

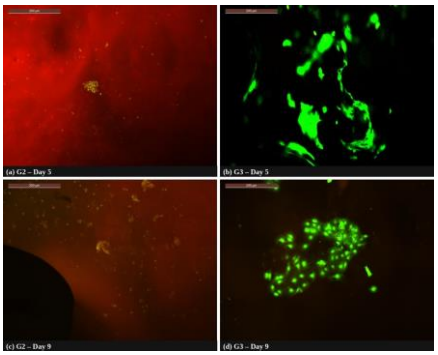


Figure 2. Calcein-AM staining of HaCaT keratinocytes seeded on the surface of G2 and G3 scaffolds, imaged in the FITC (green) channel at day 5 (a, b) and day 9 (c, d). Scale bar = 200 µm.

Conclusions

Overall, G3 appears to be the most promising formulation, from the data shown here, since it combines printability, an open and interconnected pore structure, and cytocompatibility with both primary dermal fibroblasts and keratinocytes for a longer culture period.

References

[1] I. Nacu, M. Bercea, L.E. Niță, C.A. Peptu, M. Butnaru, L. Vereștiuc, *React. Funct. Polym.* 2023, 190, 105636.

OC4. HUMAN SERUM ALBUMIN AS A MOLECULAR HOST FOR HYBRID CHIMERIC DERIVATIVES WITH PYRROLO-QUINOLINE STRUCTURE

Camelia-Georgiana Marandis[1,2]*, Dorina Amariucai-Mantu[1], Vasilichia Antoci[1], Violeta Mangalagiu[3,4], Ionel I. Mangalagiu[1], Marcela Mihai[5]
[1]*Faculty of Chemistry, "Alexandru Ioan Cuza" University of Iasi, Iasi, Romania*
[2]*RECENT AIR, "Alexandru Ioan Cuza" University of Iasi, Iasi, Romania*
[3]*CERNESIM, "Alexandru Ioan Cuza" University of Iasi, Iasi, Romania*
[4]*Faculty of Food Engineering, "Stefan cel Mare" University of Suceava, , Suceava, Romania*
[5]*Petru Poni Institute of Macromolecular Chemistry, Romanian Academy, Iasi, Romania*
**marandiscamelia01@gmail.com*

The transport and distribution of drugs in the human body represents two processes that influence their bioavailability and therapeutic efficacy. Once drugs enter the systematic circulation, they may interact with plasma proteins, which play an important role in modulating their pharmacokinetic behavior [1]. Among plasma proteins, human serum albumin (HSA) is the most abundant and serves as a major carrier of numerous endogenous and exogenous compounds. This structurally simple and stable protein represents an important model for understanding ligand-protein interactions due to the multiple binding regions and structural flexibility, which induces a remarkable ability to accommodate a wide range of ligands. The strength and nature of these interactions are relevant because molecular binding must be sufficiently favorable to realize the transport while remaining reversible to allow ligand release [2].

Building upon these findings, the interaction between different hybrid chimeric compounds with pyrrolo-quinoline-triazole structure with anticancer potential activity and HSA can provide valuable informations regarding potential use as carrier through blood system. This work presents a series of novel pyrroloquinoline-triazole hybrids obtained by a molecular hybridization strategy involving *N*-quaternization, Huisgen [3+2] dipolar cycloaddition followed by Cu(I)-catalyzed azide-alkyne 1,3-dipolar cycloaddition (CuAAC). The obtained hybrids were characterized by FT-IR and NMR spectroscopy aiming to demonstrate the proposed structure. Also, their photophysical behavior was investigated by UV-Vis absorption and fluorescence spectroscopy in order to evaluate the influence of structural modifications on their optical properties. After complete structural characterization, preliminary biological studies were performed to investigate the potential activity of the synthesized compounds. In this context, the toxicity assay on the human dermal fibroblasts (HDF) cell line revealed the lack of toxicity of our compounds and the anticancer assay against ostesarcoma HOS and MG-63 and breast adenocarcinoma MCF7 demonstrated a good activity on osteosarcoma cancer cell lines HOS and breast adenocarcinoma MCF7 and a moderate activity on osteosarcoma MG-63. Taking into the consideration of their good viability on the HDF cell line, the interactions of the obtained compounds with HSA were investigated to gain insights into their binding behavior and potential implications for transport and distribution. Thus, a comprehensive understanding of ligand-protein interactions requires the integration of complementary approaches including UV-Vis absorption spectroscopy, steady-state fluorescence spectroscopy and molecular docking simulations. Additional information regarding molecular proximity and the identification of potential binding regions was obtained through

Förster resonance energy transfer (FRET) analysis and competitive binding experiments using site-specific markers of HSA. Figure 1 illustrates the methods used to investigate the ligand-protein system.

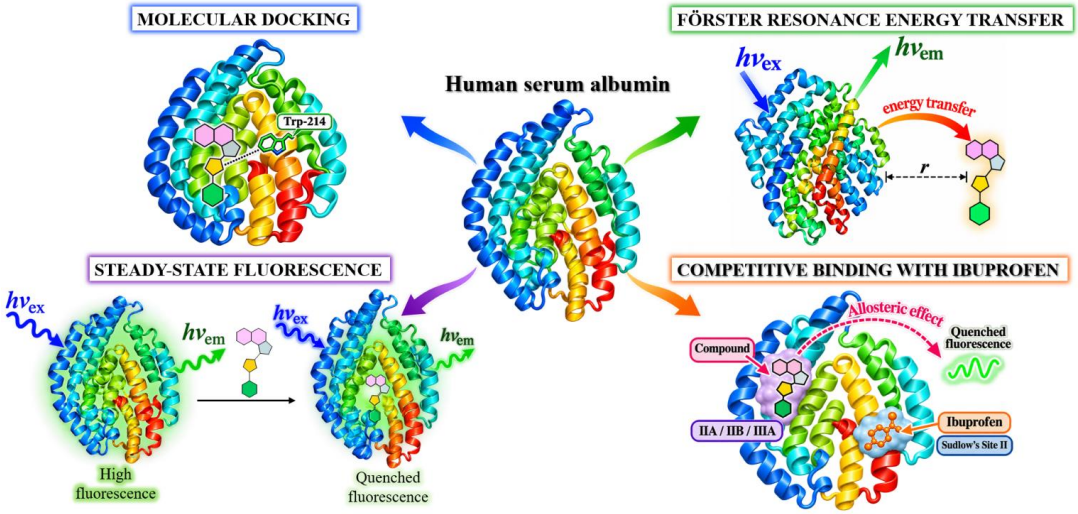


Figure 1. Schematic overview of the experimental and computational methods used to investigate the ligand-HSA system.

Overall, the computational results suggested a favorable accommodation of the investigated compounds within different regions of the protein, depending on the compound structure. Following the computational findings, steady-state fluorescence spectroscopy was employed, revealing a decrease in the intrinsic fluorescence intensity of HSA upon ligand addition in all cases. Measurements were performed at three different temperatures to assess the temperature dependence of the fluorescence quenching process and to evaluate the binding characteristics of the protein-ligand systems. Furthermore, FRET analysis was performed revealed variations in the estimated energy transfer efficiencies among the investigated compounds, suggesting a possible influence of their molecular structures. These results were in agreement with the molecular docking predictions and indicated a potential contribution to the observed fluorescence quenching. Finally, competitive binding experiments using ibuprofen as a marker of Sudlow II indicated a decrease in the apparent binding affinity, suggesting possible competitive and/or allosteric effects regardless of the structure of the compounds. These findings suggest that HSA may act as a potential carrier for the investigated heterocyclic derivatives, suggesting the possible biological relevance of their interactions.

References

[1] R. Tao, C. Ding, F. Wang, X. Zhang, G. Chen, *Transl. Gastroenterol. Hepatol.* 2026, 11, 33.
[2] S. Amézqueta, J.L. Beltrán, A.M. Bolioli, L. Campos-Vicens, F.J. Luque, C. Ràfols, *Pharmaceuticals* 2021, 14, 214.

Acknowledgements: Acknowledgment is given to infrastructure support from the Operational Program Competitiveness 2014–2020, Axis 1, under POC/448/1/1 Research infrastructure projects for public R&D institutions/Sections F 2018, through the Research Center with Integrated Techniques for Atmospheric Aerosol Investigation in Romania (RECENT AIR) project, under grant agreement MySMIS no. 127324. Authors are also gratefully for the infrastructure support provided by the Romanian National Authority for Research, by project HYBSAC, project number PNRR-III-C9-2022-I8-201, within the National Recovery and Resilience Plan.

OC5. THE SELECTIVE COMPLEXATION MECHANISM OF AN ORGANIC SALT BASED DRUG WITH β-CYCLODEXTRIN FOR THE TREATMENT OF ALOPECIA

Petru Tirnovan[1]*, Dragos-Lucian Isac[1], Narcisa-Laura Marangoci[1], Alina Nicolescu[1], Adina Coroaba[1], Andrei Neamtu[1,2], Aatto Laaksonen[1,3], Mariana Pinteala[1]

[1]*Petru Poni Institute of Macromolecular Chemistry, Romanian Academy, Iasi, Romania*

[2]*Department of Physiology, Faculty of Medicine, Grigore T. Popa University of Medicine and Pharmacy, Iasi, Romania*

[3]*Department of Materials and Environmental Chemistry, Division of Physical Chemistry, Arrhenius Laboratory, Stockholm University, Stockholm, Sweden*

**tirnovan.petru@icmpp.ro*

The active pharmaceutical ingredient of the product Minoxicapil® (Fiterman Pharma SRL), 2,6-diamino-1-N-hydroxy-4-(pyrrolidin-1′-yl)pyrimidinium L-2-oxothiazoline-4-carboxylate, is an organic salt used for the treatment of alopecia (Figure 1). The salt contains a minoxidil derived cation, in which the piperidinic ring is replaced by a pyrrolidine ring, and an anion derived from L-cysteine (a keratine component). Despite its ionic nature, the compound exhibits limited aqueous solubility requiring its formulation with additional excipients and other bioactive components [1]. As these constituents may influence drug availability and transport toward hair follicles, an alternative pharmaceutical formulation has been considered, though the use of β-cyclodextrin (β-CD) and the formation of an inclusion complex was investigated.

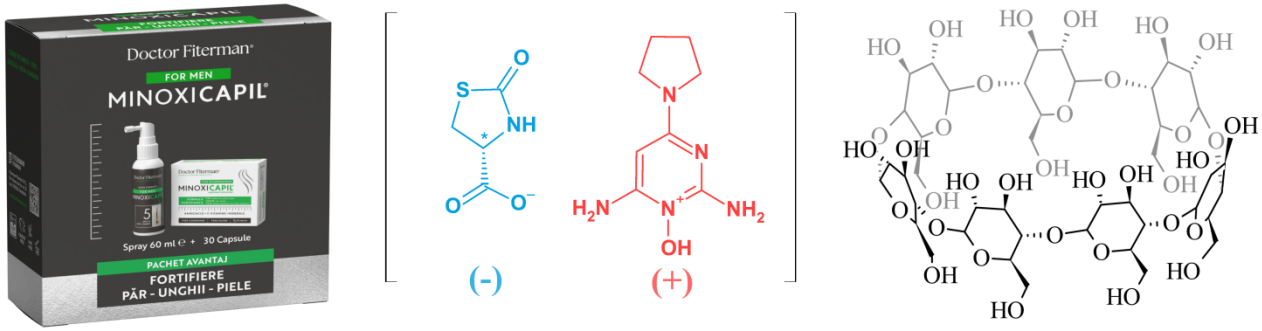


Figure 1. Depiction of the commercial Minoxicapil® formulation (image source: https://shopfiterman.ro/pachet-men-spray-60-ml-minoxicapil-30-capsule-men-doctor-fitermann) and the chemical structures of its active ingredient and β-CD.

β-CD is a biocompatible, biodegradable cyclic oligosaccharide characterized by a hydrophobic cavity and two hydrophilic rims. Its ability to form guest-host inclusion complexes has been widely explored in various pharmaceutical applications [2], to improve water solubility, increase chemical stability, reduce toxicity [3], mask the taste of drugs through a shielding effect, enhance the control over drug release and cellular viability [4].

In this study, an integrated computational and experimental approach was used to investigate the mechanism of selective complexation between the active ingredient of Minoxicapil® with β-CD. Molecular docking, molecular dynamics simulations and umbrella sampling calculations were

combined with magnetic nuclear resonance (NMR) spectroscopy, rotating-frame Overhauser effect spectroscopy (ROESY), *ex vivo* skin permeation experiments, and *in vitro* biocompatibility assays using human hair follicle dermal papilla cells (HFDPCs) [5]. Computational and experimental results consistently indicated a preferential affinity of β-CD for the cationic component compared with the anion. Although the smaller anion displayed faster initial access to the hydrophobic cavity, it did not form a persistent inclusion complex. NMR titration supports a 1:1 guest-host complex with an association constant (K_a) of 76 M^{-1}, indicating moderate binding affinity. The preferred inclusion geometry of the cation dominantly involves the pyrrolidinic ring oriented towards the hydrophobic cavity, while the more hydrophilic pyrrimidinic ring was oriented toward the secondary rim of β-CD stabilized by hydrogen bond interactions with its hydroxyl groups. This structural arrangement is supported by both computational data and changes in the NMR spin couplings.

In addition, *ex vivo* skin permeation experiments revealed that permeation remained below the analytical detection limit for both the free compound and its inclusion complex. Meanwhile, *in vitro* assays demonstrated improved HFDPC viability in the presence of the inclusion complex, compared to the free drug, across the investigated concentration range, suggesting enhanced cellular compatibility.

Overall, these findings provide molecular-level insight into the selective host-guest interactions between a minoxidil-derived organic salt and β-CD and demonstrate the potential of cyclodextrin complexation to improve biological compatibility. The results support further investigation of β-CD-based formulations as a potential strategy for developing improved topical treatments for alopecia.

References

[1] V.M. Voiculescu, M. Lupu, *Cosmetics* 2025, 12(4), 152.
[2] N. Marangoci, M. Rares, M. Silion, A. Fifere, C. Varganici, A. Nicolescu, C. Deleanu, A. Coroaba, M. Pinteala, B. C. Simionescu, *Results Pharma Sci.* 2011, 1(1), 27-37.
[3] N. Marangoci, S. S. Maier, R. Ardeleanu, A. Arvinte, A. Fifere, A. R. Petrovici, A. Nicolescu, M. Mares, S. A. Pasca, R. F. Moraru, M. Pinteala, A. Chiriac, *Chem. Res. Toxicol.* 2014, 27(4), 546-557.
[4] A. Corciova, C. Ciobanu, A. Poiata, A. Nicolescu, M. Drobota, C. D. Varganici, T. Pinteala, A. Fifere, N. Marangoci, C. Mircea, *Dig. J. Nanomater. Biostructures* 2014, 9(4), 1623-1637.
[5] P. Tirnovan, D. L. Isac, N. Marangoci, A. Nicolescu, A. Coroaba, B. Cretu, A. Laaksonen, A. Neamtu, T. Pinteala, *Carbohydr. Polym. Technol. Appl.* 2026, 14, 101155.

Acknowledgment: This work is supported by European Union's Horizon Europe research and innovation programme under grant agreement No 101086667, project BioMat4CAST (BioMat4CAST - "Petru Poni" Institute of Macromolecular Chemistry Multi-Scale In Silico Laboratory for Complex and Smart Biomaterials).

OC6. EVALUATION OF THE CHEMICAL COMPOSITION AND BIOLOGICAL ACTIVITIES OF *SIDERITIS SYRIACA*

Alexandra-Mariana Ionescu[1]*, Andreea Veronica Botezatu[1], Ana-Maria Mocanu[1], Anna Busuioc[1], Bianca Furdui[1], Alina Viorica Iancu[2], Marques Fernanda Marujo[3], Costel Vinatoru[4], Geanina Negosanu[4], Rodica Mihaela Dinica[1]*

[1]*Faculty of Sciences and Environment, "Dunarea de Jos" University of Galati, Galati, Romania*
[2]*Faculty of Medicine and Pharmacy, "Dunarea de Jos" University of Galati, Galati, Romania*
[3]*Instituto Superior Técnico, Universidade de Lisboa, Campus Tecnológico e Nuclear, Bobadela, Lisbon, Portugal*
[4]*Genetic and Vegetal Resources Bank (GVRB), Buzau, Romania*
**alexandra.ionescu@ugal.ro, rodica.dinica@ugal.ro*

Sideritis L. (Lamiaceae) comprises more than 150 annual and perennial species and subspecies worldwide, most of which are found as wild-growing plants in countries around the Mediterranean Basin and the Caspian Sea [1]. Numerous studies show the significant pharmacological activities of herba *Sideritis*, justifying its ethnopharmacological uses, and attribute these properties to its rich phytochemical profile.

S. syriaca subsp. syriaca is included as an herbal medicinal product (*Sideritis herba*) in the European Medicines Agency monograph, with indications for relieving cough associated with cold and mild gastrointestinal discomfort. In folk medicine, *Sideritis syriaca* preparations have been used as anti-inflammatory, antimicrobial, antioxidant, analgesic, antirheumatic, and tonic agents [2]. Over time, several studies have been conducted on the chemical composition of this plant, identifying compounds such as polyphenols, flavonoids, diterpenes, essential oils, and anthocyanins [3]. Due to these classes of compounds, *Sideritis syriaca* has demonstrated potential activities, including antioxidant, antimicrobial, antitumor, and antineurodegenerative effects.

This study aimed to investigate *Sideritis* species cultivated in Romania and compare the results with other data on the same species. The objectives of this study were to obtain a series of extracts using green methods and solvents of varying polarities, to determine their chemical composition, and to test them for biological activity.

The extracts were obtained using ultrasound-assisted extraction and through successive extractions with solvents of varying polarities. In this way, the classes of compounds were separated, allowing the study of various biological activities. The solvents ranged from non-polar to polar, used in different volumes and with identical extraction times.

The method used to highlight certain chemical compounds was made possible through various extraction techniques and HPLC chromatography. The chemical and biological activities evaluated in this study included determination of total polyphenol and flavonoid quantities, antioxidant, antitumor, and antimicrobial activities. Antioxidant activity was determined using the DPPH method at various concentrations of the evaluated extracts. Quantifying total polyphenols and flavonoids serves as an important test for confirming the antioxidant potential of the extracts. The antitumor effect was demonstrated using the A2780 cell line—specific to ovarian cancer—and some of the extracts were also tested for their toxicity toward fibroblasts. The efficacy of these

extracts against various bacteria and fungi was tested using the standardized Kirby-Bauer method, in accordance with international guidelines such as those from CLSI and EUCAST. Extracts demonstrating the greatest antimicrobial potential may undergo further testing using other methods, such as the determination of MIC (minimum inhibitory concentration), MBC (minimum bactericidal concentration), and the assessment of bacterial biofilm adhesion.

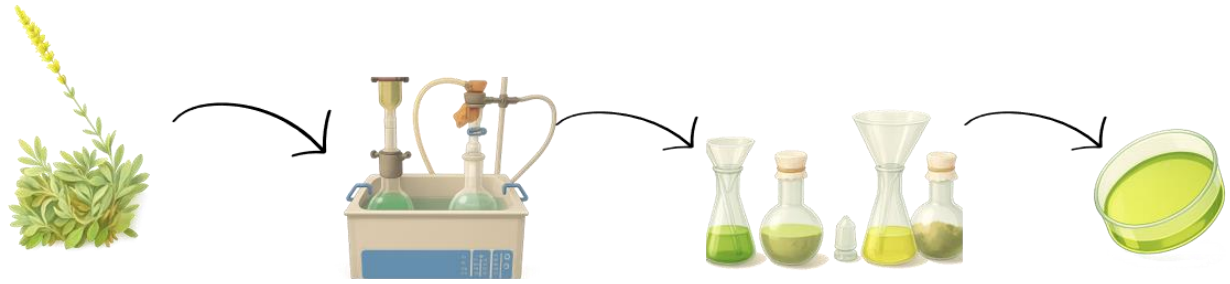


Figure 1. Ultrasound-assisted extraction method.

Thus, based on chromatographic analyses and chemical and biological tests, *Sideritis syriaca* can be considered a promising representative of its family, with significant medicinal properties for the prevention and treatment of acute and chronic diseases like infections, but also with potential for oncological pathologies.

References

[1] C. Kloukina, E. M. Tomou, N. Krigas, V. Sarropoulou, P. Madesis, E. Maloupa, H. Skaltsa, *Ind. Crops Prod.* 2020, 158, 112957.
[2] V. Goulas, V. Exarchou, L. Kanetis, I. P. Gerothanassis, *J. Funct. Foods* 2014, 6, 248.
[3] M. Armata, C. Gabrieli, A. Termentzi, M. Zervou, E. Kokkalou, *Food Chem.* 2008, 111, 179.

Acknowledgment: This work was partially supported by UDJG internal Grant ”Targeted therapeutic molecules, anti-inflammatory and antitumor, isolated from exotic plants acclimatized in Romania”, funding contract no. 7956/31.03.2025.

OC7. LINKER-DEPENDENT CONFORMATIONAL DYNAMICS OF BIS-ACRIDINE ORANGE DYES: INSIGHTS FROM MOLECULAR DYNAMICS AND ENHANCED SAMPLING

Razvan Puf[1]*, Aatto Laaksonen[1,2]
[1]*Petru Poni Institute of Macromolecular Chemistry, Romanian Academy, Iasi, Romania*
[2]*Department of Materials and Environmental Chemistry, Division of Physical Chemistry, Arrhenius Laboratory, Stockholm University, Stockholm, Sweden;*
**puf.razvan@icmpp.ro*

Nucleic acid binding fluorescent dyes serve as effective molecular probes in quantitative polymerase chain reactions (qPCR), nucleic acid detection and fluorescence bio-imaging [1]. Bis-acridine orange dyes (BAO) are particularly useful, as they give a strong and specific signal with little interference with DNA amplification. These dyes consist of two acridine orange molecules interconnected by a molecular linker. Despite enabling intramolecular stacking that may lead to fluorescence quenching, the interaction with double-stranded DNA (dsDNA) might induce conformational changes that result in fluorescence emission.

This work uses atomistic molecular dynamics (MD) simulations and enhanced sampling techniques to investigate the conformational behaviour of three thiophene linked dyes (BAO-1, BAO-2 and BAO-3) compared to a commercially available dye, EvaGreen (EG) [1]. The BAO dyes have different linker lengths and ether oxygen atoms incorporated into their structure. Initially, conventional MD simulations were applied to investigate the interaction of the compounds with dsDNA. Subsequently, umbrella sampling was employed in an explicit aqueous solvent to examine the free energy associated to the destacking of the two acridine orange moieties.

The MD simulations revealed the binding preferences (Figure 1) of each dye for dsDNA, as well as the conformational changes that each structure undergoes. The simulation duration was 1000 ns for EG and 500 ns for the three thiophene-linked dyes. Since these simulations did not provide information regarding the performance of these dyes in qPCR methods, the use of enhanced sampling techniques was further employed.

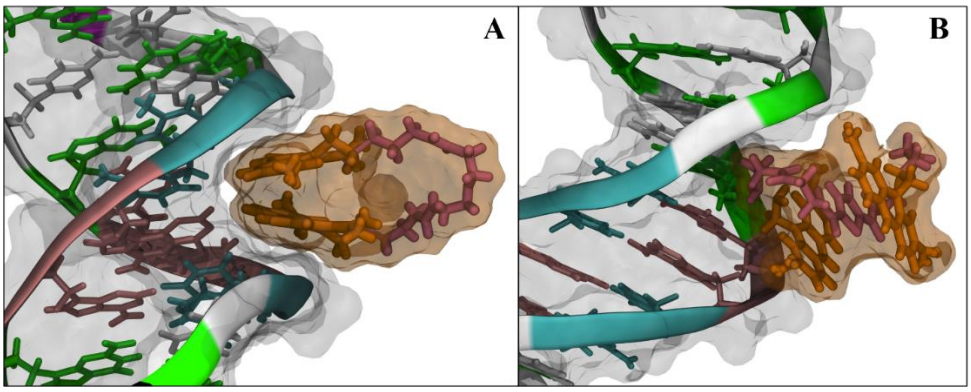


Figure 1. Examples of representative binding conformations of EvaGreen **(A)** and thiophene-linked bis-acridine orange dye **(B)** within the DNA minor groove, showing two-component and three-component stacking arrangements, respectively.

The umbrella method involves pulling the dye across a range of windows (23-26 windows, depending on the dye's structure), with a pull rate of 0.1 nm per window, from 0.4 nm to 2.7-3 nm. Each window was simulated for 40 ns to allow a large sampling of the conformational space and to reach a detailed energy profile.

From this analysis, we observed that all four dyes have a local minimum at approximately 4Å, while BAO-1 and BAO-3 exhibit a second minimum at approximately 7Å. These energy profiles allow us to estimate the free-energy difference required for each dye to transition from the stacked form to the destacked, fluorescent form. The resulting energy differences are shown in Figure 2. They show that the energy required for BAO-3 to transition from the stacked to the destacked form is considerably lower than that of the other dyes, including the commercial dye EG.

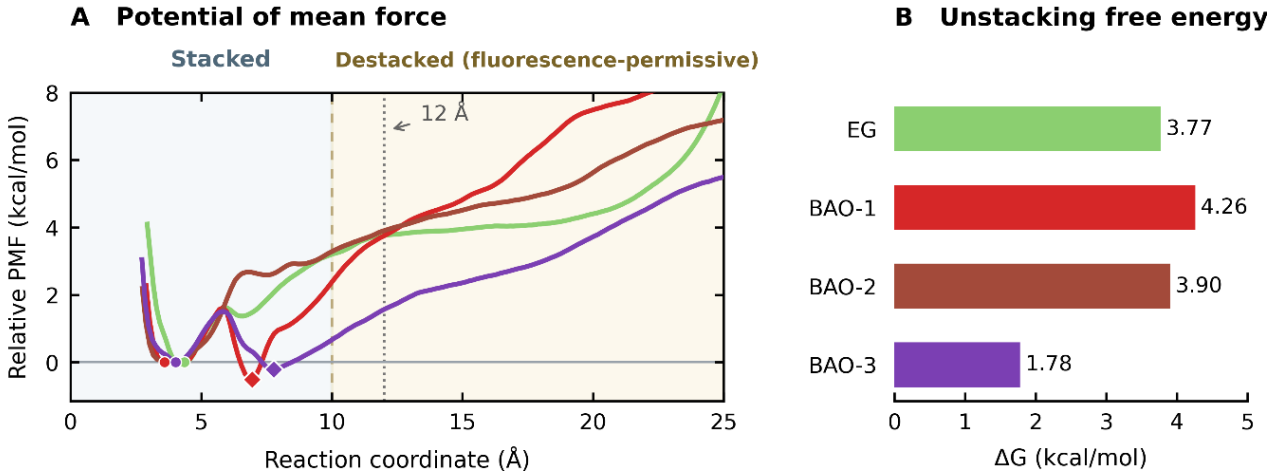


Figure 2. (A) Potential of mean force (PMF) profiles of EG, BAO-1, BAO-2, and BAO-3 obtained from umbrella sampling simulations, describing the separation of the two acridine orange chromophores. The profiles were normalized to the first energy minimum at approximately 4Å. The shaded regions indicate stacked configurations (below 10Å) and destacked, fluorescence-permissive configurations (above 10Å). The dotted vertical line marks the reference distance of 12Å. **(B)** Relative free-energy differences (ΔG) between the first minimum and the configuration at 12Å, showing the lowest energetic cost of chromophore separation for BAO-3 (1.57 kcal/mol). The results obtained in our study, suggest that BAO-3 is the most readily activated fluorophore in the series and a promising alternative to EG.

References

[1] O. Kulyk, A. Krivoshey, O. Kolosova, I. Prylutska, T. Vasiliu, R. Puf, F. Mocci, A. Laaksonen, S. Perepelytsya, D. Kobzev, R. Svoiakov, Z. Tkachuk, A. Tatarets, *J. Mater. Chem. B* **2024**, 12, 11968–11982.

Acknowledgment: This work is supported by European Union's Horizon Europe research and innovation programme under grant agreement **No 101086667**, project **BioMat4CAST** (BioMat4CAST-"Petru Poni" Institute of Macromolecular Chemistry Multi-Scale In Silico Laboratory for Complex and Smart Biomaterials).

OC8. POLYMERIC THIN FILMS FOR RASPBERRY PRESERVATION

Paula Cucu[1,2]*, Irina Apostol[2], Iuliana Spiridon[2], Mihai Mares[1]
[1]*Faculty of Veterinary Medicine, "Ion Ionescu de la Brad" University of Life Sciences, Iasi, Romania*
[2]*Petru Poni Institute of Macromolecular Chemistry, Romanian Academy, Iasi, Romania*
**paula.cucu@iuls.ro*

Guar (Gu)-based thin films with gelatin (Ge) or poly vinyl alcohol (PVA), containing carbon dot (CD) and *Rosa canina* extract (RC), were obtained (Table 1) and investigated as potential active materials for fruits preservation. The obtained materials were characterized in terms of morphology and antimicrobial activity, highlighting their effectiveness as sustainable polymeric films for extending the quality and shelf life of fresh raspberries.

Table 1. Materials composition (dry material) in 100 mL of solution.

Material	Guar	Gelatin	Poly vinyl alcohol	Carbon dot	*Rosa canina* extract
Gu/Ge	0.7 g	0.7 g	-	-	-
Gu/Ge/RC				-	0.1 g
Gu/Ge/CD				0.1 g	-
Gu/Ge/CD/RC				0.1 g	0.1 g
Gu/PVA		-	0.7 g	-	-
Gu/PVA/RC				-	0.1 g
Gu/PVA/CD				0.1 g	-
Gu/PVA/CD/RC				0.1 g	0.1 g

Regarding materials morphology (Figure 1), the Gu/Ge film displayed a relatively continuous lamellar morphology, whereas the incorporation of RC or CD produced increasingly rough, heterogeneous, and irregular surfaces.

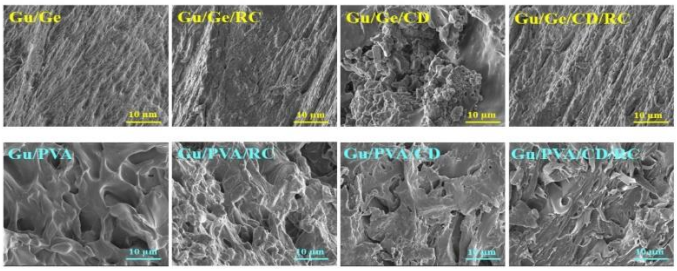


Figure 1. SEM micrographs of the obtained materials.

Similarly, Gu/PVA exhibited a relatively compact structure with irregular cavities, while the addition of RC or CD increased surface roughness and heterogeneity. Overall, these morphological changes may be associated with differences in filler dispersion and matrix–filler interactions [1].

The antimicrobial activity of the obtained films was determined using a quantitative contact method adapted from ISO 22196 (ISO 22196:2011. Measurement of antibacterial activity on plastics and other non-porous surfaces). According to the result presented in Figure 2, it can be observed that the combination of CD with the RC extract show a clear improvement in antimicrobial activity compared with the individual components, suggesting a synergistic or complementary effect between the nanomaterial and the plant-derived compounds. This enhanced activity may be related to the flavonoids present in RC, which can destabilize bacterial membranes and interfere with cellular energy metabolism [2].

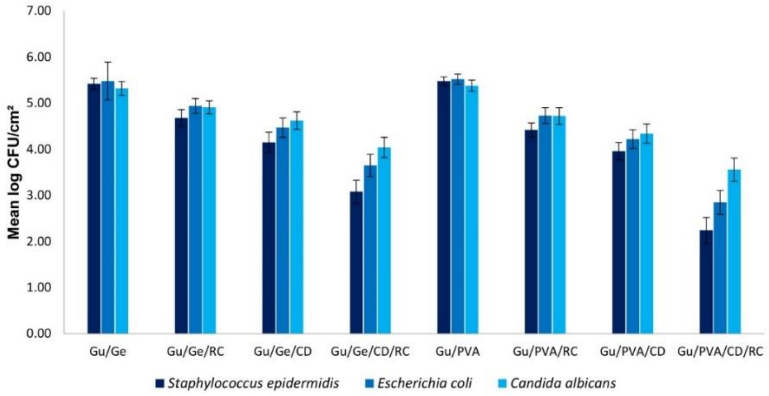


Figure 2. Antimicrobial activity of studied material.

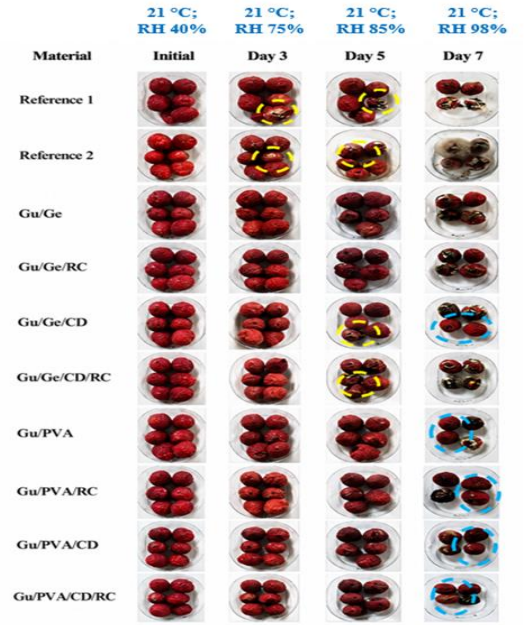


Figure 3. Visual assessment to evidence how well the material preserved raspberries compare to the two references, at different time intervals.

Figure 3 illustrates the visual changes in raspberries stored under different packaging conditions for 7 days. Initially, all fruits were in good condition, showing uniform coloration and no visible signs of fungal contamination. By day 3, the reference samples began to show visible spoilage, with localized mold colonies (yellow dashed circles), which progressively increased by day 5 and became widespread by day 7. The most severe deterioration was observed in the uncoated control, where extensive mold growth. In contrast, the fruits indicated by blue circles, including those packaged with selected Gu/Ge/CD, Gu/PVA, Gu/PVA/RC, Gu/PVA/CD, and Gu/PVA/CD/RC coatings, remained visually free of mold after 7 days of storage period.

The above-mentioned findings support the development of sustainable food preservation strategies and highlight the potential of green composites as promising materials for improving the storage of perishable fruits.

References

[1] Z. Kassab, Y. Abdellaoui, R. Idouhli, M. H. Salim, F. El Bachraoui, El-h. Ablouh, M. El Achaby *Polymers Composites* 2024, 45, 9224-9238.
[2] J. Iyyappan, S. Dhivya, P. Banupriya, V. Sahana, B. Nithisha, *Food and Humanity* 2025, 5, 100926.

OC9. HYBRID COMPOSITE AMYLOPECTIN-*g*-POLY(*N*-ISOPROPYLACRYLAMIDE)/MAGNETITE AND ITS POTENTIAL FOR CONGO RED REMOVAL

Melinda-Maria Bazarghideanu[1]*, Florin Bucatariu[1], Marius-Mihai Zaharia[1], Stergios Pispas[1,2], Marcela Mihai[1]
[1]*Petru Poni Institute of Macromolecular Chemistry, Romanian Academy, Iasi, Romania*
[2]*Theoretical and Physical Chemistry Institute, National Hellenic Research Foundation, Athens, Greece*
**melinda.bazarghideanu@icmpp.ro*

Introduction

Due to the environmental impact of industrial pollutants, especially dye pollutants, a considerable attention has been devoted in the past few years to their removal from wastewater. In the past few years, various physicochemical and biological methods have been used for dye pollutant removal, physical sorption being considered to be one of the most effective and economical techniques. Natural polymers, such as polysaccharides, have attracted significant attention as eco-friendly adsorbents mainly due to their nontoxicity, biodegradability, biocompatibility, and high structural variability [1]. Additionally, their modification with synthetic polymers, especially stimuli-responsive polymers, represents a promising approach for developing suitable materials with improved properties for wastewaters treatment. Amylopectin (AMP), is a highly branched polysaccharide containing numerous free –OH groups, which facilitate its chemical modification with different stimuli-responsive polymers to create new compounds with adapted functionalities. PNIPAM is a water-soluble, thermosensitive polymer with a LCST of 31 – 33 °C. Due to his low biodegradability and considerable biocompatibility is widely used with polysaccharides for the development of materials/hydrogels suitable for wastewaters treatment and biomedical applications [2].

Hybrid materials based on polysaccharides and stimuli-responsive polymers can be integrated with magnetic nanoparticles to form composite materials with enhanced adsorption properties. Magnetite (Fe_3O_4) nanoparticles have a wide variety of application in material science due to their low toxicity, high surface reactivity, and superparamagnetism, while their modification with polymers can further improve their stability. In this context, a novel hybrid graft copolymer based on amylopectin (AMP) and the thermosensitive polymer poly(*N*-isopropylacrylamide) (PNIPAM), was synthesized and used in electro-synthesis of an AMP-*g*-PNIPAM/Fe_3O_4 a composite material. The obtained composite, developed for the adsorption of charged pollutants, was tested for its capacity to interact with Congo Red (CR).

Experimental

The novel graft copolymer AMP-*g*-PNIPAM was obtained by grafting PNIPAM chains onto the AMP backbone via a radical-mediated coupling reaction applying the "*grafting to*" technique. The used the thermosensitive polymer PNIPAM was previously synthesized in our laboratory via RAFT polymerization, following a previously published methodology [3]. The electro-synthesis of the AMP-*g*-PNIPAM/Fe_3O_4 composite was performed via an *in-situ* formation process, during 4 h reaction under continuous electric current, using steel iron electrodes (Figure 1).

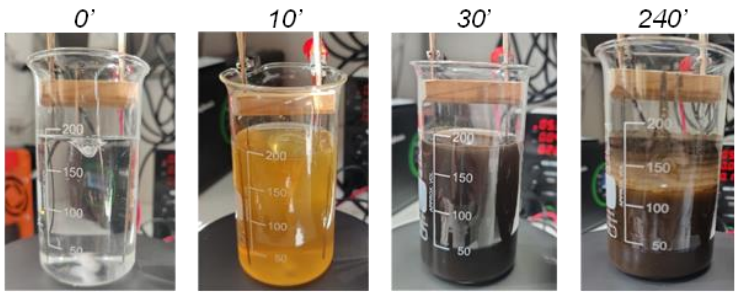


Figure 1. *In-situ* formation of AMP-*g*-PNIPAM/ Fe_3O_4 composite particles during 4 h reaction under electric current.

Results and conclusions

The characterization of the resulting grafted copolymer was performed by ATR-FTIR spectroscopy, confirming the successful grafting of PNIPAM chains onto the AMP backbone. Furthermore, for a better understanding of the self-assembly behavior of the graft copolymer in aqueous solution and its thermal stability, dynamic electrophoretic light scattering measurements were carried out as a function of temperature [2]. The AMP-*g*-PNIPAM/Fe3O4 composite has been characterized by ATR-FTIR spectroscopy ((Figure 2) and X-ray diffraction analysis, followed by an evaluation of its sorption capacity toward CR.

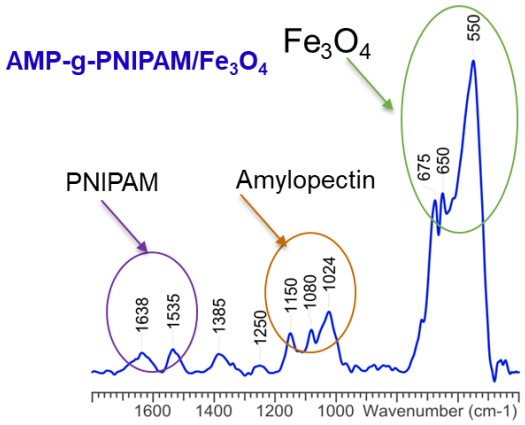


Figure 2. ATR-FTIR spectroscopy of AMP-*g*-PNIPAM/ Fe_3O_4 composite.

Summarizing, the performed analyses confirmed the chemical composition of microparticles, as evidenced by the characteristic infrared bands of Fe_3O_4 and grafted copolymer, as well as by the characteristic magnetite diffraction pattern observed in the XRD diffractograms. The obtained hybrid composite was tested for the capacity to interact with charged molecules, such us CR showing a high capacity for CR loading and release.

References

[1] M.-C. Stanciu, C.-A. Teacă, *Gels* 2024, 10, 243.
[2] M.-M. Bazarghideanu; M.-M. Zaharia; A.-M. Macsim; M. Mihai; S. Pispas, *Biomacromolecules* 2026, 27 (3), 1985–1998.
[3] M.M. Zaharia, F. Bucatariu, M. Karayianni,E.D Lotos, S. Pispas, M. Mihai, *Polymers* 2024,16(10).

Acknowledgment:

This work was supported by a grant of the Ministry of Education and Research, CCCDI - UEFISCDI, project number PN-IV-P6-6.1-CoEx-2024-0056, and by CNCS-UEFISCDI, project number PN-IV-P1-PCE-2023-0738, within PNCDI IV.

OC10. MODULATING CYCLODEXTRIN-NITROXIDE HOST-GUEST INTERACTIONS THROUGH STEREOCHEMISTRY, FUNCTIONALIZATION, AND IONIC STRENGTH

Alexandru G. Bucur[1]*, Jean P. Joly[2], Mihaela Banica[1], Sylvain R. A. Marque[2], Florenta D. Savonea[1], Gabriela Ionita[1]

[1]*Institute of Physical Chemistry - Ilie Murgulescu, Romanian Academy, Bucharest, Romania*
[2]*Aix Marseille Univ., CNRS, ICR, UMR 7273, Marseille, France*
**abucur@icf.ro*

Host-guest interactions involving stable radicals and cyclodextrins (CDs) have been extensively investigated using electron paramagnetic resonance (EPR) spectroscopy, with particular emphasis on the inclusion complexation of nitroxide radicals [1,2]. Among these systems, β-phosphorylated nitroxides are particularly interesting due to the sensitivity of their nitrogen and phosphorus hyperfine splitting constants to changes in the local environment and molecular conformation. In this work, we investigate the inclusion complexes of a series of β-phosphorylated cyclic nitroxide radicals with β-cyclodextrin (β-CD) and γ-cyclodextrin (γ-CD), focusing on the influence of stereochemistry, functionalization, and ionic strength. The investigated compounds include two hydroxymethyl-substituted diastereoisomers (Figure 1) and their corresponding acetate- and adamantane-functionalized derivatives (Figure 2).

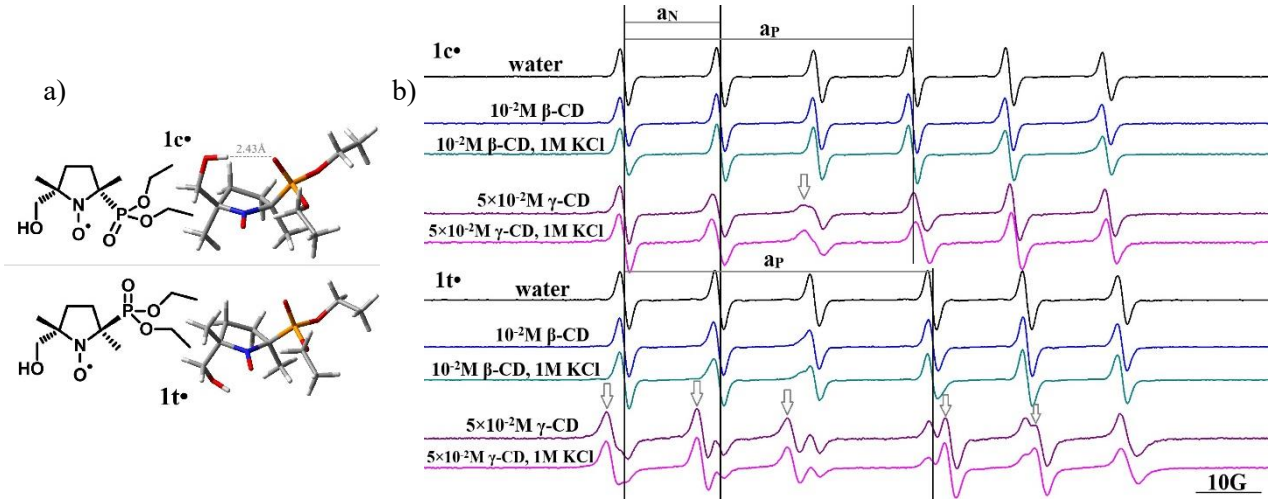


Figure 1. a) Geometries of 1c• and 1t•, b) EPR spectra in water β-CD and γ-CD of the two radicals.

EPR spectroscopy reveals distinct complexation behavior depending on molecular structure and cyclodextrin cavity size [3]. For the hydroxymethyl-substituted radicals, the cis stereoisomer can form an intramolecular hydrogen bond between the hydroxyl group and the phosphoryl moiety, whereas this interaction is not possible for the trans stereoisomer. Consequently, the trans isomer exhibits greater conformational changes upon inclusion and stronger association with γ-CD.

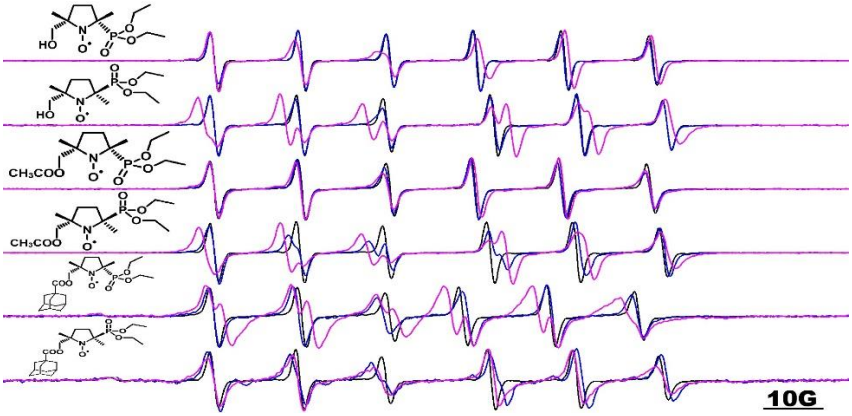


Figure 2. Structures and EPR spectra of the radicals in water (black), β-CD (pink) and γ-CD (blue).

Functionalized isomers determine different patterns of host-guest complexes as revealed by changes in the EPR parameters (Figure 2). Furthermore, increasing potassium chloride concentration enhances the stability of the complexes formed by the hydroxymethyl-substituted radicals (Figure 3), highlighting the contribution of solvation effects to host-guest interactions.

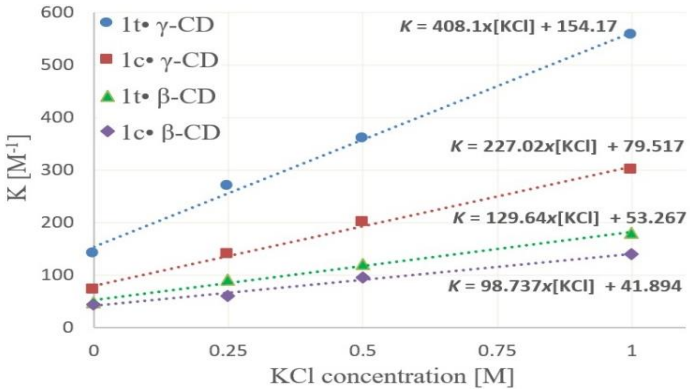


Figure 3. Graphical representation of the association constant value as a function of the KCl concentration.

Overall, these findings demonstrate how stereochemistry, functionalization, and ionic strength influence the molecular recognition of β-phosphorylated nitroxides by cyclodextrins, providing insights into the development of tunable supramolecular spin systems.

References

[1] M. Lucarini and E. Mezzina, in Electron Paramagnetic Resonance, ed. B. C. Gilbert, D. M. Murphy, V. Chechik, Royal Society of Chemistry, Cambridge, 2011, 22, p. 41-70.
[2] E.G. Bagryanskaya, S.R.A. Marque, in Electron Paramagnetic Resonance, ed. V. Chechik and D. M. Murphy, Royal Society of Chemistry, 2017, 25, p. 180-235.
[3] A.G. Bucur, N. Spataru, S.R.A. Marque, L. Preda, J.-P. Joly, G. Audran, M. Trapp, T. Spataru, F. Savonea, G. Ionita, *RSC Advances*, 2026, 16, 21756-21764.

Acknowledgment: PNRR-III-C9-2023-I8 "Chemical host–guest molecular systems for health applications (OMRI for identification of inflammatory pathologies)"

OC11. MODULATING THE THERMORESPONSIVENESS OF INTELLIGENT HYDROGELS FOR BIOMEDICAL APPLICATIONS

Adina Ferariu*, Marieta Constantin, Sanda Bucatariu, Gheorghe Fundueanu
Petru Poni Institute of Macromolecular Chemistry, Romanian Academy, Iasi, Romania
**ferariuadina@icmpp.ro*

Living systems are characterized by the presence of receptors capable of detecting specific stimuli (such as the presence of certain biomolecules or changes in temperature and pH) and transmitting this information to actuators, which trigger regulatory mechanisms essential for maintaining physiological homeostasis. A similar adaptive behavior can be mimicked by polymeric systems, enabling them to sense and respond dynamically to various changes in their surrounding environment [1]. These characteristics make stimuli-responsive polymers suitable for a wide range of biomedical applications, including controlled drug delivery, tissue engineering and the development of sensor-actuator systems [2].

The aim of this study was the design and development of three-dimensional polymer networks capable of responding to multiple stimuli, with thermosensitivity modulated by the presence of specific biomolecules. For this purpose, it was synthesized a new copolymer, poly(N-isopropylacrylamide-co-vinylphosphonic acid), capable of simultaneously responding to multiple stimuli: pH, temperature and the presence of certain biomolecules. Poly(N-isopropylacrylamide) is one of the most widely studied thermoresponsive polymers, exhibiting a lower critical solution temperature (LCST) of approximately 32 °C in aqueous media [3]. Copolymerization with hydrophilic monomers offers a way to adjust this temperature to values closer to physiological temperature. Furthermore, if the incorporated monomer contains weakly acidic or weakly basic groups, the system can also acquire pH sensitivity [4]. Based on this principle, we selected vinylphosphonic acid and synthesized copolymers and hydrogels with varying molar ratios between the two comonomers.

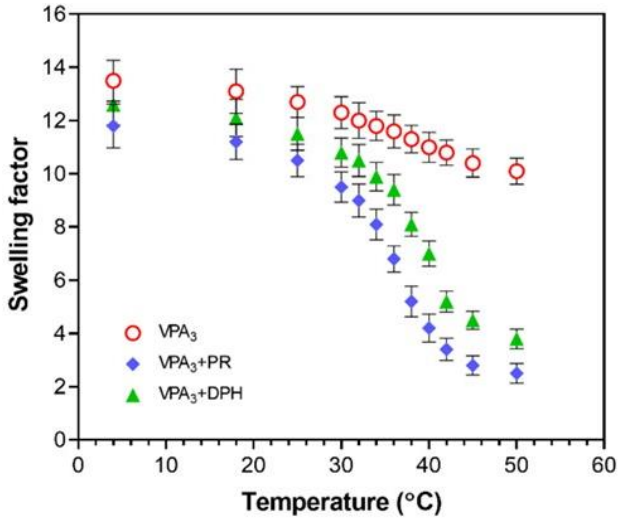


Figure 1. The effect of temperature on the degree of swelling of microgels, in the absence and presence of triggering agents.

Temperature-sensitive hydrogels can be used in biomedical applications if they exhibit a sharp phase transition within a narrow temperature range, close to the human body temperature [5]. Therefore, the transition temperature of the hydrogels was determined in simulated physiological conditions (PBS, pH = 7.4) by monitoring the change in the degree of swelling as the temperature increased (Figure 1). At this pH the phosphonic groups are ionized, much more hydrophilic and as a result the microgels in the absence of triggering agent, do not show thermosensitivity.

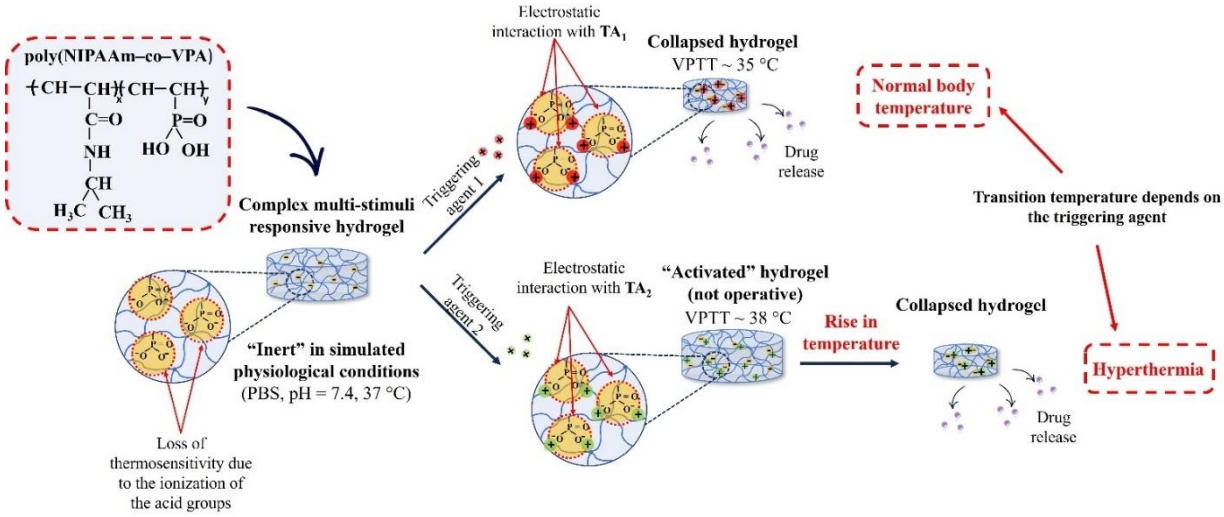


Figure 2. Schematic representation of the hydrogel's operation principle in simulated physiological conditions (PBS, pH = 7.4), at normal body temperature and in hyperthermic conditions.

On the contrary, after the interaction with model biomolecules (propranolol and diphenhydramine), the hydrogel regains its temperature sensitivity. Initially the microgels show a slow decrease in the degree of swelling followed by a sudden volume transition at a temperature close to the LCST of the corresponding linear copolymer. Therefore, the hydrogel is in a "dormant" state in the absence of the biomolecule, but becomes "active" and collapses upon interaction with the triggering agent. Depending on the physicochemical characteristics of the biomolecules, the collapse occurs either at physiological temperature (VPTT = 35.9 °C) or at febrile temperatures (VPTT = 38.5 °C), though in both cases only in the presence of the triggering agent. The operating principle of these materials was presented in Figure 2.

As opposed to traditional thermosensitive hydrogels that collapse when the temperature rises, these systems are only "activated" upon electrostatic interactions with the "triggering agent". As a result, the "triggering agent" is essential for regulating the hydrogel's thermosensitivity. Overall, the hydrogels synthesized in this study show potential as adaptable platforms for biomedical applications by combining multiple stimuli sensitivity with the ability to modulate their thermoresponsive behavior.

References

[1] D. Roy, J.N. Cambre, B.S. Sumerlin, *Prog. Polym. Sci.* 2010, 35, 278–301.
[2] H. Lee, J. Pietrasik, S.S. Sheiko, K. Matyjaszewski, *Prog. Polym. Sci.* 2010, 35, 24–44.
[3] M. Heskins, J.E. Guillet, *J. Macromol. Sci. Chem.* 1968, 2, 1441-1455.
[4] M. Constantin, S. Bucatariu, G. Fundueanu, *Sens. Actuators B: Chem.* 2025, 432.
[5] J. Meid, T. Friedrich, B. Tieke, P. Lindner, W. Richtering, *Phys. Chem. Chem. Phys.* 2011, 13, 3039-3047.

OC12. FLAME-RETARDANT PHOSPHORUS-FUNCTIONALIZED CELLULOSE OBTAINED THROUGH RADICAL GRAFTING OF PHOSPHONATE MONOMERS IN IONIC LIQUID MEDIA

Ayoub Abarkan[1]*, Ridouan El Yousfi[1], Brahim Elmekaoui[2], Nafea Achalhi[1], Abderrahman El Idrissi[1]

[1]*Laboratory of Applied Chemistry and Environment, Faculty of Sciences, Mohamed first University, Oujda, Morocco*

[2]*Materials Science, Energy and Nanoengineering (MSN) Department, Mohammed VI Polytechnic University, Benguerir, Morocco*

**ayoubabarkan98@gmail.com*

Cellulose is an abundant renewable polymer, but its inherent flammability limits its applications where fire safety is required. Upon heating, it releases combustible volatiles, particularly levoglucosan [1]. Moreover, its extensive intra- and intermolecular hydrogen-bonding network restricts the accessibility of hydroxyl groups, making chemical functionalization challenging [2]. To address these challenges, cellulose dissolution in ionic liquid media improves the accessibility of reactive sites, while radical graft polymerization introduces phosphorus-rich side chains to enhance flame retardancy. Unlike conventional substitution reactions that involve the introduction of individual phosphorus-containing groups at cellulose hydroxyl sites, radical graft polymerization enables the growth of phosphonate-rich side chains containing multiple repeating units, thereby achieving higher phosphorus loading and enhanced flame-retardant properties [3].

Herein, a homogeneous radical grafting strategy was developed to introduce phosphonate-rich polymer side chains onto cellulose. Three acrylate-functional phosphonate monomers, diethyl, dibutyl, and diphenyl acryloyloxymethylphosphonate (DEAMP, DBAMP, and DPAMP) were synthesized through the Pudovik reaction followed by acrylation, then graft-polymerized onto cellulose using ammonium persulfate (APS) in a 1-butyl-3-methylimidazolium acetate/dimethyl sulfoxide medium. The effects of monomer and initiator loading, reaction time, and temperature were systematically examined. The most favorable conditions were a monomer/cellulose mass ratio of 10:1, an APS/cellulose mass ratio of 0.1:1, 70 °C, and 6 h. Increasing the monomer concentration initially promoted graft-chain propagation, whereas excessive initiator loading favored radical termination and competing homopolymerization, reducing grafting efficiency. FTIR spectra exhibited characteristic ester carbonyl absorption near 1720 cm^{-1} and phosphorus-related vibrations, while ^{1}H and ^{31}P NMR analyses provided additional evidence of phosphonate incorporation into the grafted cellulose structures. while X-ray diffraction showed loss of the native cellulose crystalline structure. Calculated phosphorus contents reached 12.43, 9.92, and 8.64 wt% for cellulose-g-DEAMP, cellulose-g-DBAMP, and cellulose-g-DPAMP, respectively. TGA revealed increased char residues at 600 °C (58.9, 53.2, and 51.8%, respectively), compared with 9.5% for unmodified cellulose, despite earlier degradation onset. The degradation onset temperatures decreased to 177, 195, and 205 °C for cellulose-g-DEAMP, cellulose-g-DBAMP, and cellulose-g-DPAMP, respectively. This behavior is consistent with earlier phosphorus-assisted dehydration and carbonization, favoring solid residue formation.

Flame-retardant performance was evaluated using microscale combustion calorimetry (MCC), where lower peak heat release rate (pHRR) and total heat release (THR) indicate reduced combustion intensity and overall heat output. MCC showed reductions in pHRR from 257.4 W g^{-1} for cellulose to 55.9, 64.1, and 75.6 W g^{-1}, respectively, while THR decreased from 24.1 to 5.04, 6.25, and 8.01 kJ g^{-1} (Figure 1, Table 1). Furthermore, the temperatures at peak heat release (tPHRR) decreased from 359 °C for unmodified cellulose to 214, 226, and 241 °C for the corresponding grafted products, indicating earlier and substantially less intense heat-release events. This decrease, accompanied by substantially reduced heat release, is consistent with earlier char formation, which limits the generation of combustible volatiles, particularly levoglucosan. The ethyl-substituted derivative exhibited the strongest performance due to higher phosphorus loading, reduced steric hindrance, and lower phosphorus dilution associated with its shorter alkyl chains.

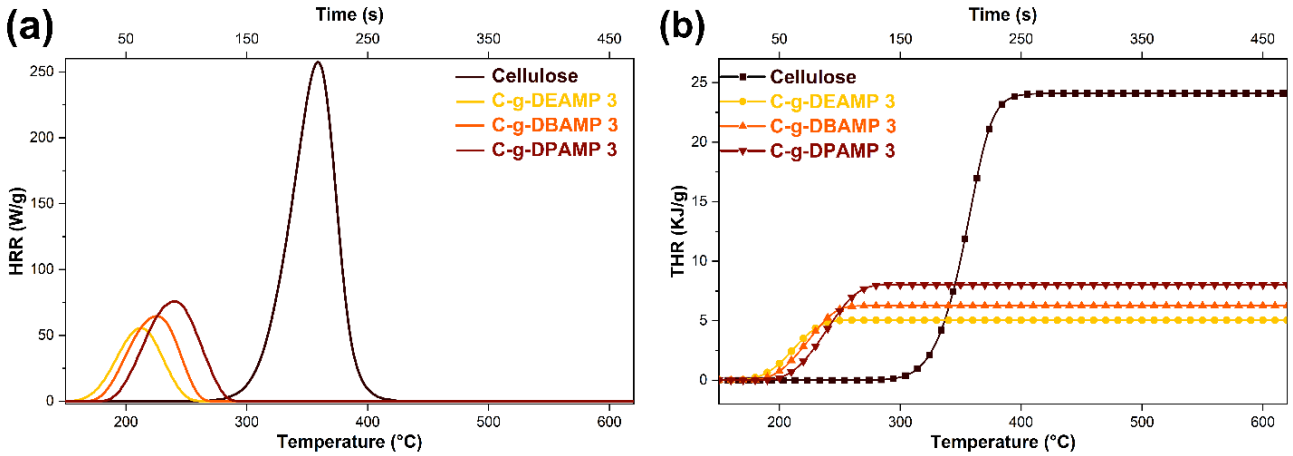


Figure 1. MCC curves of unmodified cellulose and phosphorus-grafted cellulose products: (a) HRR and (b) THR.

Table 1. MCC data of grafted phosphorylated cellulose products.

Products	PHRR (W/g)	tPHRR (°C)	THR (kJ/g)
Cellulose	*257.4*	*359*	*24.1*
C-g-DEAMP	*55.9*	*214*	*5.04*
C-g-DBAMP	*64.1*	*226*	*6.25*
C-g-DPAMP	*75.6*	*241*	*8.01*

References

[1] P. Debiagi, V. Piazza, M. Papagni, A. Beretta, A. Frassoldati, T. Faravelli, *Proc. Combust. Inst*. 2024, 40, 105651.
[2] A. Abarkan, N. Achalhi, R. El Yousfi, R. A. El Idrissi, S. El Barkany, M. Aqil, *Polym. Bull*. 2024, 81, 5375–5402.
[3] B. Liu, H. Zhao, Y. Wang, *Adv. Mater*. 2022, 34, 2107905.

Acknowledgment:
The author gratefully acknowledges the National Center for Scientific and Technical Research (CNRST) for its support. Special thanks are extended to Abdelmonaem Talhaoui for facilitating access to analytical facilities.

OC13. OPTIMIZATION OF DYE ADSORPTION PROCESS FROM SINGLE- AND MULTICOMPONENT AQUEOUS SYSTEMS USING MAGNETIC NANOCOMPOSITES

Maria Andreea Nistor*, Liliana Halip, Simona Gabriela Muntean
"Coriolan Drăgulescu" Institute of Chemistry, Romanian Academy, Timisoara, Romania
** nistor_andreea1990@yahoo.com*

The rapid growth of industrialization, modernization, and consumer demand in recent decades has led to an increasing production and use of dyed products across a wide range of industrial sectors, including the textile, leather, cosmetic, photographic, and food industries [1]. Consequently, substantial volumes of highly colored wastewater are continuously generated, often containing complex mixtures of dyes at varying concentrations [2]. If inadequately treated, the discharge of these effluents into sewage systems or directly into receiving water bodies can have significant adverse environmental impacts [3]. Therefore, the efficient removal of these contaminants from wastewater represents a major environmental priority. Among other methods investigated, adsorption has proven to be one of the most effective approaches in terms of removal efficiency, operational costs, and materials used. The main characteristics of an effective adsorbent include high adsorption capacity, good performance at low pollutant concentrations, regeneration and reuse potential, and low production costs.

In the present study, new efficient magnetic nanocomposites based on activated carbon and iron oxide**, with** different iron oxide/carbon ratios, were synthesized by the combustion method, and investigated as adsorbents for the removal of two anionic dyes (Acid Orange 7, Chromazurol S) and a cationic dye (Methylene Blue) from aqueous solutions. The synthetized materials were characterized in terms of their structural, morphological, textural, and magnetic properties using FTIR spectroscopy, X-ray diffraction (XRD), BET surface area analysis, and magnetic measurements.

Since real wastewater typically contains mixtures of dyes rather than individual dye species, investigating dye removal from multicomponent systems provides a more realistic assessment of adsorbent performance under practical treatment conditions. To determine the optimal operating conditions for achieving maximum dye removal efficiencies in single-, binary, and ternary systems, optimization studies were conducted using factorial experimental design and Response Surface Methodology (RSM). These statistical approaches enabled the quantitative assessment of the linear, quadratic, and interaction effects of the operating parameters. The effects of pH, initial dye concentration, and adsorbent dosage were investigated in single-dye systems, whereas the influence of pH and the concentrations of competing dyes was evaluated in binary and ternary systems.

The combined application of factorial design and RSM enabled the systematic evaluation of interactions between experimental variables and the identification of optimal operating conditions for maximizing dye removal. This approach also reduced the number of experiments required, thereby saving time and resources.

The optimal operating conditions were established based on contour plots and three-dimensional (3D) response surface representations generated for each pair of factors included in the statistical model.
The developed models were experimentally validated, yielding high removal efficiencies exceeding 93% for AO7 and MB and reaching up to 72% for Ch-S in single-dye systems. Remarkable removal efficiencies were also achieved in binary systems, reaching up to 85% for AO7, 95% for MB, and 70% for Ch-S. In ternary systems, removal efficiencies exceeded 73% for AO7, 79% for MB, and 59% for Ch-S. Notably, these results were obtained under relatively mild operating conditions, namely at the natural pH of the solutions and room temperature (25°C), highlighting the high adsorption performance of the synthesized magnetic nanocomposites in multicomponent aqueous systems even under normal working conditions.

In order to evaluate the regeneration and reuse performance of the synthesized magnetic nanocomposites, the study was extended to seven consecutive adsorption-desorption cycles in both single- and binary-dye systems. Removal efficiencies remained above 70% for Acid Orange 7 and Methylene Blue and above 50% for Chromazurol S in both types of systems, even after seven adsorption-desorption cycles, demonstrating the potential of the synthesized materials for repeated use.

Overall, the results demonstrate that the synthesized magnetic nanocomposites are effective and potentially sustainable adsorbents for the removal of both anionic and cationic dyes from aqueous media. The combination of high removal efficiencies, statistical optimization of the adsorption process, effective performance in multicomponent systems, and good regeneration and reuse potential highlights the promise of these materials for practical applications in the treatment of dye-containing wastewater.

References

[1] H. Mohammadi, E. Nekobahr, J. Akhtari, M. Saeedi, J. Akbari, F. Fathi, *Toxicol*. 2021, 8, 331-336.
[2] R.Al-Tohamy, S.S. Ali, F. Li, K.M. Okasha, Y.A. Mahmoud, T. Elsamahy, H. Jiao, Y. Fu, J. Sun, *Ecotoxicol. Environ. Saf*. 2022, 231, 113160.
[3] J. Fito, M. Abewaa, A. Mengistu, K. Angassa, A.D. Ambaye, W. Moyo, T. Nkambule, *Sci Rep*. 2023, 13, 5427.

Acknowledgment:

This work was partially supported by a grant of the Ministry of Education and Research, CCCDI - UEFISCDI, through the project Center of Excellence in water management, materials, by-products and waste valorization for circular bioeconomy implementation, proposal number PN-IV-P6-6.1-CoEx-2024-0056, contract 6 CoEx/02.06.2026, within PNCDI IV, and by Program no 2, Project no. 2.2 from the “Coriolan Dragulescu” Institute of Chemistry Timisoara.

OC14. *IN SILICO* EVALUATION OF ADME/TOX PROFILES USING MULTIPLE ONLINE PREDICTION TOOLS

Lucia Gradinaru*, Alina Bora, Luminita Crisan
"Coriolan Dragulescu" Institute of Chemistry, Romanian Academy, Timisoara, Romania
**lgradinaru@acad-icht.tm.edu.ro*

Early assessment of absorption, distribution, metabolism, excretion and toxicity (ADME/Tox) is essential in computer-aided drug discovery, since unfavorable pharmacokinetic or toxicity profiles are a major cause of compound attrition [1]. In silico tools offer a rapid, low-cost means of estimating these properties, but their predictions may differ owing to differences in training datasets, algorithms and decision thresholds. Comparing complementary platforms therefore allows a broader assessment and helps identify endpoints requiring further investigation. This study characterizes the ADME/Tox profiles of nine compounds, selected by pharmacophore-based virtual screening of three chemical databases, to establish a basis for their subsequent molecular-level investigation.

The compounds were evaluated with four freely accessible platforms: ADMETlab 3.0 [2], SwissADME [3], BioDockify [4], and Deep-PK [5]. The assessment covered physicochemical descriptors, drug-likeness (Lipinski [6], Veber [7], and Egan [8] rules, where supported), and absorption, distribution, metabolism, excretion, and toxicity endpoints, including gastrointestinal absorption, blood–brain barrier (BBB) permeation, transporter interactions, cytochrome P450 (CYP450) inhibition and substrate recognition, and toxicity alerts. Because the platforms differ in methodology, predictions were compared endpoint by endpoint, considering agreement and platform-specific discrepancies rather than treating outputs as interchangeable.

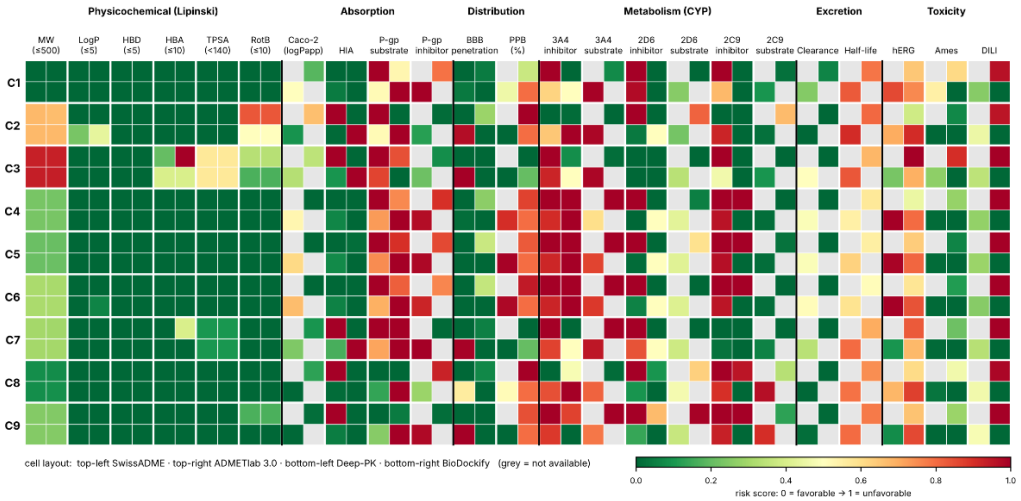


Figure 1. Integrated workflow for multi-platform ADME/Tox profiling.

The comparative ADME/Tox assessment (Figure 1) revealed the following: (i) *Physicochemical properties and drug-likeness.* Molecular weight exceeded 500 Da for eight of the nine compounds, most markedly for C2 (≈635 Da) and C3 (≈687 Da). C3 and C7 additionally showed high polarity (TPSA > 140 Å²), and C3 exceeded the hydrogen-bond acceptor limit. Lipophilicity, hydrogen-bond donor counts, and rotatable-bond profiles were

otherwise largely acceptable. Descriptor values were consistent across platforms, whereas logP estimates varied, notably for C2. (ii) *Absorption.* Gastrointestinal absorption was generally predicted to be favorable, although SwissADME and BioDockify predicted low absorption for the larger, more polar compounds (C3 and C7). Caco-2 permeability predictions varied between compounds, and P-glycoprotein (P-gp) substrate and inhibitor predictions were inconsistent across platforms, with several compounds showing potential efflux liabilities. (iii) *Distribution.* BBB permeation predictions diverged substantially between platforms, particularly for C2, C3, C7, and C9, indicating uncertainty in their predicted CNS exposure. Plasma protein binding also varied, with very high binding (>95%) predicted for C4–C6, implying a low unbound fraction. (iv) *Metabolism and excretion.* CYP3A4 inhibition was predicted for C4–C9, most consistently for C4–C6, which also showed CYP2C9 inhibition signals; CYP2D6 predictions were largely platform-dependent. Substrate predictions were more variable than inhibition predictions, underscoring the distinction between enzyme inhibition and substrate recognition. Clearance was predominantly predicted to be low to moderate, whereas half-life estimates were more variable and often less favorable, which should be considered during prioritization. (v) *Toxicity.* hERG inhibition emerged as the main liability, with C1, C2, C4–C6, and C8 receiving unfavorable predictions across several platforms. Ames alerts were limited (C1 and C3), whereas drug-induced liver injury (DILI) predictions were strongly platform-dependent. Both hERG and DILI therefore warrant particular attention in subsequent evaluation. (vi) *Consensus-based prioritization.* Physicochemical properties and absorption were comparatively favorable, whereas BBB permeation, CYP450 interactions and toxicity were the main sources of concern. C1 had the most favorable physicochemical profile but carried hERG and Ames alerts. C3 and C7 showed limited predicted absorption owing to high polarity, with fewer CYP450 alerts. C4–C6 were close analogues sharing the same liabilities (CYP450 inhibition, high plasma protein binding, P-gp interactions and hERG), while C8 and C9 showed the most favorable P-gp profiles and more moderate CYP3A4 risk. Discrepant predictions were treated as uncertainties rather than exclusion criteria.

These predictions remain computational estimates and should be interpreted within the applicability domains of the respective models. The prioritized compounds will undergo molecular docking, molecular dynamics (MD) simulations and density functional theory (DFT) calculations to examine molecular recognition, complex stability and electronic properties, respectively. Experimental validation will be required to confirm the predicted ADME/Tox profiles.

References

[1] M.E. King, M.V.F. Guzman, M.B. Ross, *Nanoscale* 2022, 14, 602-611.
[2] G. Mikami, F. Grosu, S. Kawamura, Y. Yoshida, G. Carja, Y. Izumi, *Appl. Catal. B* 2016, 199, 260-271.
[3] D. Gilea, E.M. Seftel, T. Van Everbroeck, G. Ababei, P. Cool, G. Carja, *Catalysis Today* 2024, 425, 114342.

Acknowledgment: This work was supported by Program no. 1 of the "Coriolan Dragulescu" Institute of Chemistry, Timisoara.

OC15. BORONATE-GUANOSINE-ASSISTED GROWTH OF INTERCONNECTED GOLD NANOASSEMBLIES ON DEXTRAN-COATED IRON OXIDE NANOPARTICLES FOR MAGNETICALLY RECOVERABLE SERS

Tecla Dulgheriu*, Elena-Laura Ursu, Alexandru Rotaru
Petru Poni Institute of Macromolecular Chemistry, Romanian Academy, Iasi, Romania
** dulgheriu.tecla@icmpp.ro*

Introduction

Gold nanostructures are used as SERS substrates for chemical detection and bioimaging [1,2]. In real samples, SERS analysis is limited by low analyte concentration, matrix interference, poor signal reproducibility and difficult substrate handling [3]. Fe_3O_4-Au composites allow magnetic separation, washing and preconcentration of the analyte before the Raman measurement [4]. Branched, interconnected ("black") gold shows broadband extinction in the visible and near-infrared. Hyperbranched black gold was previously prepared by gold growth on dextran templated by guanosine quartets [5]. In this work, the method was applied to dextran-coated superparamagnetic iron oxide nanoparticles (Dex-SPIONs), in order to combine the broadband plasmonic response of black gold with magnetic separation. The resulting substrate was tested for the detection of methylene blue (MB), a cationic phenothiazine dye used in aquaculture to prevent and treat fish diseases. MB is not authorised in the EU for food-producing animals, including farmed fish intended for human consumption [6], so its residues have to be monitored at low concentrations in water and aquatic products. Magnetic SERS substrates are suited to such diluted and complex samples, because the analyte can be concentrated before the measurement [4].

Experimental

Dex-SPIONs were obtained by alkaline co-precipitation of Fe^{2+}/Fe^{3+} salts in dextran solution. Guanosine was bound to the dextran shell through boronate esters formed with benzene-1,4-diboronic acid. Gold was then grown on the particles from $HAuCl_4$ in alkaline medium at elevated temperature. The final product was washed by magnetic separation and analysed in detail by XRD, DLS, ζ-potential, TEM/STEM, UV-Vis spectroscopy and VSM. For SERS investigations, the hybrid particles were incubated with MB, collected magnetically and measured at 633 nm.

Results and discussion

Low $HAuCl_4$ amounts gave incomplete gold growth, and high amounts lowered the fraction recovered by the magnet, while an intermediate amount was used in all further experiments. XRD showed the reflections of fcc gold and of the spinel iron oxide, so the magnetic core was preserved. Before controlled gold growth on the surface of Dex-SPIONs, TEM showed small, rounded nanoparticles. After the Au deposition, elongated, worm-like structures were observed (Figure 1). These structures were connected side-by-side into branched assemblies, and the junctions between them could act as SERS hot spots. The UV-Vis spectra showed broad extinction from the visible to the near-infrared, without the 520 nm band characteristic for isolated gold spheres. After gold

growth, the ζ-potential changed from +29.94 to −28.72 mV and the saturation magnetization decreased from 19.79 to 12.38 emu/g because of the added non-magnetic mass, but the particles were still separated quickly with a magnet.

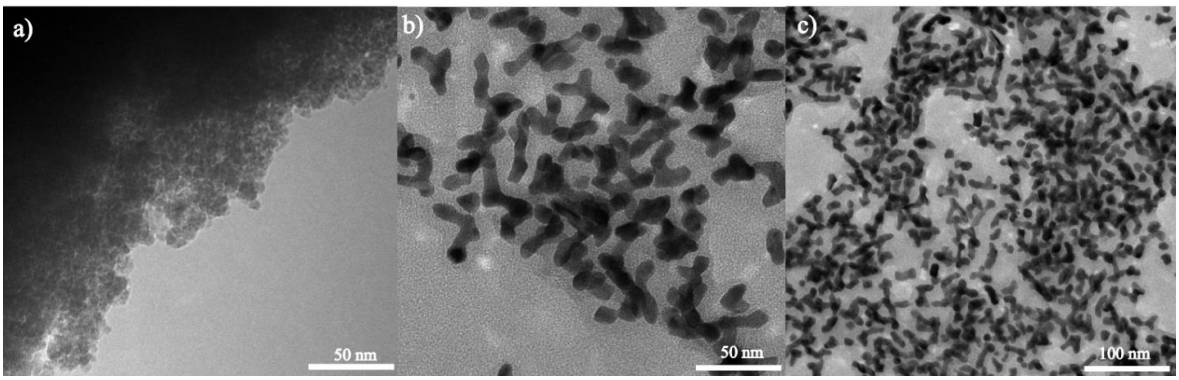


Figure 1. TEM images of (a) Dex-SPIONs and (b, c) magnetically recovered Au-Dex-SPIONs.

The characteristic MB band at 1623 cm^{-1} was used for quantification. Its intensity increased with MB concentration up to 10^{-4} M and decreased at higher concentrations, probably due to saturation of the most active sites. The log-log plot of intensity versus concentration was linear from 10^{-8} to 10^{-4} M ($R^2 = 0.968$). The detection and quantification limits calculated from the blank signal were 2.60×10^{-9} M and 1.22×10^{-8} M. The detection limit was 16–23 times lower than the values reported for a similar Fe_3O_4-Au substrate [7]. The RSD over 30 measurement points was 9.4%, and the signal was almost unchanged after 30 days of storage. The signal was recovered after washing in three reuse cycles. Interference was tested with compounds that may occur in aquaculture water. At a 100-fold higher concentration than MB, all of them gave much weaker signals at 1623 cm^{-1}. Under these conditions, crystal violet gave the strongest response, but its signal remained below that of MB.

Conclusions

Boronate-guanosine-assisted gold growth was transferred to dextran-coated magnetic nanoparticles. The Au-Dex-SPIONs show broadband plasmonic extinction, can be separated magnetically and detect MB at nanomolar concentrations with good reproducibility, stability and reusability.

References

[1] E.L. Ursu, F. Doroftei, D. Peptanariu, M. Pinteala, A. Rotaru, *J. Nanopart. Res.* 2017, 19, 181.
[2] M.C. Sardaru, N.L. Marangoci, R. Palumbo, G.N. Roviello, A. Rotaru, *Molecules* 2023, 28, 3561.
[3] S. Sloan-Dennison, G.Q. Wallace, W.A. Hassanain, S. Laing, K. Faulds, D. Graham, *Nano Convergence* 2024, 11, 33.
[4] T.T. Nguyen, S. Lau-Truong, F. Mammeri, S. Ammar, *Nanomaterials* 2020, 10, 294.
[5] E.L. Ursu, M.C. Sardaru, C. Ursu, A. Arvinte, D. Peptanariu, R. Bilyy, G. Bila, E. Bila, V. Antonyuk, I. Tiginyanu, A. Rotaru, *Int. J. Biol. Macromol.* 2026, 363, 152191.
[6] EFSA, A. Penninks, K. Baert, S. Levorato, M. Binaglia, *EFSA J.* 2017, 15, e04920.
[7] I.B. Muslimova, A.B. Khairusheva, K.A. Izbassar, Z.A. Bekbol, L.I. Lissovskaya, I.V. Korolkov, *Eurasian J. Chem.* 2026, 31, 53-65.

Acknowledgment: This work was supported by a grant of the Ministry of Research, Innovation and Digitization, CNCS/CCCDI - UEFISCDI, project number PN-IV-P8-8.1-PRE-HE-ORG-2023-0048, within PNCDI IV.

OC16. CYANOBACTERIA SPIRULINA MEDIATED BIOSYNTHESIS OF COPPER-BASED HYBRID MATERIALS AND PHOTOCATALYTIC DEGRADATION OF DYE INDIGO CARMINE

Cristina Bostaca*, Larisa-Maria Petrila, Marcela Mihai
Petru Poni Institute of Macromolecular Chemistry, Romanian Academy, Iasi, Romania
**bostaca.cristina@icmpp.ro*

The name "spirulina" is a common term used to refer to a group of cyanobacterial species, with *Arthrospira platensis* being the most widespread and most commonly used species. Spirulina grows primarily in alkaline and saline lakes. It grows rapidly, and its energy and water consumption relative to the amount of biomass produced is low [1]. Spirulina contains many components, such as proteins 55–70%, carbohydrates 15–20% (mainly polysaccharides), lipids 5–7%, vitamins less than 1%, minerals 7%, and pigments (Figure 1) [2]. Most of the protein is found in the form of phycobiliproteins: phycocyanin, allophycocyanin, and phycoerythrin. Spirulina contains three main classes of pigments: chlorophylls, carotenoids, and phycobiliproteins. Phycobiliproteins are protein-pigment complexes, and the most important one is C-phycocyanin, a blue pigment specific to cyanobacteria [3].

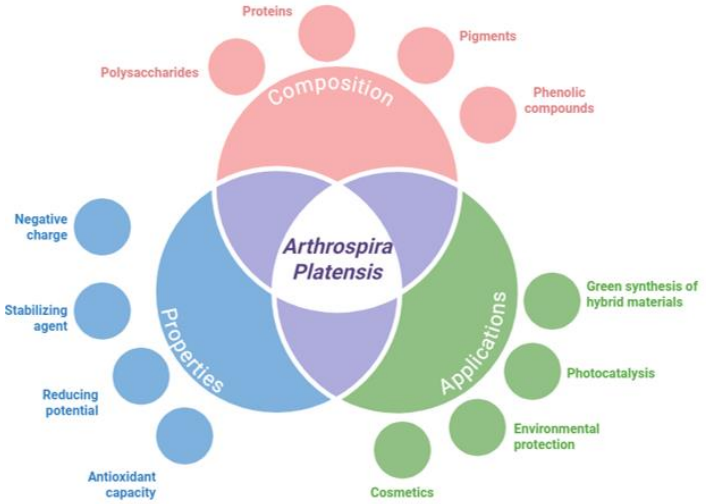


Figure 1. Composition, properties and applications of *Arthrospira plantensis.*

Spirulina can be used in various fields, including cosmetics, food, medicine, environmental protection, and catalytic applications. In catalytic processes, the spirulina biomass is used in the preparation of composite sorbents or for the preparation of metal nanoparticles, which it stabilizes, or acts as a reducing agent in their synthesis [4]. A key advantage of such materials is their easy recovery and reusability, which is particularly of interest in the context of water remediation, where such materials can be used as sorbents or catalysts.

The purpose of this study is to produce hybrid materials based on spirulina and copper and to test their effectiveness in the photodegradation of indigo carmine dye, which is an organic dye commonly found in wastewater. Firstly, the optimization of spirulina biomass solubilization was performed, testing three methods of cell disruption: mechanical agitation, an ultrasonic bath, and probe sonication. The experimental data show that probe sonication for 3 minutes was the most effective: it solubilized 95% of the biomass, and the soluble protein content reached 70.5%. The

protein content was determined using the Hartley-Lowry method and quantified by UV-Vis spectrophotometry [5]. Furthermore, the UV-Vis spectrum of the spirulina extract confirmed the presence of active compounds such as proteins, chlorophyll a, carotenoids, and c-phycocyanin. The stability of the dispersions and the self-assembly of spirulina components at different pH values were tested using techniques such as dynamic light scattering and zeta potential measurements. These analyses were used to monitor aggregates formation, hydrodynamic size distribution, and changes in surface charge. The antioxidant activity of the extract was evaluated by its ability to decolorize the 2,2'-azino-bis(3-ethylbenzothiazoline-6-sulfonic acid) (ABTS) radical.

To investigate the potential of spirulina bio-compounds to act as a matrix in the preparation of hybrid materials, the interaction between the polysaccharides and proteins present in the plant extract, pectin and Cu_2SO_4 was studied. The interaction between the components of spirulina, pectin and copper ions promoted the formation of hybrid structures of varying sizes depending on the ratio of plant extract and polysaccharide to copper ions, as evaluated using the dynamic light scattering technique. The long-term stability of the nanomaterials was assessed through zeta potential measurements conducted over an 18-day period. The results show that the hybrid materials maintain very good colloidal stability. Furthermore, DLS analysis confirms that the size distribution profile does not undergo significant changes during the 18-day storage period, demonstrating the absence of agglomeration phenomena. The morphology of the hybrid materials was analyzed using transmission electron microscopy (TEM). The TEM images show how the ratios between the components influence the appearance of the particles. To evaluate the potential of hybrid materials to act as photocatalysts, the degradation of indigo carmine dye was studied. It was observed that all the materials studied exhibited photocatalytic activity, with the degradation time varying depending on the mixing ratio between the components of the hybrid materials.

In conclusion, this study analyzed the main physicochemical and biological characteristics of spirulina extract, as well as the role of the bio-compounds in this extract in the preparation of copper-based hybrid materials. Various types of hybrid materials were obtained, characterized by dimension, morphology, and surface charge that depend on the preparation method and the ratio of the components.

References

[1] M. Chang, K. Liu, *Int. J. Food Sci. Technol.* 2024, 59, 1197-1212.
[2] K.V. Ketu, A.U. Akwo, M. Innocent, C.T. Aphrodite, *Food Chem. Adv.* 2026, 10, 101235.
[3] T. Sibiya, T. Ghazi, A. Chuturgoon, *Nutrients* 2022, 14, 3076.
[4] H. Kelebek, T. Uzlasir, H.K. Sasmaz, *Food Nutr.* 2025, 1, 10033.
[5] O.H. Lowry, N.J. Rosebrough, A.L. Farr, R.J. Randall, *J. Biol. Chem.* 1957, 193, 265-275.

Acknowledgment:

This work was supported by a grant of the Ministry of Education and Research, CCCDI - UEFISCDI, through the project Center of Excellence in water management, materials, by-products and waste valorization for circular bioeconomy implementation, proposal number PN-IV-P6-6.1-CoEx-2024-0056, contract 6 CoEx/02.06.2026.

OC17. HYDROPHOBIC NATURAL DEEP EUTECTIC SOLVENT-BASED MATERIALS AS SOLUBILIZING AND DELIVERY VEHICLES FOR FERULIC ACID

Catalin Chersan*, Raluca Nicoleta Darie-Nita, Oana Ursache, Marin-Aurel Trofin, Sergiu Coseri
Petru Poni Institute of Macromolecular Chemistry, Romanian Academy, Iasi, Romania
** chersan.catalin@icmpp.ro*

Menthol (M) is a cyclic monoterpene alcohol [1] with a wide range of biological effects such as anti-inflammatory, immunomodulatory, antioxidant, cytoprotective, antifungal, antiviral, and anticancer effects [2]. It is mainly found in Mentha essential oils, and it is a cheap compound with low solubility in water [1]. Thymol (T) is a naturally occurring monoterpene phenol, extracted from *Thyme.* The compound exhibits a hydrophobic nature and a broad spectrum of biological properties such as antioxidant, anti-inflammatory, local anaesthetic, antinociceptive, cicatrizing, antiseptic, antibacterial, and antifungal [3]. Both compounds can lead to the formation of a natural deep eutectic solvent (NADES) with good solubilization capacity of poorly water-soluble compounds [4].

Polysaccharides are naturally occurring polymers that come from renewable sources and are known for their biocompatibility, biodegradability, low toxicity, and eco-friendliness, properties that make them more attractive for medical research. They are often used in the pharmaceutical industry as suspending, binding, and thickening agents [5]. Hydroxypropyl cellulose (HPC) is a cellulose ether made by reaction of cellulose with propylene oxide. It is a semi-synthetic polymer with a broad spectrum of applications, especially in the pharmaceutical and food industry [6]. Although M-T NADES-based systems have been reported, they have mainly been obtained using low molecular weight gelators; studies employing polysaccharides as the gelling matrix remain scarce [7][8].

In this study, we intend to obtain a novel material that will combine the biological effects and solubility enhancement properties of a hydrophobic NADES based on M and T with the biocompatibility and structural properties of an HPC matrix. Ferulic Acid (FA) is a natural compound found in the seeds, leaves, and roots of different vegetables, fruits, and cereals. From a pharmaceutical point of view, it has a broad spectrum of biological effects such as antimicrobial, antioxidant, anticancer, and anti-inflammatory properties. The major drawback of this compound is the low water solubility, low bioavailability, and instability [9], limitations that make it a suitable model compound for our material. To this end, a hydrophobic NADES based on M and T was prepared in three different molar ratios. The formation of the hydrogen-bond network was confirmed by ^{1}H NMR and FTIR spectroscopy. The thermal stability of the solvent was assessed using thermogravimetric analysis (TGA), and its homogeneity was examined using polarized optical microscopy (POM). The novel materials were

Synthesized by simply adding HPC in different concentrations (from 5% to 25%), heating at 80 ^{o}C and stirring until homogeneous (Figure 1). The novel materials were not only rheologically characterized, but also by POM and FTIR spectroscopy. The solubility of FA in the three different

molar ratios was assessed using UV-VIS spectroscopy reaching a value of 9,87±0,17 mg/g of NADES, which indicates a good solubilization capacity of the solvent.

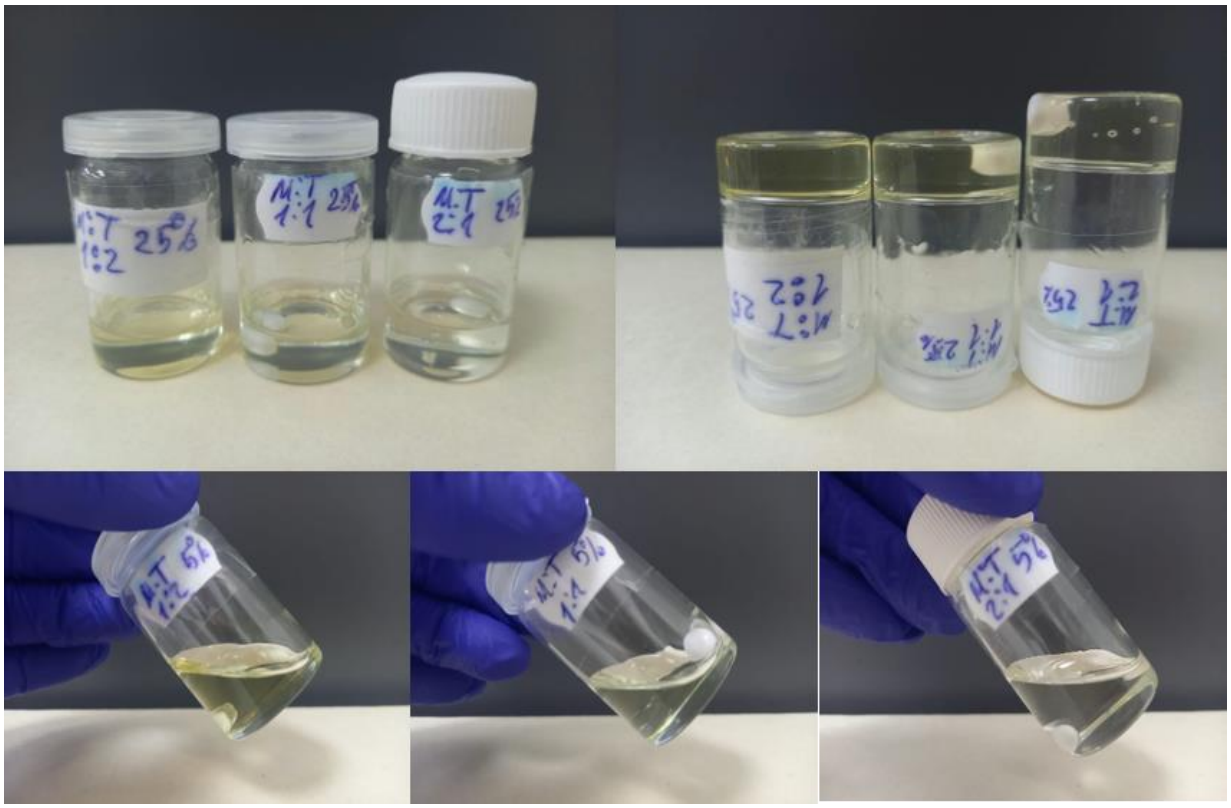


Figure 1. Appearance of the HPC-based materials (5% and 25% w/w HPC) prepared with different M-T molar ratios.

References

[1] M. Lindokuhle, K. Tumba, N. Nkosi, T. Ngema, *Chem. Thermodyn. Therm. Anal.* 2026, 21, 100249.
[2] K.H.C. Baser, E. Erdag, I.C. Haskologlu, *Nat. Prod. Commun.* 2025, 20, 1-11.
[3] A. Marchese, I.E. Orhan, M. Daglia, R. Barbieri, A. di Lorenzo, S.F. Nabavi, O. Gortzi, M. Izadi, S.M. Nabavi, *Food Chem.* 2016, 210, 402-414.
[4] M.F. Negro, P.S. Bustos, L. Bellezze, M.G. Ortega, J. Echeverría, M.F. Silva, M.A. Peralta, *Front. Pharmacol.* 2025, 16, 1643472.
[5] M. Tudu, A. Samanta, *Eur. Polym. J.* 2023, 184, 111801.
[6] D.M.M. Fertonani, B.S. Pedrosa, W.G. Silva, J.M.F. Rubim, J.C. Rinaldi, E.M. Girotto, M.R. Guilherme, A.W.A. Rinaldi, *J. Appl. Polym. Sci.* 2026, 143, e58090.
[7] D.J. Connolly, N. Blagden, L. Seton, J.W. Steed, *Cryst. Growth Des.* 2025, 25, 7834-7844.
[8] V. Vanoli, J. Pietrowska, G. de Araujo Lima e Souza, M.E. di Pietro, F. Briatico Vangosa, A. Mele, F. Castiglione, *ACS Appl. Eng. Mater.* 2024, 2, 388-396.
[9] J.R. Purushothaman, Md. Rizwanullah, *Cureus* 2024, 16, e68063.

Acknowledgment: This work was supported by a grant of the Ministry of Education and Research, CNCS – UEFISCDI, project number PN-IV-P1-PCE-2023-0558, within PNCDI IV.

OC18. RIM-SELECTIVE OLIGOCAPROLACTONE SUBSTITUTION OF β-CYCLODEXTRIN AS A STRATEGY FOR TAILORING NANOSPONGE PROPERTIES

Marius Prodan*, Valeria Harabagiu, Diana-Andreea Blaj, Cristian Peptu
Petru Poni Institute of Macromolecular Chemistry, Romanian Academy, Iasi, Romania
**prodan.marius@icmpp.ro*

Cyclodextrin-based nanosponges (NS) are three-dimensional crosslinked networks of cyclodextrin (CD) molecules, investigated for their ability to encapsulate various compounds [1]. Their properties depend on several structural factors, including the chemical nature of the CD derivatives and the crosslinking agents employed [2]. This study investigates the possibility of tailoring the properties of NS by controlling the substitution pattern of β-cyclodextrin modified with ε-caprolactone chains (β-CDCL). The possibility of obtaining β-cyclodextrin (β-CD) derivatives with preferential substitution at different rims through the organocatalyzed ring-opening oligomerization of ε-caprolactone has previously been demonstrated [3]. In the present study, two β-CDCL derivatives were synthesized, differing in the distribution of oligo(ε-caprolactone) chains: randomly substituted β-CDCL (β-CDCL-R) and β-CDCL selectively substituted at the small rim (C6 position) (β-CDCL-6). Their chemical structures were investigated using nuclear magnetic resonance (NMR) spectroscopy and matrix-assisted laser desorption/ionization mass spectrometry (MALDI-MS). The derivatives were subsequently crosslinked using citric acid (CA) or malic acid (MA) to obtain three-dimensional networks. The formation of NS through CA crosslinking of β-CDCL-R and β-CDCL-6 is represented in Figure 1. According to the literature, in the first phase, the CA undergoes a transformation into a cyclic anhydride with increased reactivity toward OH groups in comparison to its precursor [4]. In the second phase, the anhydride reacts with the OH groups from the caprolactone chain end or with the native OH groups of the β-CD and forms ester bonds.

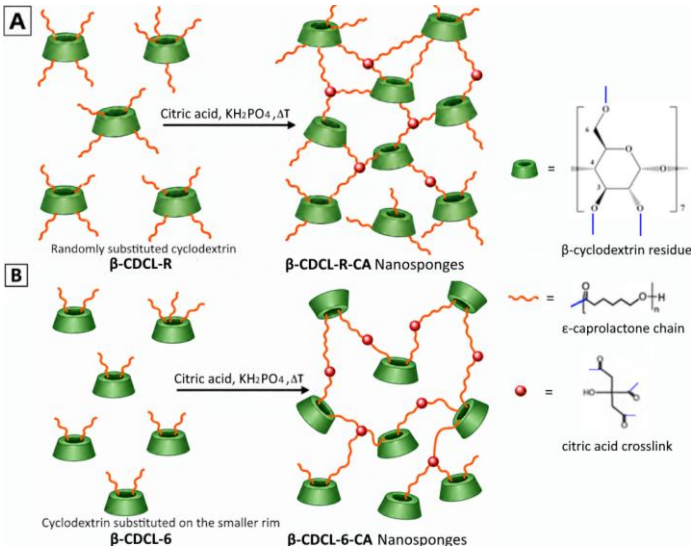


Figure 1. Schematic representation of NS formation through CA crosslinking of A: β-CDCL-R and B: β-CDCL-6.

The resulting materials were investigated to assess the influence of the precursor's structural architecture on the NS properties. Their sorption performance was evaluated using methylene blue (MB) as a model compound and UV-VIS spectrophotometry for monitoring MB solutions absorbances and calculating the solutions' concentration changes. The sorption results were also compared against NS prepared using 2-hydroxypropyl-β-cyclodextrin (HP-β-CD), reported in the literature [5]. Additionally, the effects of acid and alkaline degradation of the NS on their sorption behavior were also examined.

The results showed that nanosponges prepared from β-CDCL-6 generally exhibited higher sorption capacities than those obtained from β-CDCL-R. Furthermore, CA-crosslinked materials (β-CDCL-6-CA and β-CDCL-R-CA) displayed higher sorption capacities than their MA-crosslinked counterparts (β-CDCL-6-MA and β-CDCL-R-MA) under the investigated conditions. The prepared HP-β-CD-based nanosponges, reported in the literature, showed better sorption capacities than β-CDCL-R analogues but weaker ones than β-CDCL-6-based NS. The sorption analyses of the acid- and alkaline-treated NS showed increased sorption capacities of the β-CDCL-R nanosponges in comparison to the untreated ones. This may be associated with two possible explanations. Firstly, the partial hydrolysis of the ester bonds of the crosslinked network may generate additional hydroxyl and carboxyl groups that may interact with MB. Secondly, the ester bond cleavage may decrease the density of the network and increase the accessibility of MB to the cyclodextrin cavities, favoring the complexation. In the case of β-CDCL-6-CA, the absence of the substituents at the larger rim implies an initially high accessibility for complexation. Thus, the hydrolysis, especially at the level of oligocaprolactone ester bonds, might not produce a significant improvement in the sorption capacities of the β-CDCL-6 nanosponges. In fact, the measured sorption capacities of acid- and alkaline-treated β-CDCL-6-CA NS were smaller than the capacities of the untreated ones. This also correlates with the greater mass loss of β-CDCL-6-CA nanosponges measured after acid and alkaline treatment. In contrast, the degraded NS based on β-CDCL-R and HP-β-CD revealed an opposite trend, justified by the increase in sorption capacity. Moreover, both acid and basic degradations caused a more pronounced change in the integrity of the crosslinked network for β-CDCL-6 nanosponges compared to their β-CDCL-R homologues, as demonstrated by the gravimetric degradation experiments.

These findings suggest that controlling the substitution pattern of cyclodextrin derivatives, together with the selection of crosslinking agents, can be used to tailor the properties of cyclodextrin-based networks, including sorption performance or degradation kinetics. This approach offers opportunities for developing functional materials with adjustable characteristics for depollution applications.

References

[1] F. Trotta, M. Zanetti, R. Cavalli, *Beilstein J. Org. Chem.* 2012, 8, 2091–2099.
[2] F. Caldera, M. Tannous, R. Cavalli, M. Zanetti, F. Trotta, *Int. J. Pharm*. 2017, 531, 470–479.
[3] D.-A. Blaj, M. Balan-Porcarasu, V. Harabagiu, C. Peptu, *Carbohydr. Polym.* 2024, 334, 122032.
[4] K. Escobar, KA. Garrido-Miranda, R. Pulido, N. Nveas, M. Manso-Silvan, J. Herandez-Montelongo, *Pharm.* 2023, 15(1), 296.
[5] C. Liu, L. Song, S. Cao, H. Zhang, J. Han, *Polymer.* 2023, 280, 126043.

OC19. HYDROGELS BASED ON POLYSACCHARIDES, AMINO ACIDS AND EUTECTIC SOLVENTS

Lorena-Elena Grigoriu*, Alexandra Vieru, Diana Elena Ciolacu, Alexandru-Mihail Serban, Alina Gabriela Rusu, Loredana-Elena Nita
Petru Poni Institute of Macromolecular Chemistry, Romanian Academy, Iasi, Romania
**grigoriu.lorena@icmpp.ro*

Introduction

In this study, hydrogels were developed by first preparing amino acid- and short peptide-based supramolecular eutectogels, followed by the addition of a polysaccharide (carrageenan). Polysaccharides were selected for their excellent biocompatibility, mild gelation conditions, tunable mechanical properties, and intrinsic bioactivity, alongside their ability to stabilize and encapsulate biomolecules for controlled drug release and wound healing. Deep eutectic solvents (DES), particularly natural ones, serve as multifunctional components in these hydrogel systems.[1] They offer excellent biocompatibility, mild processing conditions, and superior solubilization of active molecules, while effectively modulating gelation, mechanical properties, hydration, and bioactivity.[2-3] Ultimately, their safe-by-design nature, tunability, and capacity to stabilize and deliver bioactive compounds make DES ideal candidates for biomedical hydrogel formulations.[4]

Materials and methods

The eutectic solvent was obtained by combining glycerol with citric acid in a 3:1 gravimetric ratio at 80 °C for 90 minutes under continuous stirring. Hydrogels were prepared using different tryptophan/glutamic acid ratios, DES and PBS amounts, with carrageenan added as the polysaccharide component. Nisin and epigallocatechin gallate (EGCG) were incorporated according to the formulations listed in Table 1.

Table 1. Composition of pristine and loaded materials.

Sample code	Composition
C_Try_GA1:1	Tryptophan + Glutamic Acid (diferent ratio) + DES + PBS(pH=7.4; 0.01M) + Carrageenan 1%
C_Try_GA1:2	
C_Try_GA2:1	
C_Try_GA1:1_N_E	Tryptophan + Glutamic Acid (diferent ratio) +DES + PBS (pH=7.4; 0.01M) + Carrageenan 1% + Nisin + Epigallocatechin gallate (EGCG)
C_Try_GA1:2_N_E	
C_Try_GA2:1_N_E	

Result and Conclusions

The structural characterization (Figure 1A) of the synthesized systems highlights high viability the successful integration of the main components within the hydrogel matrix. Scanning electron microscopy (SEM) investigations confirm the development of a well-structured, three-dimensional internal architecture characterized by a pronounced porosity, which is essential for fluid transport (Figure 1B-C). Experimental determination of the retention capacity reveals a decrease in swelling

capacity, most likely caused by additional intermolecular interactions among the polysaccharide chains, amino acids and deep eutectic solvent (Figure 1-D). The release profiles demonstrate that the active compounds were gradually released from the hydrogel matrix (Figure 1E-F).

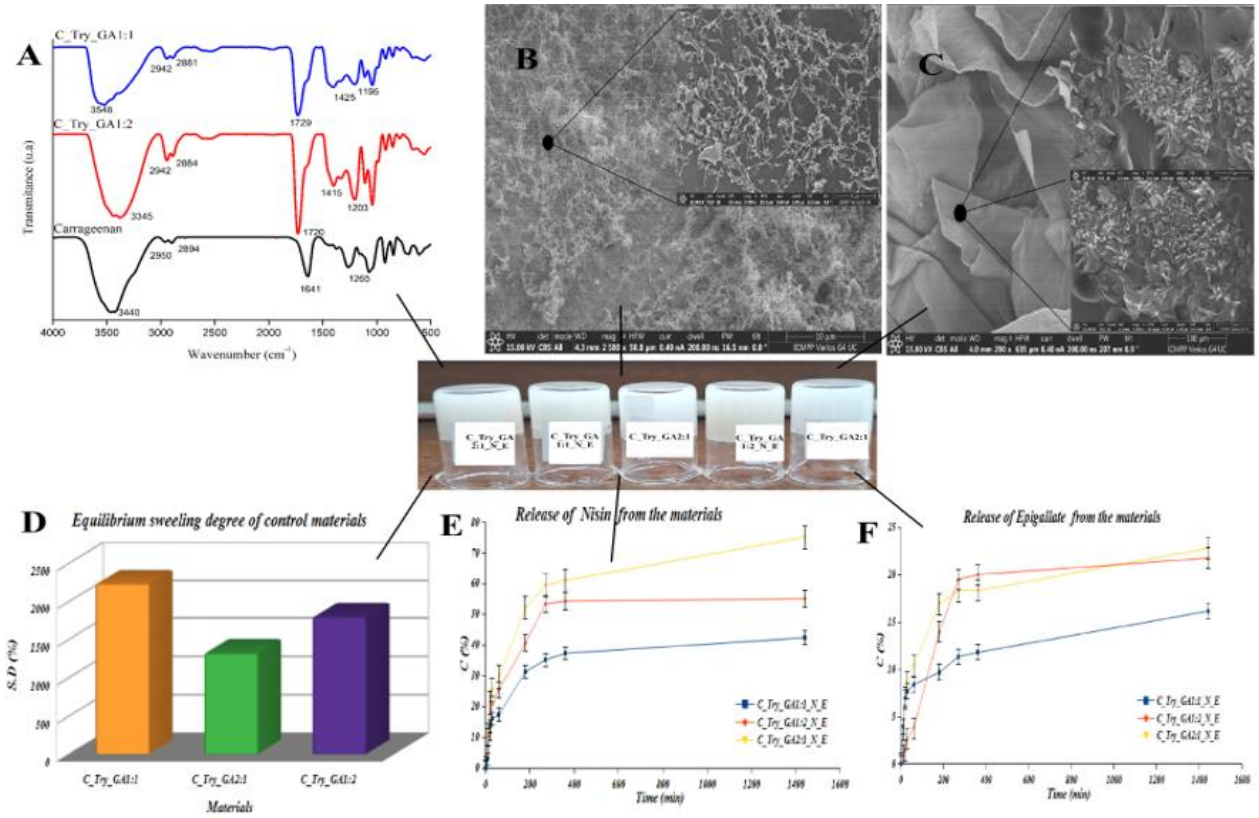


Figure 1. A-Results of FTIR spectra. B, C- Results of SEM Microscopy. D- Results of degree Swelling. E, F- Release of active principles.

References

[1] C. Zeng, H. Zhao, Z. Wan, Q. Xiao, H. Xia, S. Guo, *RSC advances* 2020, 10, 28376-28382.
[2] Y. Jiang, A. Wu, L. Yang, J. Wu, *RSC advances* 2024, 14, 25359-25368.
[3] S.N. Pedro, M.S.M. Mendes, B.M. Neves, I.F. Almeida, P. Costa, I. Correia-Sa, C. Vilela, M.G. Freire, A.J.D. Silvestre, C.S.R. Freire, *Pharmaceutics* 2022, 14, 827.
[4] M. Li, H. Cui, Y. Cao, Y. Lin, Y. Yang, M. Gao, W. Zhang, C. Wang, *Journal of Controlled Release* 2023, 354, 664-679.

Acknowledgment: This work was supported by a grant of the Ministry of Research, Innovation and Digitization, CCCDI -UEFISCDI, project number PN-IV-P7-7.1-PED-2024-1788, within PNCDI IV.


MacroYouth 2026

Poster presentations

PP1. EFFECT OF A CARBON NANOPARTICLE DISPERSION ON THE STRUCTURE AND PHOTOLUMINESCENCE OF ELECTROSPUN POLY(VINYL ALCOHOL) NANOFIBRES

Sebastian-Marian Alupoaie*, Bogdan-George Rusu, Iuliana Stoica, Magdalena Aflori
Petru Poni Institute of Macromolecular Chemistry, Romanian Academy, Iasi, Romania
**alupoaie.sebastian@icmpp.ro*

Introduction

Fluorescent carbon nanoparticles (CNPs), including carbon dots, are of growing interest for luminescent, sensing and biomedical applications. Poly(vinyl alcohol) (PVA) is a suitable matrix, being water-soluble and rich in hydroxyl groups, and PVA/carbon dot nanofibers have been proposed as wound dressings [1], while carbon dot-doped nanofibrous membranes have been used for anti-counterfeiting [2]. This study aimed to prepare PVA nanofibers with two CNP concentrations, introduced as a dispersion in ethylenediamine (EDA), and to evaluate their morphology, structure and photoluminescence, considering the possible influence of the dispersion medium.

Experimental

Aqueous PVA solutions (8.5%, w/v) were mixed with a CNP dispersion in EDA to obtain final CNP concentrations of 14.3 (PVA-CNP1) and 43.4 µg/mL (PVA-CNP2), corresponding to EDA contents of approximately 14 and 43% (v/v). A PVA solution in water, without CNPs, was used as control (PVA-M). All solutions were electrospun at room temperature under identical conditions (21.75 kV, 0.8 mL/h, 20 cm needle-to-collector distance), onto aluminium foil on a rotating collector. The mats were characterized by atomic force microscopy (AFM) (Figure 1), FTIR and photoluminescence spectroscopy.

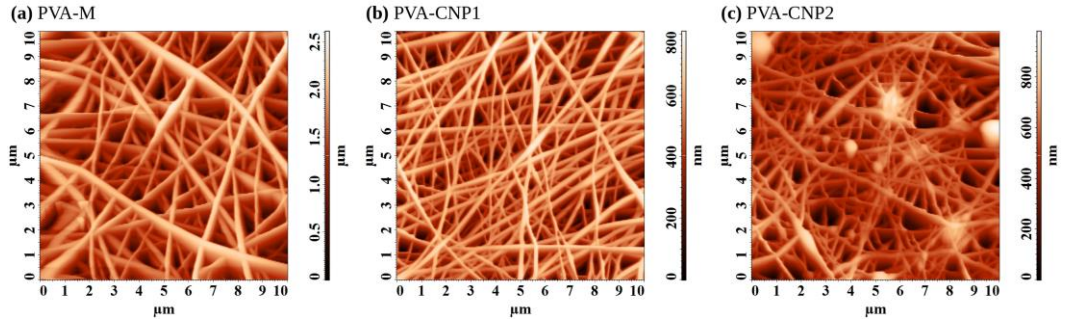


Figure 1. AFM images (10 × 10 µm^2) of PVA-M (a), PVA-CNP1 (b) and PVA-CNP2 (c).

Results and discussion

All samples consisted of continuous, randomly oriented nanofibers. The control fibers were smooth and bead-free, with a broad range of thickness, while PVA-CNP1 fibers were also bead-free but appeared thinner and more uniform. PVA-CNP2 showed very fine, branched fibers with numerous beads and partially fused junctions. Since bead formation is governed by the viscoelasticity of the solution, the charge density carried by the jet and the surface tension [3], this indicates that the EDA dispersion modifies the spinning solution.

The FTIR spectra of all samples showed the characteristic bands of partially hydrolyzed PVA, including the C=O band of residual acetate groups at ~1730 cm^{-1} [4]. In the CNP-containing fibers, the O–H stretching band shifted from 3292 to about 3270 cm^{-1} and the intensity ratio of the crystallinity-sensitive band at ~1141 cm^{-1} to the C–O band at ~1090 cm^{-1} decreased [4], indicating modified hydrogen bonding and a lower crystallinity of the PVA matrix. These changes were similar for both CNP concentrations, despite the very low CNP content (below 0.1 wt% relative to PVA), and opposite to the increase in crystallinity reported for PVA containing much higher carbon dot loadings [5]. Under UV excitation (Figure 2), PVA-CNP2 fibers exhibited a broad emission band centered at about 424 nm, more than one order of magnitude above the background of the control fibers and of the substrate. For PVA-CNP1, the emission could not be distinguished from the background, indicating that a minimum CNP concentration is required for detectable luminescence.

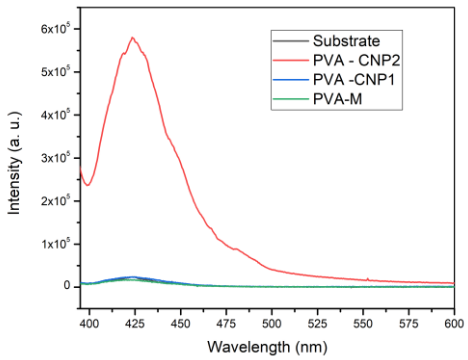


Figure 2. Photoluminescence spectra of the substrate, PVA-M, PVA-CNP1 and PVA-CNP2.

Conclusions

The addition of the CNP dispersion in EDA to PVA led to thinner fibers, bead formation at the highest EDA content, modified hydrogen bonding and lower crystallinity of PVA, changes most likely related to the dispersion medium. The emission of the fibers obtained at the highest CNP concentration makes these materials of interest for fluorescence-based labelling [2], while sensing applications could be explored after crosslinking of the water-soluble PVA matrix. A water/EDA control without CNPs will separate the two effects.

References

[1] S. Abolghasemzade, M. Pourmadadi, H. Rashedi, F. Yazdian, S. Kianbakht, M. Navaei-Nigjeh, *J. Mater. Chem. B* 2021, 9, 658-676.
[2] S. Qiang, K. Yuan, Y. Cheng, G. Long, W. Zhang, X. Lin, X. Chai, X. Fang, T. Ding, *J. Mater. Chem. C* 2023, 11, 7076-7087.
[3] H. Fong, I. Chun, D.H. Reneker, *Polymer* 1999, 40, 4585-4592.
[4] H.S. Mansur, C.M. Sadahira, A.N. Souza, A.A.P. Mansur, *Mater. Sci. Eng. C* 2008, 28, 539-548.
[5] H. Huo, J. Shen, J. Wan, H. Shi, H. Yang, X. Duan, Y. Gao, Y. Chen, F. Kuang, H. Li, L. Yang, G. Du, *Nat. Commun*. 2025, 16, 6221.

Acknowledgment: This work was supported by a grant of the Ministry of Research, Innovation and Digitization, CNCSS/CCCDI – UEFISCDI, project PN-IV-P8_1-PRE-HE-ORG-2025-0382 contract number 156PHE/2026.

PP2. EPR SPECTROSCOPIC INVESTIGATION OF SPIN-LABELLED BOVINE SERUM ALBUMIN IN ALGINATE-BASED HYDROGELS

Elena-Erika Antonia*, Elena-Gabriela Ionita
Institute of Physical Chemistry - Ilie Murgulescu, Romanian Academy, Bucharest, Romania
**antoniaerika09@gmail.com*

Introduction. Hydrogels are three-dimensional polymeric networks with a high water-retention capacity, which makes them suitable for biomedical applications, including protein encapsulation and controlled drug delivery. Alginate, a naturally occurring polysaccharide, is widely studied due to its ability to form hydrogels through ionic crosslinking with divalent cations. Bovine serum albumin (BSA), a well-established model protein, was used to examine its behavior within alginate-based hydrogels-both unmodified and functionalized-obtained through different protein-incorporation procedures. Electron paramagnetic resonance (EPR) spectroscopy is a valuable technique for investigating molecular mobility and local environment of spin-labeled species. In this study, EPR spectroscopy was applied to spin-labeled BSA encapsulated within alginate-based hydrogels, focusing on the effects of the protein-incorporation procedures and the crosslinking cation (Ba^{2+}, Ca^{2+}, Sr^{2+}, or Zn^{2+}) on the spectral characteristics of the spin label [1,2].

Materials and methods. Gel systems of different compositions were prepared using alginate (Alg), β-cyclodextrin (β-CD), adamantane (Ad), and spin-labeled BSA. The chemical structures of the main components and a schematic representation of spin-labelled BSA are shown in Figure 1. The study focused on the spectroscopic characterization of these systems using electron spin resonance (EPR), with emphasis on how gel composition, protein incorporation procedure and the crosslinking cation affect the spectral features of the spin-labelled protein [3].

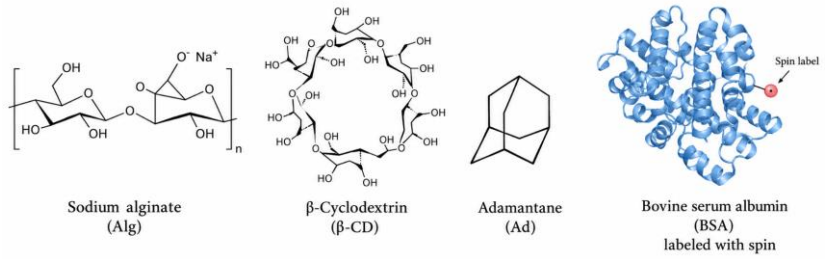


Figure 1. Chemical structures of the main components of the investigated systems.

The experimental work was organized in three series designed to compare different approaches to protein incorporation and to evaluate the influence of the ionic crosslinking agent. In Series 1, the alginate-based formulations were first crosslinked using an aqueous solution of hydrated barium chloride ($BaCl_2$), after which spin-labelled BSA was added dropwise to the preformed gels, in order to assess the behaviour of the labelled protein in contact with an existing polymeric network. In Series 2, spin-labelled BSA was incorporated into the alginate-based solutions before crosslinking. Series 3 investigated the influence of the crosslinking cation on spin-labelled BSA in simple alginate hydrogels. The alginate solutions were crosslinked using solutions of barium chloride, calcium chloride, strontium nitrate, or zinc nitrate. Spin-labelled BSA was introduced after gel formation in each case, allowing the influence of the crosslinking cation to be examined under comparable preparation conditions. The EPR measurements were performed on the prepared

samples to evaluate the spectral characteristics of spin-labelled BSA in various alginate gels as a function of cation type and polysaccharide functionalization.

Results and Discussion. The EPR results revealed variations in the spectral parameters of spin-labelled BSA depending primarily on the composition of the alginate-based systems, especially in the presence of β-cyclodextrin. The comparison between the two preparation procedures showed broadly similar spectral features for several formulations, suggesting that the sequence of protein incorporation and gel formation did not produce major changes. The third experimental series further explore the influence of the crosslinking cation (Ba^{2+}, Ca^{2+}, Sr^{2+} or Zn^{2+}) on the EPR spectral features of spin-labelled BSA [4].

Table 1. EPR spectral parameters of spin-labelled BSA in alginate-based hydrogels and corresponding residual solutions across the three experimental series.

GEL	DISTANCE 1 (Azz1)	DISTANCE 2 (Azz2)
Gel_Alg_Ba_BSA	64.53	35.25
Gel_Alg-bCD_Ba_BSA	64.86	35.25
Gel_Alg-Ad_Ba_BSA	65.36	35.25
Gel_Alg-Ad_Alg-Bcd_Ba_BSA	65.11	35.25
RESIDUAL SOLUTION	**DISTANCE 1 (Azz1)**	**DISTANCE 2 (Azz2)**
Sol_Alg_Ba_BSA	66.24	35.37
Sol_Alg-bCD_Ba_BSA	66.32	35.37
Sol_Alg-Ad_Ba_BSA	64.33	35.30
Sol_Alg-Ad_Alg-bCD_Ba_BSA	63.93	35.14
GEL	**DISTANCE 1 (Azz1)**	**DISTANCE 2 (Azz2)**
Gel_Alg_BSA_Ba	64.75	35.06
Gel_Alg-bCD_BSA_Ba	65.95	35.14
Gel_Alg-Ad_BSA_Ba	65.39	34.98
Gel_Alg-Ad_Alg-Bcd_BSA_Ba	64.91	35.46
RESIDUAL SOLUTION	**DISTANCE 1 (Azz1)**	**DISTANCE 2 (Azz2)**
Sol_Alg_BSA_Ba	65.56	35.39
Sol_Alg-bCD_BSA_Ba	65.96	35.39
Sol_Alg-Ad_BSA_Ba	65.16	35.23
Sol_Alg-Ad_Alg-bCD_BSA_Ba	65.56	35.23
GEL	**DISTANCE 1 (Azz1)**	**DISTANCE 2 (Azz2)**
Gel_Alg_Ca_BSA	67.40	35.20
Gel_Alg_Sr_BSA	65.52	35.20
Gel_Alg_Zn_BSA	66.38	35.20
RESIDUAL SOLUTION	**DISTANCE 1 (Azz1)**	**DISTANCE 2 (Azz2)**
Sol_Alg_Ca_BSA	67.72	35.22
Sol_Alg_Sr_BSA	69.04	35.14
Sol_Alg_Zn_BSA	67.47	34.97

References

[1] K.Y. Lee, D.J. Mooney, *Progress in Polymer Science*, 2012, 37(1), 106–126.
[2] C. Colin, E. Akpo, A. Perrin, D. Cornu, J. Cambedouzou, *Molecules,* 2024, 29(11), 2515.
[3] G. Ionita, C.M. Topala, E.E. Antonia, A.G. Bucur, ***Gels***, 2026, **12(3)**, 217.
[4] V. Chechik, E. Carter, D.M. Murphy, *Oxford Chemistry Primers,* 2016.

Acknowledgment: ”Chemical host-guest molecule systems for health applications’’ (OMRI for identification of inflammatory pathologies), PNRR-III-C9-2023-I8-CF97, contract no. 760283/ 27.03.2024, project code CF97/ 31072023.

PP3. OPTIMIZATION OF THE UGI REACTION FOR ALGINATE FUNCTIONALIZATION: CHARACTERIZATION AND ANTIMICROBIAL ACTIVITY

Raluca-Elena Avram*, Gabriela Liliana Ailiesei, Maria Marinela Lazar, Maria Valentina Dinu
Petru Poni Institute of Macromolecular Chemistry, Romanian Academy, Iasi, Romania
**munteanu.raluca@icmpp.ro*

As global technological progress intensifies, the demand for advanced functional materials continues to grow. Lately, polysaccharide-based materials have attracted considerable attention owing to their natural origin, structural diversity, and potential for chemical functionalization. Among the most effective methods for polysaccharides functionalization are multicomponent reactions (MCR).

MCRs are chemical reactions in which three or more compounds react in a single step form a compound with a complex molecular structure, incorporating many atoms from the starting materials. These reactions offer several advantages, including a ”one-pot” reaction, reduced solvent consumption, versatility, and high yields.

Sodium alginate (ALG) is a naturally occurring polysaccharide with numerous features, including hydrophilicity, chemical reactivity, and the presence of functional groups that enable structural modification. Chemical modification of alginate allows its hydrophilic–hydrophobic balance to be adjusted, potentially leading to materials with improved physicochemical properties [1]. Among the most versatile, economical, and rapid approaches to functionalize ALG is the UGI multicomponent reaction.

In this study, ALG was functionalized through the Ugi multicomponent reaction using propylamine (PPA), various aldehydes (hexanal (Hex), dodecyl aldehyde (DDA), citral (Cit), and benzaldehyde (Bz), and tert-butyl isocyanide (TbI) (Figure 1). The reaction conditions were optimized by varying the initial pH and the molar ratio of ALG carboxyl groups to the low-molecular-weight reactants ($RM_{COOH: reactants}$).

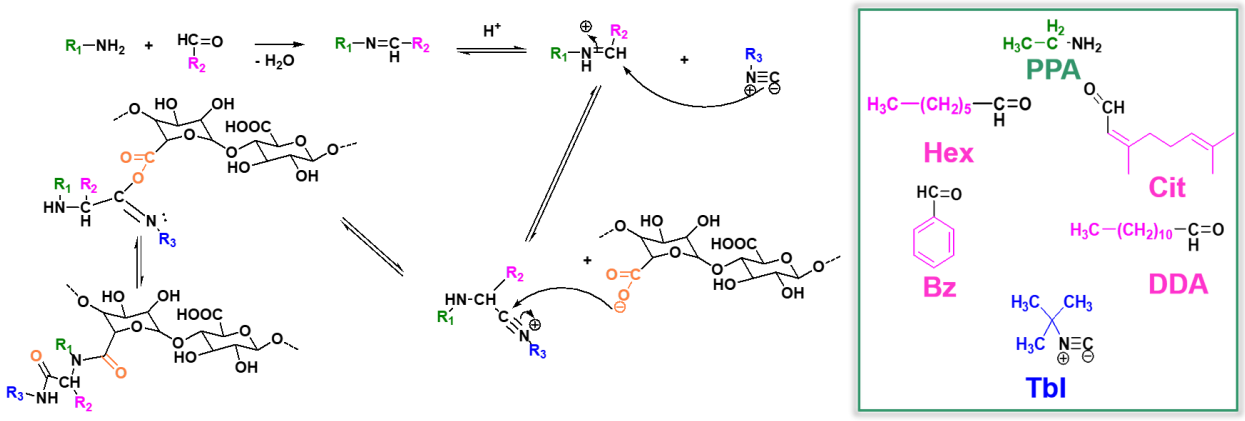


Figure 1. The mechanism of ALG functionalization through Ugi reaction.

Successful ALG functionalization was confirmed by ^{1}H-NMR and FTIR spectroscopy. The stability of the resulting ALG derivatives (ALG-Ugi) was investigated over a period of 77 days by monitoring their ^{1}H-NMR spectra (Figure 2). DS was determined using ^{1}H-NMR spectroscopy, conductometric titration, and polyelectrolyte titration to assess the influence of the initial pH, reactant molar ratio, and analytical method on the determined DS values. At pH 5, increasing the molar ratio of the low-molecular-weight reactants to the carboxyl groups of alginate generally led to higher DS values, indicating that pH 5 was the most favorable condition for achieving a high degree of substitution.

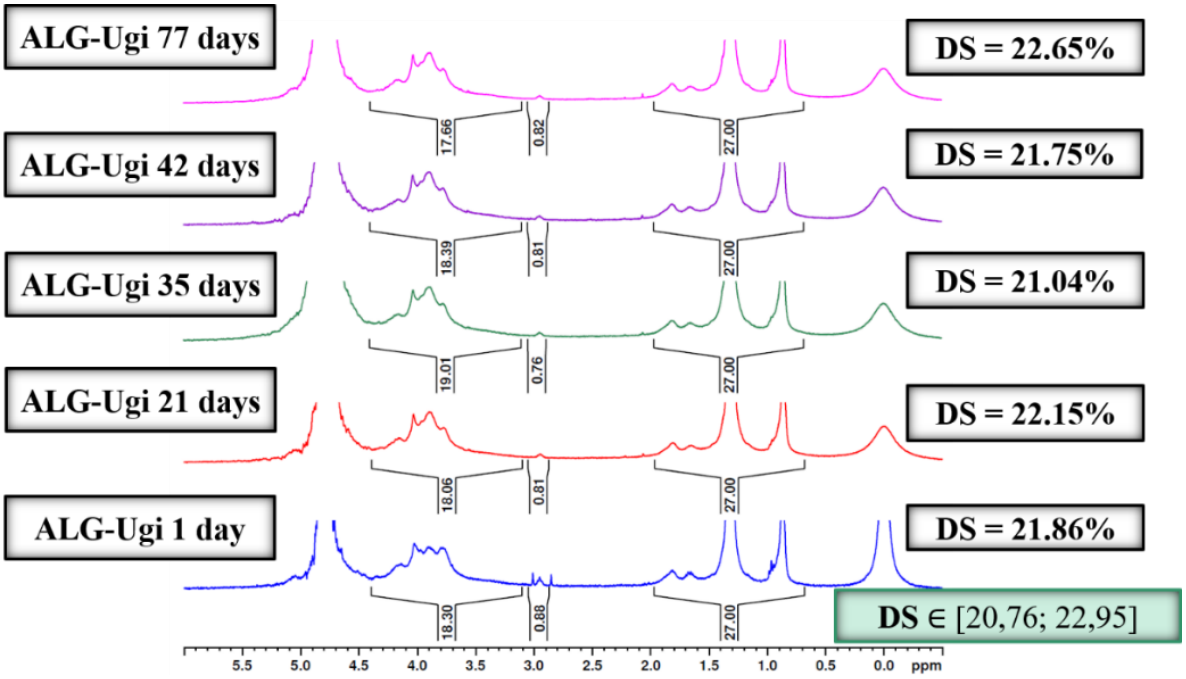


Figure 2. Comparative ^{1}H-NMR spectra of the ALG-Ugi derivatives recorded for eleven weeks.

The antibacterial activity of the ALG derivatives was evaluated against two Gram-negative bacteria (*Escherichia coli* and *Salmonella Typhimurium*) and two Gram-positive bacteria (*Listeria monocytogenes* and *Staphylococcus aureus*). The influence of DS and the type of aldehyde used in the modification reaction was investigated. All films prepared from the synthesized derivatives demonstrated improved antibacterial activity compared with films prepared from unmodified ALG. The most pronounced effect was observed for the derivative obtained using DDA, which exhibited bacterial inhibition exceeding 95% against all four bacterial strains.

References

[1] S. Akshaya, A.J.A. Nathanael, *ACS OMEGA* 2024, 9, 4246-4262.
[2] M.B. Carpio, P.M. Thompson, C. Moody, J.G. Pierce, Brudno, Y. *Carbohydrate Polymers* 2025, 369, 124299.

Acknowledgment: This work was supported by a grant of the Ministry of Research, Innovation and Digitization, CNCS-UEFISCDI, project number PN-IV-P1-PCE-2023-1968, within PNCDI IV.

PP4. INFLUENCE OF DEEP EUTECTIC SOLVENT PRETREATMENT ON PRODUCTION AND PROPERTIES OF CELLULOSE NANOFIBERS

Madaina-Roxana Birtea*, Gabriela Biliuta, Raluca-Ioana Baron, Raluca Nicoleta Darie-Nita, Sergiu Coseri
Petru Poni Institute of Macromolecular Chemistry, Romanian Academy, Iasi, Romania
**birtea.madalina@icmpp.ro*

Introduction

Cellulose nanofibers represent a highly versatile class of nanomaterials that have attracted significant interest for numerous applications, especially in composite systems, due to their remarkable mechanical strength and stiffness. When incorporated into hydrogels, either as the main network-forming component or as an active reinforcing phase, they contribute to the development of materials exhibiting superior mechanical, structural, and functional properties [1]. Traditional approaches for cellulose nanofiber isolation rely on multiple chemical pretreatment steps, often involving large quantities of aggressive chemicals such as sulfuric acid and sodium hydroxide. While effective, these processes raise significant environmental and economic concerns. Consequently, recent research has increasingly focused on the development of sustainable pretreatment technologies that reduce or eliminate the need for harsh chemical reagents while maintaining processing efficiency. The primary objectives are to minimize energy requirements, decrease environmental footprint, and enable the environmentally responsible production of cellulose nanofibers [2]. Deep eutectic solvents (DESs) are a distinctive class of solvents obtained through the combination of two or more components, typically a hydrogen-bond donor and a hydrogen-bond acceptor. The extensive hydrogen-bonding interactions between these components give rise to a eutectic mixture with a melting point substantially lower than that of each individual constituent. This unique physicochemical behaviour has attracted considerable interest in the development of sustainable and environmentally friendly processing technologies. One of the most well-known DESs is *reline*, consisting of a mixture of choline chloride and urea in a molar ratio of 1:2 (Figure 1).

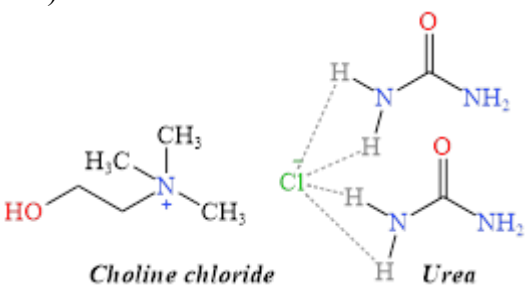


Figure 1. Chemical composition of *reline.*

Experimental strategy

The experimental strategy of this study consisted of performing two pretreatments on α-cellulose using two different deep eutectic solvents. The first deep eutectic solvent used is choline chloride and urea (*DES-1*) in a molar ratio of 1:2. This eutectic solvent has already been described in the literature and employed as a pretreatment medium for fibrillated nanocellulose production.

The second eutectic solvent used is a new formulation, consisting of choline chloride, 1-methylimidazole, and water (*DES-2*) in a molar ratio of 1:2:1. Both pretreated cellulose batches were then oxidized using the NaBr/NaClO/TEMPO (radical 2,2,6,6-tetramethylpiperidine 1-oxyl) system [3]. For comparison purposes, α-cellulose was also oxidized under identical conditions without prior pretreatment. The oxidation products were purified by dialysis, freeze-dried, and subsequently characterized. FT-IR and ^{13}C-CPMAS analyses confirmed the chemical modifications and the introduction of surface carboxyl groups, while atomic force microscopy verified the formation of fibrillated nanocellulose. Surface charge density was determined by conductometric titration with sodium hydroxide, and suspension stability was evaluated through Zeta potential measurements.

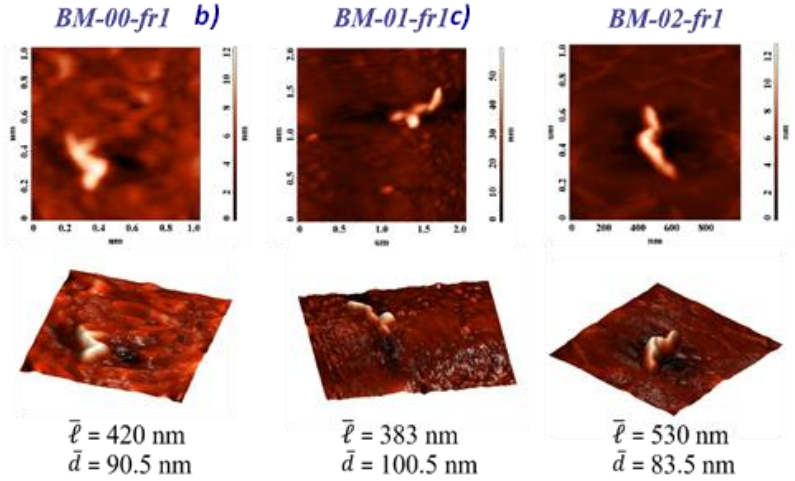


Figure 2. The images obtained by atomic force microscopy and the average dimensions of the cellulose nanofibers obtained by oxidation: a) α-cellulose without pretreatment; b) α-cellulose pretreated with DES-1; c) α-cellulose pretreated with DES-2.

Results

FT-IR spectroscopy revealed that pretreatment with deep eutectic solvents did not induce detectable chemical changes in the cellulose structure. Both pretreatments successfully yielded fibrillated nanocellulose, as evidenced by the AFM images presented in Figure 2, although with different carboxylic group contents. The fractions obtained from the oxidation of α-cellulose pretreated with DES-2 exhibited the highest carboxyl group content and a zeta potential of approximately −50 mV, indicating excellent colloidal stability and the formation of stable suspensions in polar solvents.

References

[1] B. Thomas, M. C. Raj, K. B. Athira, M. H. Rubiyah, J. Joy, A. Moores, G. L. Drisko, C. Sanchez, *Chem. Rev.* 2018, 118, 11575-11625.
[2] A. Arivendan, X. Chen, Y. F. Zhang, W. Gao, *Int. J. Biol. Macromol*. 2024, 281, 135925.
[3] G. Biliuta, A. Dascalu, I. Stoica, R. I. Baron, D. Bejan, M. Bercea, S. Coseri, *Wood Sci. Technol.* 2023, 57 1443-1465.

Acknowledgment: This work was supported by a grant of the Ministry of Research, Innovation and Digitization, CNCS-UEFISCDI, project number PN-IV-P1-PCE-2023-1020 (6PCE/08.01.2025), within PNCDI IV.

PP5. SYNTHESIS AND STRUCTURAL CHARACTERIZATION OF PYRIDINE SCHIFF BASES WITH ALIPHATIC AND SILOXANE UNITS

Alexandra Birzu*, Mihaela Dascalu, Sergiu Shova, Maria Cazacu
Petru Poni Institute of Macromolecular Chemistry, Romanian Academy, Iasi, Romania
**birzu.alexandra@icmpp.ro*

Schiff bases constitute a versatile platform for the development of new compounds. Their azomethine bonds provide a convenient route to molecules whose structure can be varied through the choice of aldehyde and diamine. In bis-Schiff bases, two imine groups connect the terminal aromatic fragments to a common bridge, allowing both the terminal groups and the central segment to be modified. This modular approach is useful for preparing related compounds, in which individual structural features can be compared systematically.

Siloxane-containing Schiff bases are of particular interest because the Si–O–Si unit introduces a flexible inorganic segment into an otherwise organic framework. The preparation and crystallographic characterization of a bis(pyrrole) Schiff base derived from 1,3-bis(3-aminopropyl)tetramethyldisiloxane illustrate the suitability of this diamine for constructing structurally defined bis-imines [1]. Studies of related siloxane-spaced salen-type compounds have also highlighted the influence of the spacer on their synthesis and physicochemical behaviour [2]. In particular, comparisons with organic analogues have identified differences in imine formation and surface behaviour. These observations establish a basis for investigating further aldehyde-derived series while recognizing that their properties must be determined individually. The biological relevance of comparing siloxane and aliphatic spacers is supported by investigations of related Schiff-base metal complexes. In a recent study, cobalt(II) complexes bearing siloxane or hexamethylene bridges displayed different cytotoxic responses in cancer-cell assays [3]. These findings motivate further comparative investigations, while providing no direct evidence of anticancer activity for the metal-free pyridine-based compounds described here.

This work presents the synthesis and structural characterization of six pyridine Schiff bases, organized into two series of three positional isomers. The compounds were obtained by condensation of pyridine-2-, pyridine-3-, and pyridine-4-carboxaldehyde with either 1,3-bis(3-aminopropyl) tetramethyldisiloxane or 1,12-diaminododecane (Figure 1). Each molecule contains two pyridyl-azomethine units connected through a tetramethyldisiloxane-containing spacer or a dodecamethylene chain. This design allows the position of the pyridine nitrogen and the chemical nature of the spacer to be considered within the same comparative study. The three pyridine carboxaldehyde isomers retain the same elemental composition but place the ring nitrogen at different positions relative to the imine substituent. The two diamines introduce a second structural variable: an organic chain containing twelve methylene groups or two aminopropyl-derived segments joined by a tetramethyldisiloxane unit. Thus, each pyridyl substitution pattern can be examined in both spacer environments, and each spacer can be examined across the three positional isomers. Because the spacers also differ in length and composition, any subsequent differences in behaviour will require interpretation in terms of the complete molecular structures.

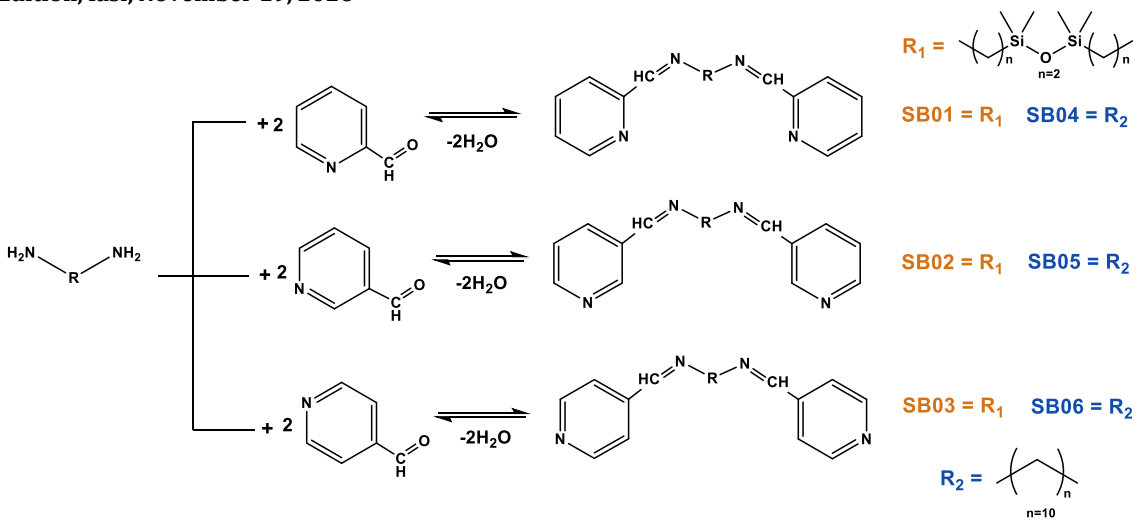


Figure 1. Synthesis of bis-Schiff bases SB01-SB03 by condensation of 1,3-bis(3-aminopropyl)tetramethyldisiloxane with pyridine-2-, -3-, and -4-carboxaldehyde, respectively, in dichloromethane at room temperature for 2 h, and SB04-SB06 by condensation of 1,12-diaminododecane with the corresponding aldehydes in ethanol under reflux temperature for 2h.

All six compounds were characterized by ^{1}H and ^{13}C NMR spectroscopy, FTIR spectroscopy, mass spectrometry and single-crystal X-ray diffraction. The combined data establish their molecular structures and enable a systematic comparison of the influence of pyridyl substitution and spacer composition on molecular conformation and crystal packing. Further work will focus on the complexation of these Schiff bases with different metal ions, alongside investigations of their stability in solution, surface tension and hydrophilic-hydrophobic balance. *In vitro* anticancer testing of all six Schiff bases is also planned to explore the influence of spacer composition and pyridyl substitution on their biological activity. The planned biological assessment will compare the responses of the aliphatic and siloxane-containing derivatives and explore whether the position of the pyridine nitrogen influences their effects on cancer-cell viability. These experiments constitute the next stage of the study; no anticancer activity is claimed at the present stage.

Conclusion

This study establishes two series of structurally characterized pyridine-based bis-Schiff bases containing aliphatic or siloxane spacers. These compounds provide a basis for further investigations into metal complexation, solution stability, surface activity and hydrophilic-hydrophobic balance. Planned *in vitro* anticancer studies will explore how their structural differences influence biological activity.

References

[1]. A. Vlad, C. Turta, M. Cazacu, E. Rusu, S. Shova, *Eur. J. Inorg. Chem.* 2012, 5078–5084.
[2]. M. Damoc, A.-C. Stoica, A.-M. Macsim, M. Dascalu, M.-F. Zaltariov, M. Cazacu, *J. Mol. Liq.* 2020, 316, 113852.
[3]. M. Damoc, A.-C. Stoica, M.-F. Zaltariov, D. Peptanariu, M. Dascalu, M. Cazacu, *R. Soc. Open Sci.* 2025, 12, 250279.

Acknowledgments: This work was supported by a grant of the Ministry of Research, Innovation and Digitization, CCCDI - UEFISCDI, project number PN-IV-P7-7.1-PED-2024-2479 (SMM-ChaPS), within PNCDI IV.

PP6. CARBON QUANTUM DOT-LOADED SODIUM ALGINATE/K-CARRAGEENAN HYDROGELS

Cosmina-Maria Bogza*, Carmen-Mihaela Popescu, Maria-Cristina Popescu
Petru Poni Institute of Macromolecular Chemistry, Romanian Academy, Iasi, Romania
**bogza.cosmina@icmpp.ro*

Introduction

Polysaccharide-based hydrogels provide hydrophilic networks whose properties can be tailored through polymer selection and crosslinking strategies. Incorporating fluorescent carbon dots into these networks enables the development of composite materials with additional optical functionality [1-3]. In this study, sodium alginate/κ-carrageenan hydrogel beads containing biomass-derived CQDs were prepared and characterized.

Preparation and physico-chemical properties of hydrogels

The hydrogel beads were prepared by mixing separately dissolved sodium alginate (1%) and κ-carrageenan (1%) solutions at a 1:1 ratio under heating and stirring (Table 1). After that, we incorporated an aqueous CQD dispersion before gelation (0.1% CQD loading). The mixture was added dropwise into a bath containing 1.5% $CaCl_2$ and 0.3% KCl, and the resulting beads were washed and then dried overnight at 40 °C. The resulting materials were evaluated in terms of morphological, physical, and micromeritic properties.

Table 1. Morphological, physical and micromeritic properties.

	SA+K-car	SA+K-car+CQD
Projected area	2.5749±0.5596	1.9794±0.143966
Projected perimeter	6.3266±0.62687	5.329±0.239499
Equivalent diameter	1.8013±0.183723	1.586683±0.05795
Circularity	0.8098±0.1314	0.8768±0.0525
Aspect ratio	1.2917±0.21546	1.26232±0.13641
Roundness	0.7915±0.1175	0.7992±0.084028
Solidity	0.96±0.0150	0.967±0.009434
Elongation	0.3526±0.2264	0.329464±0.15378
Eccentricity	0.5830±0.1533	0.587428±0.11311
Rectangularity ratio	0.7870±0.0550	0.786057±0.05990
Roughness	3.0184±0.3158	2.866543±0.05851
Mean bead size (mm); n=90	1.38782±0.31647	1.52411±0.31034
Bulk density (g/ml)	0.62551	0.6706
Tapped density (g/ml)	0.66721	0.7185
Particle density (g/ml)	1.61	1.25
Porosity (%)	61.14845	46.352
Hausner's ratio	1.06667	1.07143
Carr's index (%)	6.24991	6.66667
Settling velocity (cm/s)	4.77941	6.5

Following physicochemical characterization, the water sorption behavior of the hydrogel beads was evaluated over three consecutive cycles to assess their water uptake capacity and retention upon repeated use.

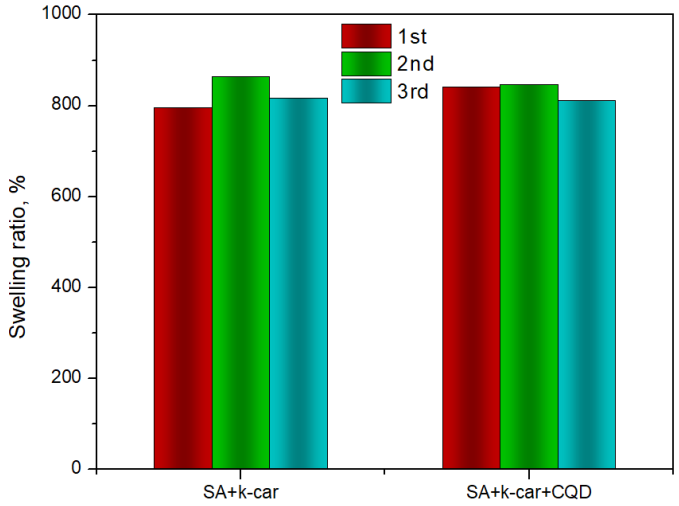


Figure 1. Sorption profiles of CQD-free and CQD-loaded hydrogels across the three cycles.

All hydrogel formulations exhibited maximum water sorption values above 800% in each of the three consecutive adsorption–desorption cycles (Figure 1).

Additionally, we monitored fluorescence in the aqueous medium at 24 h intervals up to 96 h to investigate the release of fluorescent species from the CQD-loaded hydrogels.

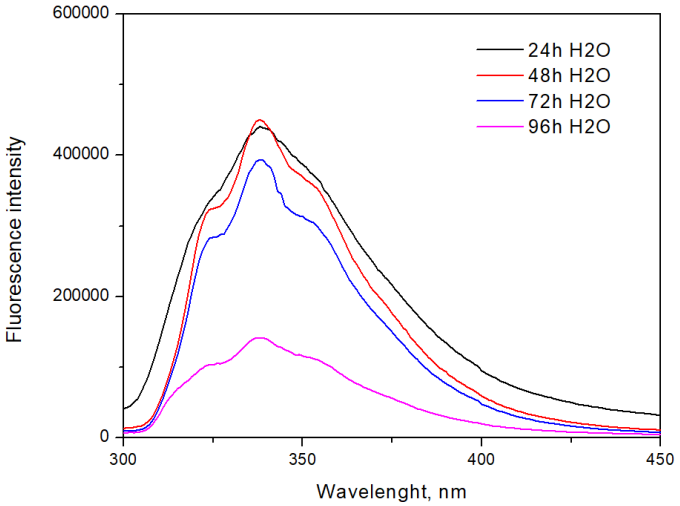


Figure 2. Fluorescence spectra of aqueous fractions collected during hydrogel immersion.

Detectable fluorescence in the 72–96 h fraction suggests prolonged release of CQD-associated fluorescent species from the hydrogel beads over the investigated period (Figure 2).

Reference

[1] X. Yang, S. Fu, A.H. Basta, L. Lucia, *BioResources* 2024, 19, 6838-6858.
[2] Y. Wang, Z. Liang, Z. Su, K. Zhang, J. Ren, R. Sun, X. Wang, *ACS Appl. Bio Mater*. 2018, 1, 1398-1407.
[3] Z. Li, Z. Lin, *Aggregate* 2021, 2, e21.

PP7. EXTENDED π-CONJUGATED SCHIFF BASE COMPLEXES OF TRANSITION AND RARE-EARTH METALS

Robert I. Botea*, Augustin Madalan
Faculty of Chemistry, University of Bucharest, Bucharest, Romania
**ioan.botea@s.unibuc.ro*

We report the synthesis of mononuclear and heterometallic binuclear complexes of 3d, 4d, and 4f metals based on Schiff base ligands featuring extended p-conjugated systems. These polydentate ligands were reacted with Zn(II) triflate or perchlorate and Pd(II) chloride, generating mononuclear complexes with tetrahedral and square-planar coordination geometries. The synthetic route for the Zn(II) complexes is shown in Figure 1. The corresponding 4f complexes were obtained by reacting the ligands with rare-earth hexafluoroacetylacetonates, $Ln(hfac)_3 \cdot nH_2O$, resulting in square-antiprismatic coordination geometries. The structures and coordination environments of the complexes were established by single-crystal X-ray diffraction.

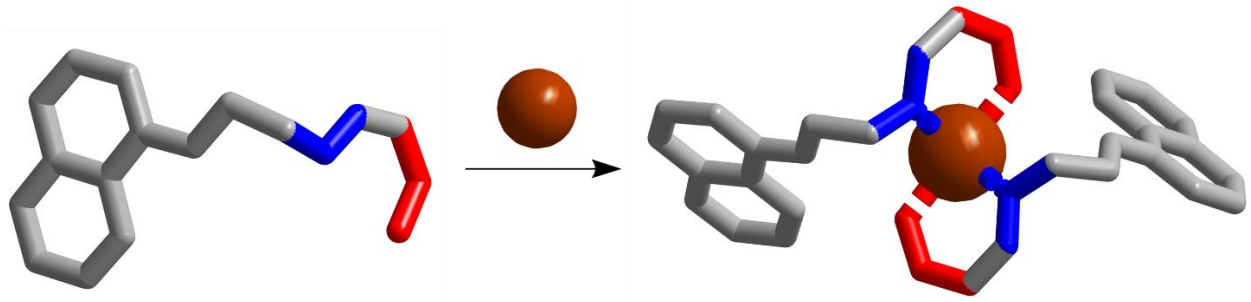


Figure 1. Schematic synthesis of 3d complexes using Schiff base ligands.

The photophysical properties of the Eu(III) and Tb(III) complexes were also investigated. The extended π-conjugated systems can act as antenna chromophores, facilitating energy transfer to the lanthanide centres and sensitizing their characteristic emission. In particular, near-infrared emission is of interest for potential biomedical imaging applications, owing to its relatively high tissue penetration and reduced photodamage [2]. We also employed a sequential synthetic approach to obtain 3d-4f heterometallic assemblies, using the pre-formed Zn(II) complex as a coordination platform for lanthanide incorporation. This approach provides an opportunity to investigate how the introduction of lanthanide ions influences the photophysical properties of the resulting systems.

In addition, we are investigating the potential DNA-binding properties of these complexes, with particular emphasis on the Pd(II) derivatives. Their extended aromatic systems may favor p - p stacking interactions with the nucleobases of DNA [3]. Figure 2 presents the proposed intercalation and covalent binding mechanisms, which provide a basis for further investigating the interaction of these complexes with DNA and their potential biological activity.

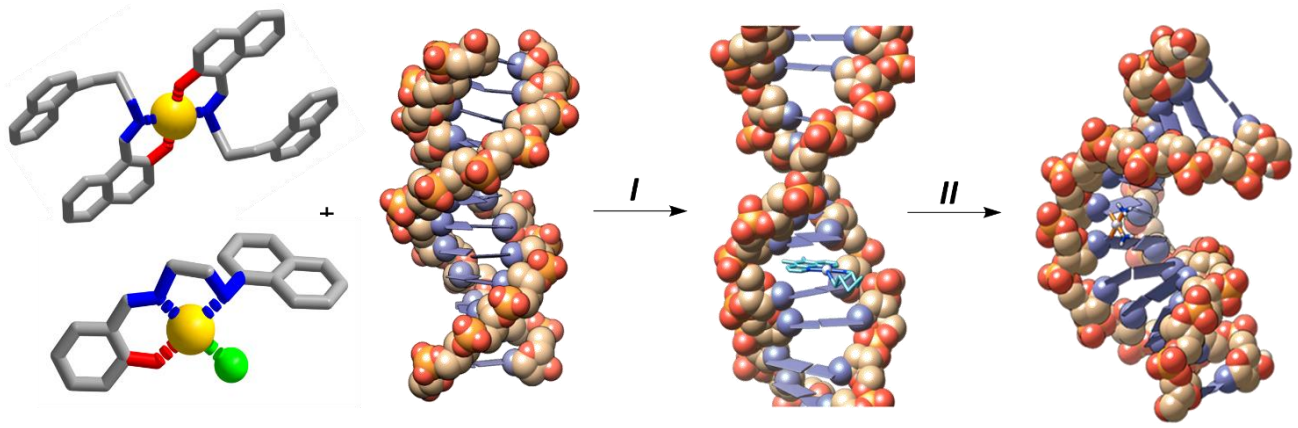


Figure 2. Proposed intercalation mechanisms and corresponding conformational changes; Intercalation (I) and covalent bonding (II).

References

[1] M. Andruh, *Dalton Trans.* 2015, 44, 16633-16653.
[2] Y. Ning, M. Zhu, J.-L. Zhang, *Coord. Chem. Rev*. 2019, 399, 213028.
[3] S.N. Mbugua, N.R. S. Sibuyi, L.W. Njenga, *ACS Omega* 2020, 5, 14942-14954.

PP8. EXPLORING LIGNIN MODEL DIMER INTERACTIONS IN IMIDAZOLIUM-BASED IONIC LIQUIDS THROUGH MOLECULAR DYNAMICS SIMULATIONS

Narcis Cibotariu[1]*, Aatto Laaksonen[1,2]
[1]*Petru Poni Institute of Macromolecular Chemistry, Romanian Academy, Iasi, Romania*
[2]*Department of Materials and Environmental Chemistry, Division of Physical Chemistry, Arrhenius Laboratory, Stockholm University, Stockholm, Sweden*
**cibotariu.narcis@icmpp.ro*

Lignin comprises about 15% to 40% of lignocellulosic biomass and is a large renewable source of aromatic compounds; however, most of the industrially separated lignin is still burned to produce heat [1]. To convert it to chemicals or materials, the lignin needs to be dissolved. Its aggregation hinders the dissolution and, in model compounds, it even creates a higher barrier for cleaving the ether bonds [2].

In this context, ionic liquids (ILs) are attractive solvents because they are able to dissolve lignin and their properties can be adjusted through the choice of the anion and the cation [3]. The number of possible ion combinations is large; however, selecting among them necessitates an understanding of the interactions between the ions and lignin, as well as the interactions among lignin fragments, which determine the dispersion of lignin. Lignin fragments can associate through hydrogen bonds between hydroxyl groups and through contacts between aromatic rings, either π–π stacking [3] or less specific hydrophobic contacts. Hydrogen bond associations are relatively straightforward to identify with current analytical tools, whereas ring contacts are harder to characterize: rings can meet face to face, offset or edge to face, and a measurement averaged over the whole sample hardly separates these arrangements. Molecular dynamics (MD) is a computational technique through which each contact can be examined individually, with its partner, the groups involved and its geometry, and we used it to study how the anion of an IL changes the balance between these two modes of association.

Because native lignin has no unique molecular structure, we chose a model dimer built around the *β*-O-4 ether linkage, the most prevalent bond in lignin [4]. This dimer contains two methoxylated aromatic rings and three hydroxyl groups and, due to its simple structure, it has also been used in other studies involving ILs [2, 3]. In this study, the lignin dimer was simulated in four imidazolium-based ILs that share the same cation, bearing an acidic group at the end of its side chain, and differ in the anion, from a weakly coordinating one (A1) to stronger hydrogen-bond acceptors (A2-A4). Each IL system contained 100 dimers, and was simulated in three independent replicas of 1 μs. Each aromatic ring was represented by its ring center of mass (COM), the six carbons of a lignin ring, the five ring atoms of the imidazolium cation. The radial distribution function (RDF), $g(r)$, between ring COMs of different dimers compares the number of rings found at a distance r with the number expected for a random distribution at the same density. A cation ring was counted as stacked on a lignin ring when the two COMs were closer than 5.5 Å, the ring planes deviated by less than 30° from parallel and the lateral offset was below 2.5 Å [5].

Hydrogen bonds between different dimers were rarely observed in our simulations. Anions formed hydrogen bonds with the dimer more frequently at the phenolic hydroxyl compared to either aliphatic hydroxyl group. Figure 1 shows the interaction between a lignin ring and the ring structure of another lignin or cation. The intermolecular ring RDFs exhibit their first maximum at approximately 6 Å, with $g(r) > 1$ in all liquids, indicating an excess of ring proximity compared to a uniform reference. The average population values for the four liquids (A1-A4) were ~20, 23, 32, and 39 ring pairs per 100 dimers, with the average for A4 being around 1.9 times greater than that of A1. The data on ring orientation at small separation distances indicated comparable enrichment of nearly parallel orientation angles for rings across different dimers.

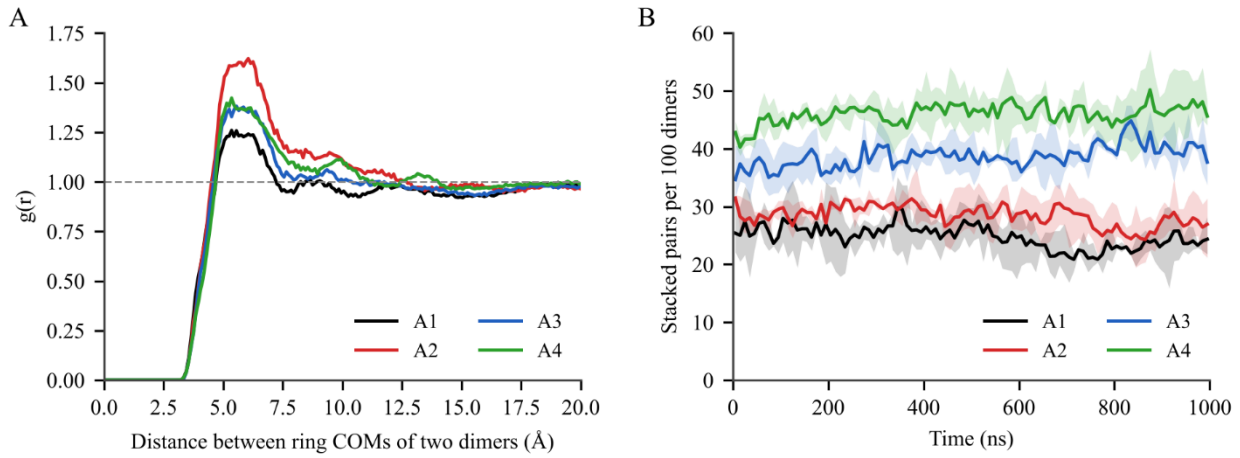


Figure 1. (A) RDF between the ring COMs of different lignin dimers. (B) Cation rings stacked on lignin rings per 100 dimers over the 1 μs trajectories, with the line indicating the mean of three replicas and the band illustrating the range between replicas.

These results demonstrate that in the investigated ILs, the anion typically interacts with the hydroxyl groups of lignin, while the cation occupies the space surrounding the aromatic rings of lignin. Moreover, neither ion reduces the proximity between the rings of different lignin fragments. Therefore, assessing the ability of an ionic liquid to solubilize lignin requires an investigation of both types of interactions, with molecular dynamics providing a direct method for this evaluation.

References

[1] A.J. Ragauskas, G.T. Beckham, M.J. Biddy, R. Chandra, F. Chen, M. F. Davis, B.H. Davison, R.A. Dixon, P. Gilna, M. Keller, P. Langan, A.K. Naskar, J. N. Saddler, T.J. Tschaplinski, G.A. Tuskan, C.E. Wyman, *Science* 2014, 344, 1246843.
[2] Y. Zhang, F. Huo, Y. Wang, Y. Xia, X. Tan, S. Zhang, H. He, *Front. Chem.* 2019, 7, 78.
[3] M. Mohan, H. Choudhary, A. George, B.A. Simmons, K. Sale, J.M. Gladden, *Green Chem.* 2021, 23, 6020-6035.
[4] J. Zakzeski, P.C.A. Bruijnincx, A.L. Jongerius, B.M. Weckhuysen, *Chem. Rev.* 2010, 110, 3552-3599.
[5] K. Hackenstrass, N. Tabudlong Jonasson, M. Hartwig-Nair, T. Rosén, S. Florisson, M. Wohlert, *Faraday Discuss.* 2026, 263, 52-64.

Acknowledgment: This work is supported by European Union's Horizon Europe research and innovation programme under grant agreement No 101086667, project BioMat4CAST (BioMat4CAST - "Petru Poni" Institute of Macromolecular Chemistry Multi-Scale In Silico Laboratory for Complex and Smart Biomaterials).

PP9. MOLECULARLY IMPRINTED POLYMER-BASED ELECTROCHEMICAL SENSORS FOR BIOGENIC AMINES DETECTION – A REVIEW

Andreea-Loredana Comanescu*, Andra-Georgiana Trifan, Constantin Apetrei
Faculty of Sciences and Environment, "Dunarea de Jos" University of Galati, Galati, Romania
**Andreea.Comanescu@ugal.ro*

Biogenic amines (BAs) are organic compounds produced by the microbial decarboxylation of amino acids in fermented products. Therefore, the biogenic amine content in fermented products can serve as an indicator of their freshness or spoilage and can be used to assess food quality, as well as to prevent health issues caused by abnormal levels of these compounds. Food products such as dairy (cheese, yogurt), meat and processed meat products (chicken breast, salami), fish (tuna, anchovies) as well as fermented beverages (beer and wine)—which are consumed in large quantities worldwide— may contain significant amounts of biogenic amines, such as cadaverine, putrescine, histamine, tyramine, phenylethylamine, etc.; and upon ingestion, these can cause allergies, food poisoning, abdominal pain, and hypotension [1]. Therefore, it is necessary to develop a simple, rapid, and effective method for detecting these compounds of interest.

Several techniques for the detection of BAs have been proposed in the specialized literature, namely: chromatographic techniques (ultra-high-performance liquid chromatography (UHPLC) [2], gas chromatography–mass spectrometry (GC-MS) [3], ion chromatography (IC) [4], and electrophoretic techniques (capillary electrophoresis (CE) [5]). Although these techniques exhibit sensitivity and selectivity in the detection of biogenic amines, they require complex and expensive equipment, qualified personnel, and elaborate sample preparation—consequently consuming large quantities of reagents and solvents. In contrast, electrochemical sensors based on molecularly imprinted polymers (MIP) appear to be a promising alternative to chromatographic and electrophoretic techniques; this is because, in addition to the advantages offered by electrochemical methods (rapidity, simplicity, and sensitivity), their modification with MIP also provides selectivity (due to a design specific to the target analytes) [6].

MIP is formed by combining a functional monomer and a template (the target analyte) in the presence of a cross-linking agent, followed by polymerization of the mixture and removal of the template. Essentially, MIP contains sites specific to the target molecule and is capable of selectively identifying and binding only the molecule of interest (as can be seen in Figure 1). The most frequently used functional monomers are carboxylic acids (vinylbenzoic acid, acrylic acid), sulfonic acids, and heteroatomic bases (vinylimidazole, vinylpyridine), while the most commonly used cross-linking agents are ethylene glycol dimethacrylate (EGDMA), divinylbenzene (DVB), and trimethylolpropane trimethacrylate (TRIM) [7]. MIP-based electrochemical sensors are typically obtained by depositing a polymer—synthesized in the laboratory—onto the surface of a commercial electrochemical sensor. They are used to rapidly, sensitively, and selectively detect the analyte of interest.

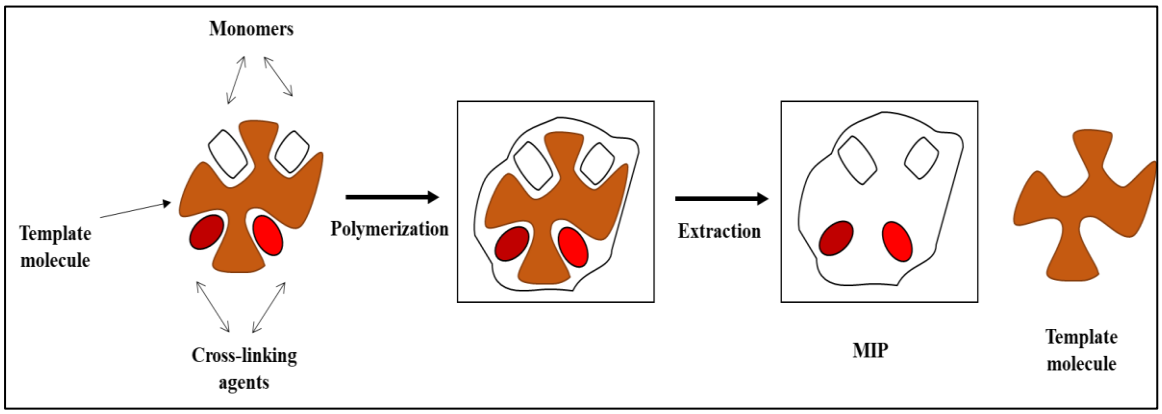


Figure 1. Graphical representation of the molecular imprinting of a polymer.

Over the years, several studies related to the detection of biogenic amines using MIP-based electrochemical sensors have been published in the scientific database (Google Scholar). Therefore, the aim of this study was to evaluate existing research to identify new configurations of MIP sensors and to determine the extent to which these polymers have improved the detection limit for the biogenic amine of interest. The MIP-based electrochemical sensors reported in the scientific literature generally rely on the detection of histamine and tyramine, likely due to the fact that histamine and tyramine poisonings are the most frequent. The electrochemical performance of the developed MIP sensors was investigated using electrochemical techniques such as cyclic voltammetry (CV), amperometry (Amp), square-wave voltammetry (SWV), and differential pulse voltammetry (DPV). By combining MIPs with various nanomaterials (gold nanoparticles, MXene, carbon nanotubes), researchers achieved detection limits in the micromolar-femtomolar range (due primarily to the nanomaterials) as well as rapid analysis, increased selectivity, stability, and repeatability (due to the polymers used). To demonstrate their practical applicability, the sensors were tested and validated on various sample matrices: food samples such as fish (tuna, black pomfret, mackerel), yogurt, beef, and soy sauce; fermented beverages such as beer and wine; and biological samples such as human serum. Good analytical recoveries confirm that the sensors developed by the researchers can be used for both biomedical and food industry applications [8], [9], [10], [11], [12].

References

[1] S.K. Kannan, B. Ambrose, S. Sudalaimani, M. Pandiaraj, K. Giribabu, M. Kathiresan, *Anal. Methods* 2020, 12, 3438-3453.
[2] E. Dadáková, M. Křížek, T. Pelikánová, *Food Chem.* 2009, 116, 365-370.
[3] W. Wojnowski, J. Namieśnik, J. Płotka-Wasylka, *Microchem. J.* 2019, 145, 130-138.
[4] A. Jastrzębska, A. Piasta, E. Szłyk, *J. Anal. Chem.* 2015, 70, 1131-1138.
[5] N. Zhang, H. Wang, Z.-X. Zhang, Y.-H. Deng, H.-S. Zhang, *Talanta* 2008, 76, 791-797.
[6] L. Wang, M. Pagett, W. Zhang, *Sens. Actuators Rep.* 2023, 5, 100153.
[7] G. Vasapollo, R. Del Sole, L. Mergola, M.R. Lazzoi, A. Scardino, S. Scorrano, G. Mele, *Int. J. Mol. Sci.* 2011, 12, 5908-5945.
[8] S. Li, T. Zhong, Q. Long, C. Huang, L. Chen, D. Lu, X. Li, Z. Zhang, G. Shen, X. Hou, *Microchem. J.* 2021, 171, 106844.
[9] M. Akhoundian, A. Rüter, S. Shinde, *Sensors* 2017, 17, 645.
[10] J. Huang, X. Xing, X. Zhang, X. He, Q. Lin, W. Lian, H. Zhu, *Food Res. Int.* 2011, 44, 276-281.
[11] Z. Shi, H. Guo, X. Jia, X. Song, X. Zhao, Y. Zhu, S. Wu, *J. Alloys Compd.* 2026, 1076, 189392.
[12] S. Khumngern, P. Khanaaekwichaporn, A. Numnuam, N. Nontipichet, P. Limsakul, P. Thavarungkul, C. Thammakhet-Buranachai, *Food Chem.* 2026, 519, 149699.

PP10. POTENTIAL APPLICATIONS OF PHYTOCHEMICAL AND SYNTHETIC ANTI-INFLAMMATORY COMPOUNDS

Manuela Elena Covit[1], Denis Ionut Defta[1], Fanica Balanescu[2], Anna Busuioc[1], Andreea Veronica Botezatu[1]*, Rodica Mihaela Dinica[1]*
[1]*Faculty of Science and Environment, "Dunarea de Jos" University of Galati Galati, Romania*
[2]*Faculty of Medicine and Pharmacy, "Dunarea de Jos" University of Galati, Galati, Romania*
**rodica.dinica@ugal.ro, andreea.botezatu@ugal.ro*

Chronic inflammation is associated with the physiological and pathological processes of various diseases, including obesity, atherosclerosis, rheumatoid arthritis, gout, Alzheimer's disease, depression, Parkinson's disease, and cancer. Worldwide, more than 50% of deaths are attributed to conditions such as strokes, cancer, obesity, and diabetes [1,2].

Modern medicine treats inflammatory disorders primarily with non-steroidal anti-inflammatory drugs (NSAIDs) and corticosteroids. Currently available anti-inflammatory drug therapies are often insufficient or lead to intolerable side effects [3]. Plant-derived compounds are used in the formulation of pharmaceutical products currently available on the market. Their topical administration in dosage forms such as ointments offers the advantage of reducing the risk of systemic adverse effects on the stomach, kidneys, and liver. In this context, topical formulations containing plant extracts represent a promising alternative for the relief of localised pain.

This study aimed to obtain plant extracts from *Symphytum officinale* (comfrey) rich in bioactive phytochemicals, to evaluate the *in vitro* antioxidant and anti-inflammatory effects of plant extracts, and to develop an ointment containing plant extract and a synthetic anti-inflammatory agent. Future studies will focus on physicochemical properties and stability of the ointment, alongside evaluating its anti-inflammatory efficacy through *in vitro* and *in vivo* assays.

The plant material, *Symphytum officinale* (comfrey) roots, was purchased from a special store and ground into a powder using an electric grinder. Extraction was performed using 80% ethyl alcohol under conventional reflux conditions, and alternatively *via* ultrasound-assisted extraction (Figure 1). The extracts were analysed for allantoin content, and their potential anti-inflammatory activities were assessed in comparison with a synthetic drug using the HSA thermal denaturation inhibition test [4]. Diclofenac sodium (Merck), plant extracts, cholesterol, lanolin, and petrolatum were used to prepare the ointment. The obtained ointment was analysed using FT-IR and UV–Vis spectroscopy after 1 day, 7 days, 30 days, and 90 days. Ultrasound-assisted extraction (UAE) yielded higher yields than conventional reflux extraction (CE). These differences demonstrate ultrasound's effectiveness in facilitating mass transfer and accelerating the release of compounds soluble in the extraction solvent. A higher allantoin content was determined in the comfrey root extract obtained by UAE (29.97 µg/mg extract) compared with that obtained by CE (25.98 µg/mg extract). The extracts demonstrated *in vivo* anti-inflammatory potential, similar to a synthetic drug (diclofenac sodium). From an organoleptic perspective, the ointment was characterised by a greasy consistency, dark chartreuse colour, and a characteristic herbal odour. Furthermore, no aggregation or phase separation was observed. Regarding pH, the initial value was 6.00, slightly decreasing to 5.90 three months after preparation.

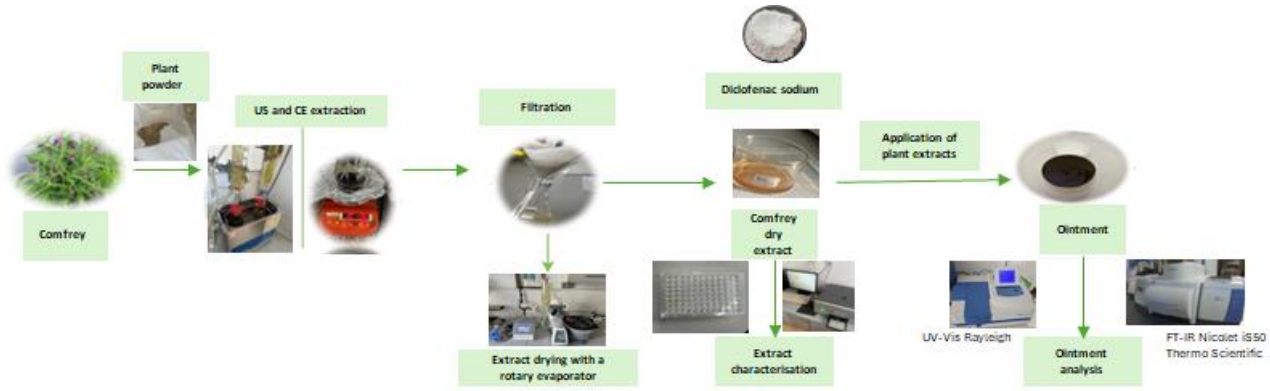


Figure 1. The schematic representation of plant extraction and its potential application in obtaining an ointment.

Furthermore, no aggregation or phase separation was observed. Regarding pH, the initial value was 6.00, slightly decreasing to 5.90 three months after preparation. In the IR spectrum of the ointment, characteristic vibrational bands corresponding to chemical bonds in the structures of the active ingredients (diclofenac sodium and plant extract) were observed, along with other lower-intensity bands attributable to the excipients. The persistence of the vibrational bands over time, together with the absence of newly appearing bands, indicates the stability of the obtained pharmaceutical formulation and suggests that no detectable chemical changes occurred over the 90 days. Comparison of the UV–Vis spectra of the ointment immediately after preparation, after 1 day, after 30 days, and after 90 days revealed that the overall spectral profile and the positions of the absorption maxima were maintained, with no new bands appearing. These findings suggest good chemical stability of the compounds containing chromophore groups. Thus, the ointment spectrum reflected the overlapping contributions of synthetic and naturally occurring chromophores, as well as their stability over a 90-day period.

In conclusion, the data obtained support the utilisation of plant materials as sources of bioactive phytochemicals with anti-inflammatory properties, with the potential for integration into the pharmaceutical and cosmetic industries, thereby reducing reliance on animal-derived resources or synthetic compounds and contributing to the development of more sustainable products.

References

[1] D. Furman, J. Campisi, E. Verdin, P. Carrera-Bastos, S. Targ, C. Franceschi, L. Ferrucci, D.W. Gilroy, A. Fasano, G.W. Miller, A.H. Miller, A. Mantovani, C.M. Weyand, N. Barzilai, J.J. Goronzy, T.A. Rando, R.B. Effros, A. Lucia, N. Kleinstreuer, G.M. Slavich, *Nat. Med*. 2019, 12, 1822-1832.
[2] R. Bai, C. Yao, Z. Zhong, J. Ge, Z. Bai, X. Ye, T. Xie, Y. Xie, *Eur.J.Med.Chem.* 2021, 213, 113165.
[3] G.M. Slavich, *Brain.Behav.Immun.* 2015, 45, 13–14.
[4] R.M. Dinica, C. Sandu, A.V. Dediu Botezatu, A. Cazanevscaia Busuioc, F. Balanescu, M.D. Ionica Mihaila, C.N. Dumitru, B. Furdui, A.V. Iancu, *Sustainability*. 2021, 13, 10170.

Acknowledgement: This work was partially supported by the UDJG internal Grant" Targeted therapeutic molecules, anti-inflammatory and antitumor, isolated from exotic plants acclimatised in Romania", funding contract no. 7956/31.03.2025.

PP11. ELECTROCHEMICAL DETECTION OF POLYPHENOLIC COMPOUNDS OF INTEREST IN WINES – A REVIEW –

Andrei-Daniel Geman*, Constantin Apetrei
Faculty of Science and Environment, "Dunarea de Jos" University of Galati, Galati, Romania
**gemanandreiga@gmail.com, constantin.apetrei@ugal.ro*

Phenolic compounds are natural compounds found in plants and are divided into two main groups: flavonoids and non-flavonoids. They are found in numerous plant-based foods, such as fruit, vegetables, cereals, tea, coffee, wine and spices, although their quantities vary depending on the source. Regular consumption of these foods can deliver numerous health benefits thanks to the antioxidant properties of phenolic compounds. These substances help to scavenge free radicals and reduce oxidative stress, thereby protecting cells from damage. As a result, they may help to lower the risk of certain diseases, including cardiovascular disease, atherosclerosis, inflammatory conditions and some types of cancer. For these reasons, phenolic compounds are being extensively studied for their role in human health and their contribution to the nutritional value of plant-based foods [1]. Traditional analytical methods, including capillary electrophoresis, spectroscopy, chromatography and nuclear magnetic resonance (NMR), are widely used to identify and quantify chemical compounds in wines. Although these methods are effective in detecting certain polyphenolic compounds, they often require expensive equipment, specialized laboratories and highly qualified staff, and the instruments are often bulky. Furthermore, their implementation may involve complex sample preparation procedures and relatively long analysis times, as well as large quantities of solvents, which can limit their suitability for rapid, routine measurements. Therefore, in this context, researchers have begun to look for more effective alternatives, and electrochemical detection has emerged as a promising alternative due to its simplicity, cost-effectiveness, rapid response and ease of use.

This approach is based on monitoring changes in electric current or potential generated by the electrochemical processes taking place at the electrode surface, enabling both the qualitative identification of analytes and the quantitative determination of their concentrations. Despite these advantages, the electrochemical determination of polyphenols in wines presents a number of analytical challenges. The development of more sensitive and selective electrochemical methods could, therefore, facilitate the reliable determination of polyphenols at lower concentrations and broaden the scope of these techniques in wine analysis and quality assessment. Consequently, these criteria have become factors of interest in studies conducted in recent years. The aim of this review is to highlight recent developments in the field of electrochemistry, the most commonly used electrochemical techniques, the screen-printed electrode variants employed, as well as to highlight the main areas of development and identify gaps in the specialist literature, which may serve as starting points for future studies. In this context, electrochemical techniques such as cyclic voltammetry, differential pulse voltammetry, and square-wave voltammetry have been widely employed to assess both total polyphenol content and individual polyphenol classes by measuring anodic signals, including peak currents and the areas under voltammograms, within characteristic potential ranges [2].

Screen-printed electrodes have been widely used by scientists for the electrochemical analysis of polyphenols in wine. Of the various types available, screen-printed carbon electrodes (SPCE) are commonly used as detection platforms due to their simplicity, low cost and adaptability to the analyte of interest. To improve their sensitivity and selectivity, researchers used various nanomaterials and biologically active compounds, such as single-walled carbon nanotubes, metal oxide nanoparticles - Zinc oxide (ZnO), iron oxide nanoparticles Iron oxide nanoparticles (Fe_3O_4 NPs), manganese oxide (MnO_2), copper oxide nanoparticle (CuONP), cerium oxide nanoparticles (CeO_2 NPs), and enzymes such as laccase and tyrosinase to modified these electrodes [3]. These modifications to screen-printed electrodes and the development of electrochemical biosensors can improve the electrochemical response and contribute to the development of more efficient methods for the detection and quantification of polyphenols in wine samples. Biosensors have attracted the attention of researchers primarily due to their remarkable advantages in terms of detection and quantification limits, as they are much more sensitive to the analyte of interest – in this case, polyphenolic compounds. SPCE and SPCE-based biosensors offer an innovative approach to analytical methods, as they enable the development of an analytical platform capable of analyzing the compounds of interest on-site, thereby reducing the costs associated with traditional analyses [4]. Among spectroscopic techniques, FTIR (Fourier Transform Infrared Spectroscopy) has been successfully used to characterize the modified SPCE surface, as it provides information on the chemical composition and functional groups present on the electrode. This technique allows the surface modification to be confirmed and contributes to the assessment of the material's chemical stability following electrochemical measurements. This approach is non-destructive and non-invasive, which allows the screen-printed electrodes to be reused in further experimental measurements. Furthermore, FTIR analysis can provide information on possible interactions between the electrode surface and the analyte during the detection process [5]. By reviewing recent advances in open-access literature on the electrochemical analysis of polyphenols in wine samples, this review provides information on the analytical performance of various voltametric techniques, nanotechnologies and surface-modified materials, as well as their applicability in various sample matrices – supported by the results obtained in recent years.

References

[1] P.C. Pwavodi, V.H. Ozyurt, S. Asir, M. Ozsoz, *Micromachines* 2021, 12(3), 312.
[2] Y. Cheng, J. Yu, *Sensors and Actuators A: Physical* 2024, 365, 114912.
[3] M. Moreno, A. Sánchez Arribas, L. González, E. Bermejo, A. Zapardiel, M. Chicharro, *Microchemical Journal* 2021, 162, 105836.
[4] E.R. Ahmed, F.M. Abou-Elella, A.M. Abdelmonem, M.A. Ali, *Chemical and Biological Technologies in Agriculture* 2025, 12(1), 171.
[5] X. Chen, Q. Xi, F. Sun, L. Zou, Y. Li, *Naunyn-Schmiedeberg's Archives of Pharmacology* 2025, 398(4), 4247–4263.

PP12. DNA CONDENSATION BY 4-ARM PEG–HISTIDINE/LYSINE PEPTIDE POLYPLEXES: TUNING TRANSFECTION AND BIOCOMPATIBILITY

Razvan Ghiarasim*, Dragos Peptanariu*, Mihaela Silion, Alina Nicolescu, Lucian Bahrin, Mariana Pinteala
Petru Poni Institute of Macromolecular Chemistry, Romanian Academy, Iasi, Romania
**peptanariu.dragos@icmpp.ro; ghiarasim.razvan@icmpp.ro*

Histidine- and lysine-rich peptides are versatile building blocks for non-viral gene delivery, combining DNA-binding capacity with functionalities relevant to intracellular transport [1,2]. Their conjugation to multi-arm polyethylene glycol (PEG) provides a modular approach to controlling carrier architecture and biological performance. This study investigates the influence of peptide length and PEG molecular weight on DNA condensation, colloidal behaviour, transfection efficiency and biocompatibility. Two peptide sequences, Cys-$(His)_6$-$(Lys)_3$-$(His)_6$ (HL1) and Cys-$(His)_6$-$(Lys)_3$-$(His)_6$-$(Lys)_3$-$(His)_6$ (HL2), were conjugated to maleimide-functionalized 4-arm PEG cores of 2 or 20 kDa through thiol–maleimide coupling (Figure 1).

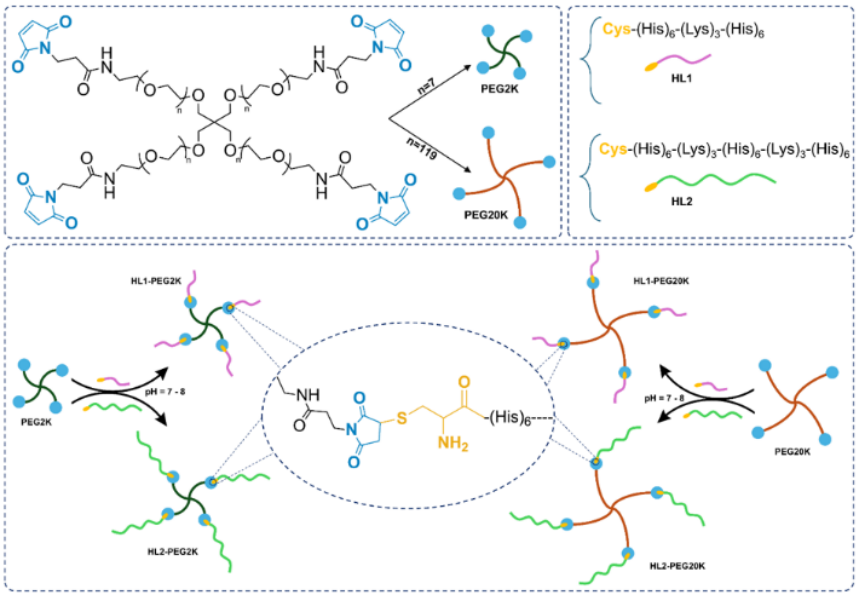


Figure 1. Schematic illustration of the design of vectors based on a PEG core functionalized with HL1 (HL1-PEG2K and HL1-PEG20K) and HL2 (HL2-PEG2K and HL2-PEG20K) peptide sequences.

The resulting conjugates, HL1-PEG2K, HL1-PEG20K, HL2-PEG2K and HL2-PEG20K, were investigated alongside the corresponding free peptides. Conjugation was confirmed by ^{1}H NMR and MALDI-TOF mass spectrometry. DNA complexation and polyplex properties were evaluated using GelRed displacement, DNase I protection, dynamic light scattering, zeta potential measurements and atomic force microscopy. The longer HL2 peptide exhibited higher DNA-binding affinity and displacement capacity than HL1. Nevertheless, all formulations provided strong protection against DNase I over 30 min at a peptide/DNA mass ratio of 100.

PEG molecular weight strongly influenced polyplex organization: PEG2K improved the short-term colloidal stability of HL1-based complexes in complete culture medium, whereas PEG20K formulations exhibited heterogeneous dispersions and aggregate or network-like morphologies. HL2/DNA and HL2-PEG2K/DNA retained measurable particle populations for 24 h in medium supplemented with 10% serum, although DLS alone cannot establish preservation of intact polyplexes. Luciferase assays in human osteosarcoma (HOS) cells demonstrated a pronounced dependence of transfection on carrier architecture (Figure 2).

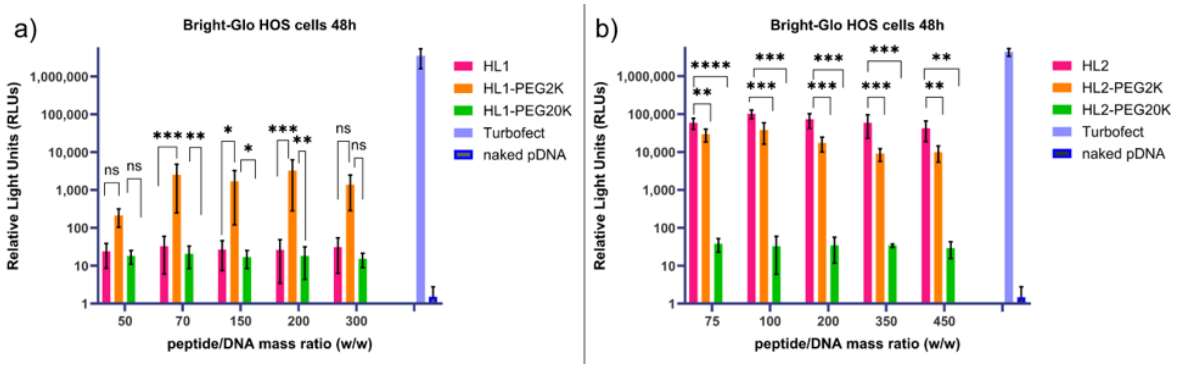


Figure 2. Transfection efficiency of (a) HL1- and (b) HL2-based polyplexes in HOS cells. Luciferase activity was measured 48 h after delivery of 500 ng/well pCS2+MT-Luc plasmid. Results represent mean ± SD (n = 8); TurboFect and naked plasmid DNA served as controls.

Unmodified HL2 achieved the highest transfection efficiency at a peptide/DNA mass ratio of 100. PEG2K enhanced HL1-mediated transfection approximately 100-fold but reduced HL2-mediated transfection by 2–6-fold, while PEG20K impaired both systems, highlighting the balance between PEG-mediated stabilization and cellular interactions [3]. HL1 polyplexes and HL2/DNA maintained HOS cell viability above 90%, whereas HL2-PEG2K/DNA reduced viability to approximately 72% at a mass ratio of 100. In human dermal fibroblasts, HL2-PEG2K/DNA viability decreased with increasing mass ratio, reaching approximately 66% at 150. No significant acute ROS response was detected after 60 min. The 4-arm PEG–peptide architecture provides a tuneable scaffold for DNA delivery. While free HL2 offered the highest transfection efficiency, HL2-PEG2K combined gene delivery activity with a modular PEG framework. Further optimization of peptide density and PEG functionalization is required to balance transfection and biocompatibility and to explore future targeting-ligand conjugation.

References

[1] J. Thomas, K. Punia, J.K. Montclare, *Pept. Sci.* 2021, 113, e24189.
[2] M.L. Read, S. Singh, Z. Ahmed, M. Stevenson, S.S. Briggs, D. Oupicky, L.B. Barrett, R. Spice, M. Kendall, M. Berry, J.A. Preece, A. Logan, L.W. Seymour, *Nucleic Acids Res.* 2005, 33, e86.
[3] J.J.F. Verhoef, T.J. Anchordoquy, Drug Deliv. *Transl. Res.* 2013, 3, 499–503.

Acknowledgment: This paper is supported by European Union's Horizon Europe research and innovation programme under grant agreement No 101086667, project BioMat4CAST (BioMat4CAST - "Petru Poni "Institute of Macromolecular Chemistry Multi-Scale in Silico Laboratory for Complex and Smart Biomaterials) and by a grant from the National Research Authority, project no. PNRR-III-C9-2023-I8-161, MultiPodGaN, contract no. 760285/27.03.2024, within the National Recovery and Resilience Plan.

PP13. Mn-DOPED ALUMINIUM IRON OXIDES AS ADVANCED MATERIALS FOR WASTEWATER REMEDIATION

Ionela Grecu[1]*, Maria Emiliana Fortuna[1], Alexandra Lapusneanu[2], Ioan-Andrei Dascalu[1], Andra-Cristina Enache[1], Corneliu Cojocaru[1], Petrisor Samoila[1]
[1]*Petru Poni Institute of Macromolecular Chemistry, Romanian Academy, Iasi, Romania*
[2]*"Costache Negruzzi" National College, Iași, Romania*
**grecu.ionela@icmpp.ro*

Environmental pollution has emerged as a critical global challenge, driven by accelerated industrialization, urban expansion, population growth, and escalating resource consumption. These anthropogenic activities have intensified the release of hazardous pollutants into natural ecosystems, threatening ecological integrity and human health. Aquatic systems are particularly susceptible to contamination due to the continuous discharge of industrial effluents, agricultural discharges, pharmaceutical residues, and untreated or inadequately treated domestic wastewater. The increasing prevalence of toxic and recalcitrant contaminants, including toxic heavy metals, synthetic dyes, pesticides, pharmaceutical compounds, and microplastics, further complicates wastewater treatment strategies owing to their chemical stability, toxicity, resistance to degradation, and significant ecological and public health risks. Although conventional treatment technologies, such as coagulation–flocculation, membrane filtration, biological processes, and chemical oxidation, are widely implemented, their effectiveness may be constrained by incomplete contaminant removal, limited selectivity, substantial operational costs, and the potential generation of secondary waste streams. These challenges highlight the growing demand for developing advanced and sustainable materials with enhanced adsorption and catalytic capabilities, capable of efficiently removing a broad spectrum of pollutants from complex wastewater matrices [1, 2].

In this context, metal oxide nanomaterials have emerged as particularly promising candidates owing to their structural versatility, tunable physicochemical properties, high surface reactivity, and excellent chemical stability. Moreover, their large specific surface area, together with the possibility of tailoring their morphology, defect concentration, and surface chemistry, enables enhanced adsorption and photocatalytic performance, making them highly effective for the removal of a broad range of environmental contaminants [3, 4]. Among these materials, aluminum iron oxide ($AlFeO_3$) has attracted growing interest due to its multifunctional character. $AlFeO_3$ is a multiferroic oxide isostructural with $GaFeO_3$ (orthorhombic, $Pna2_1$), in which Al and Fe are distributed over both octahedral and tetrahedral sites, giving rise to the coexistence of magnetic and polar ordering [5]. This unique combination of properties has enabled its exploration in sensing devices [6] and catalysis [7,8]. Previous studies have shown that transition-metal substitution at the Fe site represents an effective strategy for tailoring the structural, magnetic, and ferroelectric characteristics of $AlFeO_3$. In particular, Mn incorporation has been reported to fine-tune the magnetic behavior of this family. Nevertheless, while significant efforts have been devoted to the synthesis, structural characterization, and multiferroic behavior of pristine and doped $AlFeO_3$ systems, their catalytic response remains underexplored. Therefore, a comprehensive investigation of Mn-doped $AlFeO_3$ is essential for assessing its suitability in wastewater applications.

In this respect, this study is focused on the synthesis of new doped aluminium iron oxides with the

general formula $AlFe_{1-x}Mn_xO_3$ (x = 0, 0.02, 0.05) using the Pechini method (Scheme 1). As a low-cost and environmentally friendly synthesis technique, the Pechini route enables enhanced stoichiometric control, homogeneous cation distribution, and reproducibility [9, 10]. Briefly, stoichiometric amounts of metal nitrates were dissolved in ultrapure water and mixed with citric acid and ethylene glycol. The resulting solution was heated at 80 °C under continuous stirring until a viscous gel was obtained. Citric acid served as a complexing agent, promoting the formation of stable complexes with metal cations, and ensuring homogeneous cation distribution while limiting the precipitation of metal species. Ethylene glycol acts as a polyesterification agent, reacting with citric acid to generate a polymeric network that immobilizes the metal-citrate complexes within a resin matrix. Subsequently, the gel was transferred to a sand bath and heated to 350 °C, where self-combustion occurred, yielding a dark-brown precursor powder. The powder was calcined at 750 °C for 4 h and then at 800 °C for an additional 2 h to remove residual organic species and promote the crystallization of the oxide phase. The materials were characterized using X-ray diffraction (XRD), vibrating-sample magnetometry (VSM), and transmission electron microscopy (TEM) to assess the impact of Mn substitution and calcination temperature on their structural, magnetic, and morphological properties.



Scheme 1. Graphical representation of the Pechini synthesis route.

References

[1] H.M. Solayman, Muna E. Raypah, Azrina Abd Aziz, Kang Kang, Md. Badiuzzaman Khan, Yoshifumi Horie, Thanh-Binh Nguyen, Jheng-Jie Jiang, *J. Environ. Chem. Eng.* 2026, 14, 5, 123531.
[2] N. Asghar, A. Hussain, D.A. Nguyen, S. Ali, I. Hussain, A. Junejo, A. Ali, *J. Nanobiotechnol.* 2024, 22, 26.
[3] D.B. Olawade, O.Z. Wada, B.I. Egbewole, O. Fapohunda, A.O. Ige, S.O. Usman, O. Ajisafe, *Front. Nanotechnol.* 2024, 6, 1466721.
[4] M. Gopika, T. Nair, Sajini, M. Beena, *Talanta Open* 2022, 5, 100080.
[5] F. Bourée, J. L. Baudour, E. Elbadraoui, J. Musso, C. Laurent, A. Rousset, *Acta Crystallogr.* B 1996, 52, 217.
[6] L. B. Farhat, S. B. Ahmed, S. Ezzine, M. Amami, *Mater. Chem. Phys.* 2020, 255, 123631.
[7] R. Smarak, S. Bhuvanasundari, S. Kavita, N.K. Debendra, T. Thomas, *Ceram. Int.* 2024, 50, 13, A, 22817-22828.
[8] S. Bhuvanasundari, G. Venkatachalam, M. Doble, T. Thomas, *Ceram. Int.* 2022, 48, 21,32326-32337.
[9] J.D.G. Fernandes, D.M.A. Melo, L.B. Zinner, C.M. Salustiano, Z.R. Silva, A.E. Martinelli, M. Cerqueira, C. Alves Júnior, E Longo, M.I.B Bernardi, *Mater. Lett.* 2002, 53, 1-2, 122-125.
[10] M.P. Pechini, *U.S. Patent* 1967, 3, 330, 697, 1967.

Acknowledgment: This work was supported by a grant from the Ministry of Research, Innovation and Digitization, CNCS-UEFISCDI, project number PN-IV-P6-6.1-CoEx-2024-0056, within PNCDI III.

PP14. SORBTION OF NITRONYL NITROXIDE BENZALDEHYDE IN POLY(ETHYLENE GLYCOL)/B-CD HYDROGELS HYBRID AuNPs

Alexandra Ana-Maria Iancu*, Alexandru Gabriel Bucur, Mihaela Banica, Gabriela Ionita
Institute of Physical Chemistry – Ilie Murgulescu, Romanian Academy, Bucharest, Romania Country
**addaada36@gmail.com*

Polysaccharide hydrogel properties can be tuned by simple structural modifications. A particular case is that of hydrogels with inorganic nanoparticles embedded in the gel structures, which represent excellent candidates for applications in several diverse fields including catalysis, sensing, electronics, and biomedicine. Gold nanoparticles (AuNPs) have a broad spectrum of application areas including medicine, the food industry, water purification, and biological applications. In particular, AuNPs are applied in drug delivery, photothermal therapy, imaging, sensing, catalysis, and even as antimicrobials. Embedding AuNPs in gels favors their stability and enables their reuse, especially in catalytic processes [1]. In this study, we used a polymer gel formed by coupling PEG900 with β-cyclodextrin (PEG900/β-CD), as well as the hybrid material resulting from the in situ formation of AuNPs within this polymer gel matrix (PEG900/β-CD/AuNPs) [1, 2].

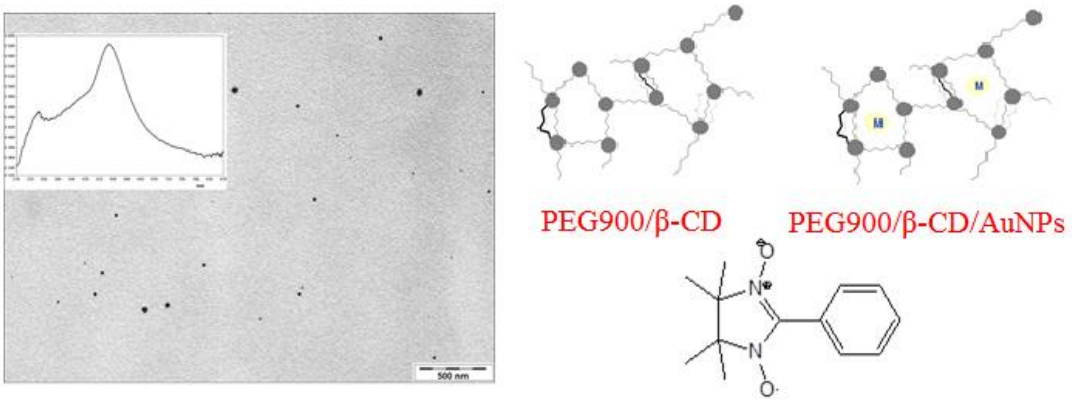


Figure 1. TEM image of a PEG900/β-CD gel section with Au nanoparticles (the inset shows the UV-Vis spectra of the gel), schematic representation of gels, and the structure of the nitronyl-nitroxide derived from benzaldehyde (NNB).

The UV-Vis spectrum of the $[AuCl_4]^-$-loaded gel after reduction shows a strong surface plasmon band at 538 nm, confirming the formation of nanoparticles. The TEM image of a gel section shows that the particle size is in the range of 10–50 nm (Figure 1). These particles do not diffuse out of the gel, thereby offering the possibility of using this material in catalysis. Our study pursued the following directions: 1) encapsulation of nitronyl-nitroxide (NNB) within the two hydrogels and determining the regions preferred by this radical inside the gel matrices, and 2) monitoring the reaction between NNB and reduced glutathione within the gels. Analyzing the spectra in Figure 2, it can be observed that NNB prefers complexation with the cyclodextrins that form the network nodes of the gels, as indicated by a decrease in the hyperfine splitting constant (a_N) by approximately 0.4 G, along with a decrease in the rotational correlation time. The presence of gold nanoparticles does not hinder access to the cyclodextrin cavities within the gel, as the NNB signal intensities remain similar in both gels.

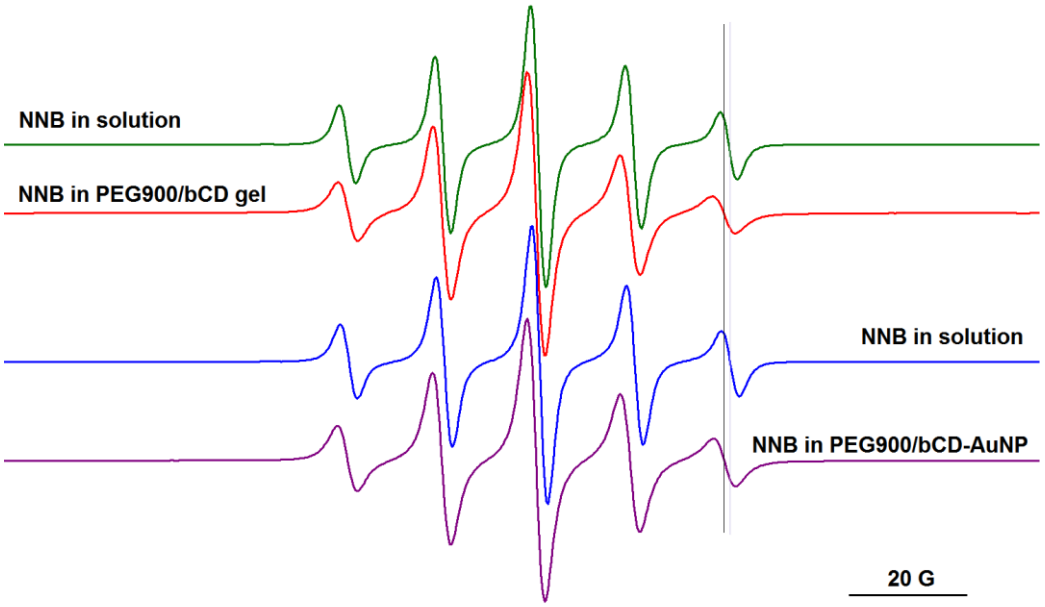


Figure 2. The EPR spectra of NNB in solution and in gels.

NN radicals are known to participate in redox reactions with biologically important reducing agents, most notably thiols, such as glutathione (GSH), which is the most abundant intracellular antioxidant and a key regulator of cellular redox homeostasis [3]. The rate of NNB reduction by GSH in gels provides quantitative information on the accessibility of the radical and protective effects arising from supramolecular interactions with cyclodextrin units.

References

[1] G. Ionita, G. Marinescu,C. Ilie, D.F. Anghel, D. Smith, V. Chechik, *Langmuir*, 2013, 29(29), 9173-9178.
[2] G. Ionita, V. Chechik, *Chem. Commun*. 2010, 8255-8257.
[3] L. Ciutu, A.-G..Bucur, A.V.F. Neculae, G. A. Sanda, A.R. Petrovici, P. Ionita, A. Fifere, I.A. Turin-Moleavin, A. Salifoglou, S. Matsia, G. Ionita, *CHEMBIOCHEM*, 2026, 27(20), e70561.

Acknowledgment: Project PNRR-III-C9-2023-I8 “Chemical host–guest molecular systems for health applications (OMRI for identification of inflammatory pathologies)”, contract no. 760283/27.03.2024, Ministry of research, innovation and digitalization, Romania, funded by European Union – NextGenerationEU.

PP15. RHENIUM TRICARBONYL COMPLEXES-LOADED POLYESTER NANOPARTICLES FOR POTENTIAL BIOMEDICAL APPLICATIONS

Andrei-Alexandru Ivu[1]*, Alina Gabriela Rusu[1], Alexandru Mihail Serban[1], Isabella Nacu[2], Fabio Zobi[3], Liliana Verestiuc[2], Loredana Elena Nita[1]

[1]*Petru Poni Institute of Macromolecular Chemistry, Romanian Academy, Iasi, Romania*
[2]*Department of Biomedical Sciences, Faculty of Medical Bioengineering, Grigore T. Popa University of Medicine and Pharmacy Iasi, Iasi, Romania*
[3]*Department of Chemistry, Fribourg University, Fribourg, Switzerland*
**ivu.andrei@icmpp.ro*

Metallodrugs are attracting growing interest as potential new theranostic agents, given the limitations of conventional antitumor and antimicrobial therapies, particularly in the context of increasing drug resistance. In this context, rhenium tricarbonyl complexes have stood out for their distinct molecular geometries, which enable unique biological interactions and biocompatibility [1,2]. The lipophilicity of these compounds promotes intracellular uptake, where they can generate reactive oxygen species (ROS), acting as photosensitizers in photodynamic therapy (PDT), and serve as photoCORMs for hypoxia-based therapy. Furthermore, their intrinsic luminescence is characterized by large Stokes shifts and long emission lifetimes that can be tuned through ligand design, making them useful fluorophores for imaging applications [3,4]. Beyond their promising properties, limitations such as poor pharmacological profile, non-self recognition, the presence of endogenous competing ligands and reactivity toward biological species require encapsulation in nanocarriers [5]. In particular, nanoparticles based on copolyesters exhibit (bio)degradability *via* enzymatic degradation or acid-catalysed hydrolysis of ester bonds, thereby facilitating the controlled release of bioactive compounds at the desired site [6].

The primary objective of this work is to describe the strategy for encapsulating rhenium tricarbonyl complexes in copolyester-based nanocarriers for potential theranostic applications in the biomedical field. To achieve this goal, two diimine-based organometallic complexes, *fac*-[$Re(CO)_3$(**NN**)Br], where **NN** represents 2,2'-bipyridine (Bipy) and 4,4'-di-tert-butyl-2,2'-bipyridine (t-Bu-Bipy), were successfully loaded into poly[ethylene brassylate-co-glycidyl methacrylate] (PEBGMA)-based nanoparticles, colloidally stabilized with a Tween 80/Span 85 surfactant system. The selected approach involved a modified solvent displacement method governed by copolymer self-assembly arising from differences in chain polarity and hydrophobic interactions with the rhenium complexes. The resulting nanosuspensions were evaluated in terms of their physicochemical properties using Dynamic Light Scattering (DLS) and Electrophoretic Light Scattering (ELS), with the obtained results correlated with morphological investigations performed by Transmission Electron Microscopy (TEM). Fluorescence spectroscopy was employed to characterize the photophysical properties of organometallic complexes. *In vitro* release kinetics were performed by dialysis under physiological conditions (pH 7.4, 37 °C), and the concentrations of the released complexes and encapsulation efficiency (EE%) were quantified spectrophotometrically.

The findings of this study highlighted the capacity of PEBGMA copolymers to self-assemble into nanostructures capable of encapsulating lipophilic $Re(CO)_3$ complexes. This observation is supported by DLS measurements (Figure 1.A.), which revealed distributions of monomodal hydrodynamic diameters (D_H) for all samples. The control nanosuspension exhibited a D_H of approximately 155 nm, with a narrow size distribution characteristic of a monodisperse system. The PG2_Re(Bipy) and PG2_Re(t-Bu-Bipy) formulations exhibited D_H of 185.5 nm and approximately 200 nm, respectively, with an increase in dispersity index (PDI). This trend may be attributed to the bulkier structure of the t-Bu-Bipy ligand, whose tert-butyl substituents may introduce steric effects that influence the arrangement of the encapsulated complexes within the polymer matrix.

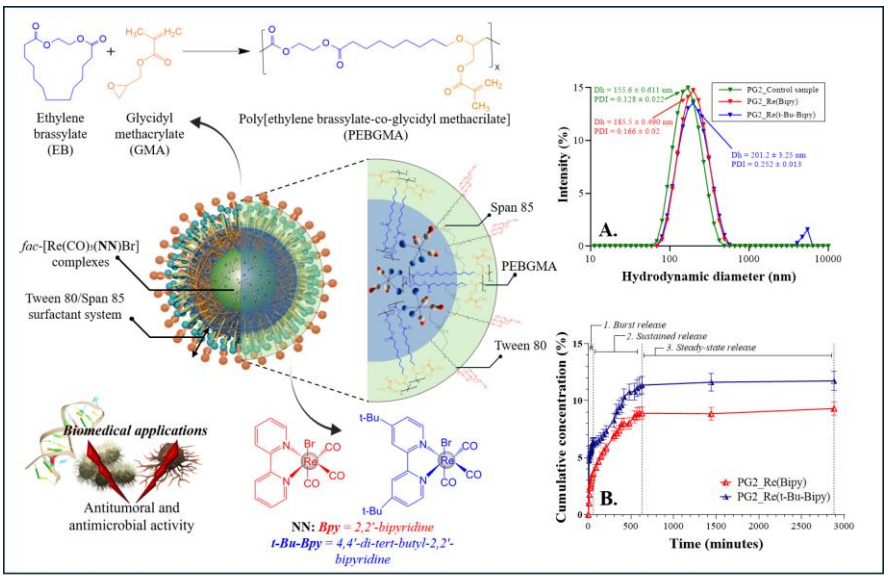


Figure 1. Schematic overview of the study. (A) D_H distribution of the nanoformulations. (B) *In vitro* release profiles of the encapsulated rhenium complexes.

As shown in Figure 1.B., the nanosystems provided controlled release of complexes in three phases: initial burst, sustained release, and plateau. Despite its higher lipophilicity, Re(t-Bu-Bipy) was released more than Re(t-Bu-Bipy), likely because its tert-butyl groups hinder $\pi - \pi$ stacking and tight packing within the hydrophobic core, enabling diffusion.

References

[1] A.A. Haase, E.B. Bauer, F.E. Kühn., D.C. Crans, *Coord. Chem. Rev.* 2019, 394, 135-161.
[2] K. Schindler, Y. Cortat, M. Nedyalkova, A. Crochet, M. Larttuada, A. Pavic, F. Zobi, *Pharmaceuticals* 2022, 15(9), 1107.
[3] A. Acosta, J. Antipan, M. Fernandez, G. Prado, C. Sandoval-Altamirano, G. Gunther, I. Gutierrez-Urrutia, I. Poblete-Castro, A. Vega, N. Pizarro, *RSC Adv.* 2021, 11(51), 31959-31966.
[4] K. Schindler, F. Zobi, *Chimia* 2021, 75(10), 837.
[5] V.M. Chiriac, A.-A. Ivu, A.G. Rusu, A. Ghilan, A.M. Serban, A. Vieru, L.E. Nita, A.P. Chiriac, *Gels* 2026, 12(11), 964.
[6] L.E. Nita, A.-A. Ivu, A.G. Rusu, A.M. Serban, A.M. Macsim, D. Timpu, I. Nacu, L. Verestiuc, A.P. Chiriac, *Polymer* 2026, 366, 130870.

Acknowledgment: This research is carried out and financed within the framework of the Second Swiss Contribution MAPS (Project No. IZ11Z0_230668).

PP16. FROM COUMARIN-CONTAINING QUATERNARY SALTS TO CYCLOADDUCTS: A COMPARATIVE UV–VIS STUDY

Florentina-Gabriela Lazar[1]*, Cristina AL-Matarneh[1], Dorina Amariucai-Mantu[2], Ashraf AL-Matarneh[1,2], Mariana Pinteala[1]
[1]*Petru Poni Institute of Macromolecular Chemistry, Romanian Academy, Iasi, Romania*
[2]*Faculty of Chemistry, "Alexandru Ioan Cuza" University of Iasi, Iasi, Romania*
**lazar.florentina@icmpp.ro*

3-(Bromoacetyl)coumarin is a useful building block for the synthesis of structurally diverse coumarin-containing heterocycles. Its synthetic importance arises from the combination of the conjugated coumarin scaffold and the reactive α-bromoketone side chain, which provides a convenient site for chemical functionalization. The displacement of bromide by nitrogen nucleophiles enables the attachment of heteroaromatic units while preserving the coumarin moiety (Figure 1). This approach has been employed in the preparation of coumarin-containing pyridinium and quinolinium salts, illustrating its value for the construction of hybrid molecular structures [1]. Nitrogen-containing heterocycles offer further possibilities for structural diversification through quaternization and subsequent transformations of the resulting salts [2]. Among these systems, pyridine, quinoline, and isoquinoline constitute a particularly useful group for comparative investigations (Figure 1). Pyridine contains a single six-membered aromatic ring with one nitrogen atom, whereas quinoline and isoquinoline are bicyclic systems formed by the fusion of a benzene ring with a pyridine ring. The latter two heterocycles differ in the position of the nitrogen atom relative to the ring junction. Consequently, their selection allows two structural features to be considered: the extension of the aromatic framework through benzannulation and the influence of nitrogen position within isomeric heterocyclic systems. Previous studies have demonstrated that structural modifications of coumarin derivatives can influence the positions and shapes of their absorption bands [3]. In this context, the incorporation of the mentioned heterocycles into coumarin-containing structures provides an opportunity to investigate relationships between molecular architecture and optical absorption properties. UV–Vis absorption spectroscopy is therefore a suitable technique for comparing the cumarine and the resulting compounds and evaluating how changes in the heterocyclic framework affect their spectral characteristics. The present work focuses on three related series of compounds: coumarin-containing monoquaternary salts derived from pyridine, quinoline, and isoquinoline, and the corresponding cycloadducts obtained using ethyl propiolate and dimethyl acetylenedicarboxylate. The synthetic route involves the *N*-alkylation of the selected heterocycles with 3-(bromoacetyl)coumarin. The resulting salts serve as precursors for heterocyclic ylides generated under basic conditions, which subsequently undergo [*3+2*] dipolar cycloaddition with the activated alkynes (Figure 1). The two dipolarophiles provide access to cycloadducts with different ester substitution patterns, extending the structural diversity available for comparison. The UV–Vis investigation follows two complementary directions. First, compounds derived from pyridine, quinoline, and isoquinoline are compared within each series to examine the influence of the heterocyclic core. Second, each monoquaternary salt is considered alongside its corresponding cycloadducts to investigate the changes in absorption associated with the transformation of the charged heteroaromatic

precursor into a fused heterocyclic system.

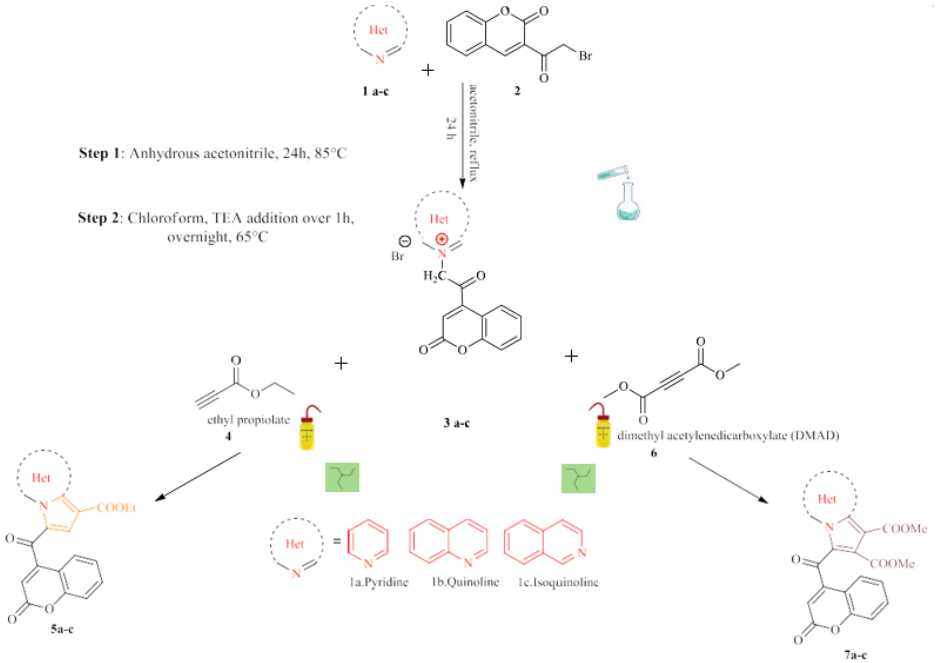


Figure 1. Synthetic route to coumarin-containing quaternary salts and their corresponding cycloadducts derived from pyridine, quinoline, and isoquinoline.

Comparison of the ethyl propiolate and dimethyl acetylenedicarboxylate derivatives additionally addresses the influence of their different substitution patterns. Particular attention is directed towards the positions of absorption maxima, the shapes and relative contributions of individual bands, and absorption extending towards the visible region. Spectral comparisons require consistent solvent and measurement conditions, while the interpretation of absorption intensities takes account of concentration and optical path length. This comparative framework aims to distinguish the influence of the nitrogen heterocycle from the effects of the subsequent synthetic transformation. Complementary *in silico* ADME profiling is used to compare selected physicochemical descriptors and predicted pharmacokinetic properties across the compound series. This analysis examines how structural changes accompanying cycloaddition affect parameters relevant to further biological investigation, while distinguishing computational predictions from experimentally established behavior [4]. Overall, the study aims to clarify structure–absorption relationships among the synthetized compounds and to provide a basis for selecting representative derivatives for further photophysical investigation.

References

[1] B. Porwal, B. S. Jayashree, M. Attimarad, *J. Basic Clin*. Pharm. 2010, 1, 29–32.
[2] M.-C. Sardaru, C.-M. Al Matarneh, N. Simionescu, I.I. Mangalagiu, M. Pinteala, R. Danac, *Rev. Roum. Chim.* 2024, 69, 63–74.J. Donovalová, M. Cigáň, H. Stankovičová, J. Gašpar, M. Danko, A. Gáplovský, P. Hrdlovič, *Molecules* 2012, 17, 3259–3276.
[3] A. Daina, O. Michielin, V. Zoete, *Sci. Rep*. 2017, 7, 42717.

Acknowledgment: This work was supported by a grant of the Romanian National Authority for Scientific Research, CNCS – UEFISCDI, project PN-IV-P7-7.1-PED-2024-1008. (76PED/05.05.2025).

PP17. PREPARATION OF THE COPPER ALGINATE COMPLEXES USING ION EXCHANGER COLUMN METHOD

Alina-Petronela Moraru*, Marius-Mihai Zaharia, Marcela Mihai
Petru Poni Institute of Macromolecular Chemistry, Romanian Academy, Iasi, Romania
**moraru.alina@icmpp.ro*

Introduction

Polysaccharides are abundant natural biomacromolecules that have attracted considerable attention due to their biocompatibility, biodegradability, low toxicity, and diverse biological activities. Their functional groups, such as hydroxyl, carboxyl, and amino groups, enable interactions with metal ions and the formation of polysaccharide-metal complexes with a wide variety of properties [1]. Metal ions have an essential role in numerous biological processes occurring in living organisms. Ion exchangers (IE) are materials that contain ionic-charged functional groups, capable of retaining oppositely charged ions from electrolyte solutions, generally aqueous, concomitantly with the release into solution of an equivalent amount of ions having the same charge. Depending on the nature of the ions involved in the ion exchange process, they are classified into cation exchangers and anion exchangers. Materials capable of interacting with both cations and anions are called amphoteric or zwitterionic exchangers [2].

In this study, the ion exchange column method was used for the preparation of soluble polysaccharide-metal ion complexes, allowing initially the retention of sodium alginate on the surface of an ion exchanger, the exchange with copper ions both with the functional groups of the ion exchangers and with the functional groups of the polysaccharide and subsequently the elution of the soluble polysaccharide-Cu(II) complexes. The sorption of sodium alginate (AlgNa) was investigated using ion-exchange resins with amino (IE-EDA) and zwitterionic (IE-EDA-Zw) functionalities to assess their ability to retain the polysaccharide and identify suitable matrices for subsequent metal-ion loading.

Experimental

The sorption of AlgNa on IE was carried out using a polysaccharide solution with a concentration of 7×10^{-3} M, with the initial pH adjusted to 4. For the sorption experiments, 4 mL of IE and 5 mL of AlgNa solution were introduced into 20 mL flasks. The mixtures were agitated at 250 rpm using an orbital shaker (Orbital Shaker-Incubator ES-20) at room temperature (25 °C) for 24 hours to reach sorption equilibrium. The IE impregnated with alginate solution were introduced into a chromatographic column (Diba Omnifit Labware). A volume of $CuSO_4 \cdot 5H_2O$ solution was passed over them at a controlled flow rate to allow their interaction with the carboxylate groups of alginate and promoting the formation of copper alginate complex (AlgCu). The obtained fractions were characterized by atomic absorption spectrophotometry (AAS) to determine the content of Cu^{+2} ions sorbed by the difference between the initial concentration and after passing through the column. The elution of the AlgCu formed in the column was carried out by passing 0.1M HCl solution. The eluate fractions were characterized by AAS, FTIR-ATR spectroscopy and by potentiometric titration.

Results and Discussion

The AAS analysis quantified the amount of Cu^{2+} ions retained for both investigated IE (IE-EDA and IE-EDA-Zw) impregnated with alginate. By elution with 0.1 M HCl solution, soluble AlgCu complexes were obtained. In the FTIR spectra obtained for fractions F1–F4, the characteristic bands of sodium alginate are maintained, but changes in their intensity and position can be observed, especially in the regions corresponding to the bands 1611-1412 cm^{-1} and 1032 cm^{-1}, which can be correlated with the interaction of Cu^{2+} ions with the $–COO^-$ groups of sodium alginate (Figure 1). The potentiometric titrations showed the behavior of the AlgCu complexes as a function of pH. At acidic pH, the protonation of carboxylate groups can reduce the negative charge of AlgCu. At basic pH, their deprotonation leads to a negative ionic charge, thus influencing the streaming potential values.

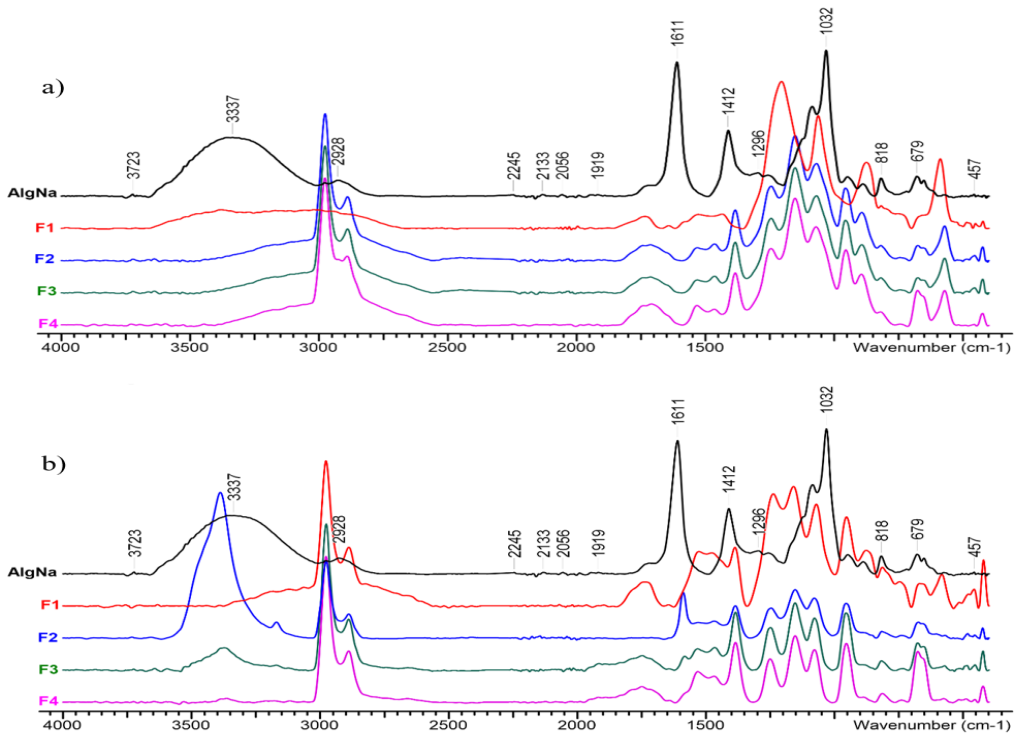


Figure 1. FTIR spectra of AlgNa and of the AlgCu fractions eluted with 0.1 M HCl (F1-F4) from the columns filled with (a) IE-EDA/Alg and (b) IE-EDA-Zw/Alg.

The proposed ion-exchange column method provides a suitable approach for the formation of AlgCu complexes. The use of ion-exchange resins facilitates the interaction between sodium alginate and Cu^{2+} ions in aqueous media. The obtained results highlight the potential of ion-exchange materials for the preparation of natural polysaccharide-metal complexes and functional hybrid materials.

References

[1] X. Li, F. Jiang, M. Liu, Y. Qu, Z. Lan, X. Dai, C. Huang, X. Yue, S. Zhao, X. Pan, C. Zhang; in Journal of Agricultural and Food Chemistry, 2022, 70(23), pp. 6922–6942.
[2] Z. Hubicki, M. Wawrzkiewicz, G. Wójcik; in Ion Exchange: Studies and Applications, 2015, p. 1.

Acknowledgment: This work was financially supported by a grant of the Ministry of Research, Innovation and Digitization, CNCS-UEFISCDI, project number PN-IV-P1-PCE-2023-0738, within PNCDI IV.

PP18. HYDROPHOBIZED SILICA-BASED NANOCOMPOSITE FORMULATIONS FOR SUPERHYDROPHOBIC WOOD SURFACES

Monica-Georgiana Musteata*, Maria-Cristina Popescu, Carmen-Mihaela Popescu
Petru Poni Institute of Macromolecular Chemistry, Romanian Academy, Iasi, Romania
**musteata.monica@icmpp.ro*

Introduction

Superhydrophobic surfaces are characterized by their exceptional water repellent properties, which result from a combination of specific surface roughness and low surface energy [1]. Silane-functionalized silica nanoparticles can be used to tailor the surface wettability of different substrates [2-5]. In this study, we investigated the development of a superhydrophobic wood surface using formulations based on hydrophobized silica nanoparticles with and without an acrylic copolymer, and examines their effects on surface chemistry, morphology and water contact angle.

Experimental procedure

Silica nanoparticles were synthesized using the Stöber sol-gel method [2]. Briefly, 10 mL of tetraethyl orthosilicate (TEOS) was added dropwise into a mixture containing 90 mL of ethanol and 10 mL of ammonium hydroxide, under continuous stirring for 2 h. The resulting mixture was aged overnight, followed by the gradual addition of 1 mL of FAS-octyl (1H,1H,2H,2H-perfluorooctyltriethoxysilane) (Table 1). The reaction mixture was further stirred at 60 °C and 1000 rpm, for 2 h to allow the surface functionalization of the silica nanoparticles. The resulting formulation was divided into 2 parts: the first one was used without further modification, while in the second was an acrylic copolymer was added (MA23) to obtain a polymer-based nanocomposite formulation. Birch wood samples (20 × 20 × 5 mm), previously oven-dried at 100 °C for 24 h, were impregnated in the resulting dispersion under vacuum for 2 h (Figure 1). After the treatment, the samples were kept at room temperature for 24 h to allow solvent evaporation then oven-dried at 100°C for an additional 24 h.

Table 1. Composition of the two formulations, used for individual impregnation of wood samples.

Prepared formulations	EtOH (mL)	NH_4OH (mL)	TEOS	FAS octyl (ml)	MA23 3%
A	90	10	10	1	-
B	90	10	10	1	34



Figure 1. Photos of untreated (control) and treated birch wood samples after drying.

Physico-chemical and morphological characterization

Infrared spectroscopy and scanning electron microscopy (SEM) were used to characterize physico-chemical and morphological characteristics of the 2 formulations: the FAS-octyl-functionalized silica nanoparticles (A) and FAS-octyl-functionalized silica nanoparticles incorporated into MA23 acrylic copolymer (B) (Figure 2). The first method was used to identify the characteristic functional groups and assess the chemical modifications associated with silica functionalization and the incorporation of the acrylic copolymer, while SEM analysis was performed to assess the particle morphology, apparent size, and agglomeration. SEM images revealed predominantly spherical particles. Compared to A, the B formulation displayed a more closely packed, aggregated particle arrangement, indicating changes in particle organization. The treated wood surfaces present differences compared to control sample. The SEM images highlight morphological architectures (Figure 3). The wood treated with A shows a particulate surface texture, while the wood surface treated with B appears to form a more continuous, fine-grained coating. The infrared spectra also indicate changes after the treatment.

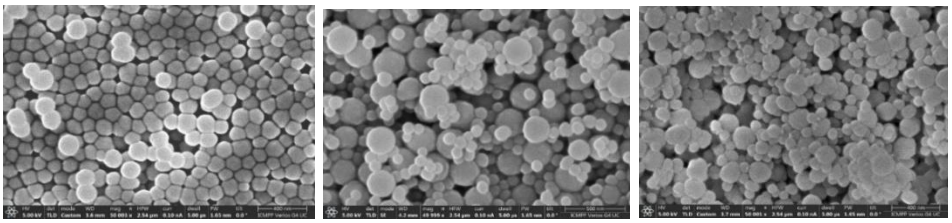


Figure 2. SEM images of silica nanoparticles, hydrophobized silica nanoparticles and nanocomposites (~50,000×).

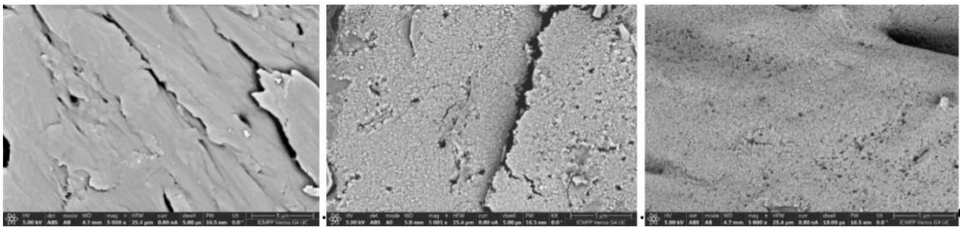


Figure 3. SEM images of wood samples control and treated with A and B.

Static water contact angles increased from 118.84° for untreated wood sample to 161.62° for wood treated with A and 148.89° for the wood treated with B. Thus, A exceeded the conventional 150° contact-angle threshold for superhydrophobicity, whereas B was 1° below. The addition of a polymeric matrix into the hydrophobized silica nanoparticles reduced the contact angle, but improved the surface resistance.

Conclusions. FAS-octyl-functionalized silica nanoparticles indicated an increased water contact angle of the treated birch wood, but adding MA23 altered the coating morphology and reduced the mean contact angle compared to silica only formulation. These findings underline the importance of formulation composition and surface texture in designing water-repellent wood surfaces.

References

[1] H. Chang, K. Tu, X. Wang, J. Liu, *RSC Advances* 2015, 5(39), 30647-30653
[2] W. Stöber, A. Fink, E. Bohn, *Journal of Colloid and Interface Science* 1968, 26(1), 62-69
[3] A. Mitani, P. Terzopoulou, V. Kamperidou, *Materials* 2026, 19(11), 2339.
[4] X. Wang, Y. Chai, J. Liu, *Holzforschung* 2013, 67(6).
[5] X. Zhang, F. Shi, J. Niu, Y. Jiang, Z. Wang, *J. Mater. Chem.* 2008, 18(6), 621-633.

PP19. SCAFFOLD ARCHITECTURE AS A DESIGN PARAMETER IN 3D-PRINTED SCAFFOLDS FOR TISSUE REGENERATION

Isabella Nacu*, Anca Toma, Liliana Verestiuc
Department Biomedical Sciences, Faculty of Medical Bioengineering, "Grigore T. Popa" University of Medicine and Pharmacy, Iasi, Romania
** isabella.nacu@umfiasi.ro*

Introduction

Skin repair process following burns, wounds or chronic lesions remains a clinical challenge, motivating the development of skin substitutes able to mimic the native extracellular matrix (ECM) [1]. Autologous grafts, the clinical gold standard, are limited by donor-site availability, whereas allografts, xenografts and commercial substitutes are costly, risk immune rejection and rarely restore native skin function. This has motivated the development of ECM-mimicking engineered skin substitutes. Among the methods used to develop tissue substitutes, extrusion-based 3D (bio)printing allows the fabrication of porous scaffolds with a controlled architecture, which offer mechanical support and promote nutrient diffusion, cell adhesion and proliferation [2–4]. Gelatin and sodium alginate, particularly in their methacrylated forms (GelMA and AlMA), are widely used in (bio)inks preparation process due to their biocompatibility, biodegradability, and stability in physiological conditions [4,5]. This study aims to compare the properties of square and honeycomb 3D-printed lattices based on GelMA/AlMA compositions, in order to establish the influence of scaffold design and polymer ratio on the functional and biological behavior of scaffolds for skin tissue regeneration.

Materials and Methods

GelMA/AlMA inks prepared in three ratios between polymers were processed by extrusion-based 3D printing under square-lattice and honeycomb structures. Scaffolds were crosslinked by UV irradiation and calcium chloride treatment, to enhance scaffolds stability. Stereomicroscopy was used for the examination of shape fidelity and pore morphology. Fluid uptake was measured gravimetrically in specific culture medium, DMEM/HAM F-12, with an equilibrium swelling degree assessed after 60 min experiment interval. Furthermore, compressive Young's modulus was calculated from the linear region of the stress–strain curve under uniaxial compression. Moreover, scaffolds 'cytocompatibility was assessed by MTT assay and confirmed through fluorescent morphological analysis of human dermal fibroblasts.

Results and Discussion

Stereomicroscopy (Figure 1) showed good structural uniformity and shape fidelity to the digital models for both architectures, with the exception of the GelMA_AlMA$_3$ honeycomb scaffolds, which displayed partially closed pores. Square lattices showed symmetric, open and interconnected pores delimited by perpendicular filaments. Honeycomb lattices displayed elongated pores with diagonal filaments and higher apparent porosity, favorable for oxygen and nutrient transport. From the fluid interaction behaviour point of view, the printed scaffolds exhibited suitable swelling values influenced by GelMA content (presented in Table 1), due to its preserved hydrophilic functional groups. Further, the compressive Young's modulus ranged from 2.09 to 20.28 kPa, the highest

value being measured for the matrix with the highest AlMA content, presenting the stiffening effect of the ionically and covalently crosslinked alginate network. Rather than a limitation, this indicates that the GelMA/AlMA ratio offers a versatile method for tailoring scaffold stiffness, with the 50/50 formulation providing a particularly soft matrix suitable for tissues regeneration.

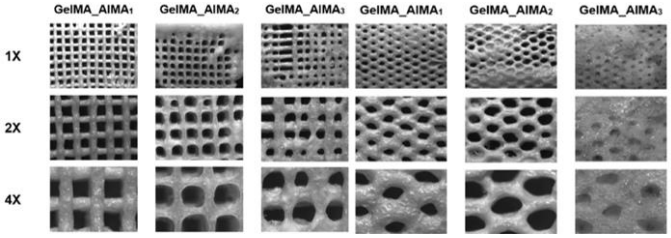


Figure 1. Stereomicroscopy images of square (left) and honeycomb (right) lattices.

Table 1. Composition, equilibrium swelling degree and Young's modulus of printed scaffolds

Sample	GelMA/AlMA ratio	Swelling degree (60 min), %	Young's modulus, kPa
GelMa_AlMA$_1$	40/60	~431	20.28
GelMa_AlMA$_2$	50/50	~501	2.09
GelMa_AlMA$_3$	60/40	~575	10.44

As it can be seen in Figure 2a, MTT results showed a cell viability above the 80% treshhold in ISO 10993-5, supporting citocompatibility under tested conditions. After 72 hours, and fluorescence images showed spindle-shaped fibroblasts forming a confluent monolayer in contact with all scaffolds (presented in Figure 2b). This typical fibroblast morphology indicates good cell adhesion and spreading, likely supported by the cell-binding motifs of GelMA.

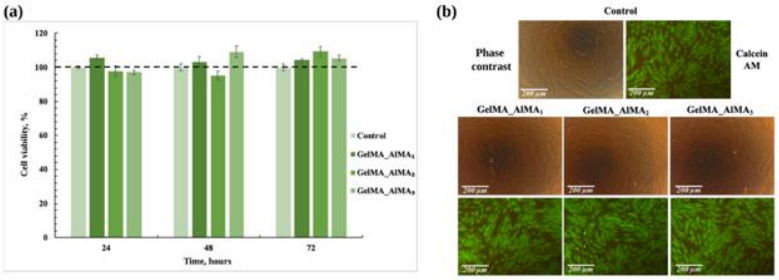


Figure 2. (a) Cell viability (%) at 24, 48 and 72 h; (b) cell morphology after 72h (phase contrast and Calcein AM).

Conclusions

GelMA/AlMA inks were successfully 3D-printed into square and honeycomb scaffolds form with high shape fidelity, and honeycomb design had greater apparent porosity. Swelling and stiffness varied with composition, and *in vitro* testing indicated non-cytotoxicity with preserved fibroblast morphology. These findings support the influence of architecture and polymer ratio on designing scaffolds for skin tissue regeneration.

References

[1] T. Weng, L.Zhang, Y.Liu, X.Zhao,X.Yue, J. Funct Biomater., 17(1):3, 2025. [2] K. Sindhi, R.B.Pingili, V.Beldar, S.Bhattacharya, J.Rahaman, D.Mukherjee, J. Tissue Viability., 34(2):100858, 2025. [3] V.T. Hoang,Q.T. Nguyen, T.T. K.Phan, T.H. Pham, N.Thi H.Dinh, Le P.H. Anh, L.T. M. Dao, Van D. Bui, H.-N. Dao, D Son Le, A.T. L.Ngo, Q.-D. Le, L.N.Thanh, MedComm, 6, 2025. [4] L. Xiaorui, F. Zheng, X. Wang, X. Geng, S. Zhao, H. Liu, D. Dou, Y. Leng, L. Wang, Y. Fan, Int J Bioprint.;9(2):649, 2023. [5] Tarassoli S.P., Z.M. Jessop, T. Jovic, K. Hawkins, S.I. Whitaker, Front. Bioeng. Biotechnol. 9, 2021.

Acknowledgment: This work was supported by a grant of the Grigore T. Popa University of Medicine and Pharmacy, Iași, Romania, project number 7381/2026.

PP20. VOLATILE ORGANIC COMPOUNDS FROM COFFEE AS POTENTIAL BIOACTIVE AGENTS IN CHITOSAN BASED MATERIALS

Andrei-Razvan Pana[1]*, Grigore Ungureanu[1], Cristopher Anel Boya[2], Mihai Brebu[1], Elena Stoleru[1]

[1]*Petru Poni Institute of Macromolecular Chemistry, Romanian Academy, Iasi, Romania*
[2]*Center for Biodiversity and Drug Discovery, Institute for Scientific Research and High Technology Services (INDICASAT AIP), Panama City, Panama*
**pana.andrei@icmpp.ro*

According to International Coffee Association, the coffee beans are the second most traded products in the world after crude oil [1], therefore the interest on the chemical profile of what gives our coffees the distinguished aromas and flavours. Acknowledging the work of Santamaría et al., who investigated Panamanian Geisha (*Coffea arabica)* and commercial Robusta (*Coffea canephora)* coffee blends using headspace solid-phase microextraction coupled with gas chromatography–mass spectrometry (HS-SPME–GC/MS), sensory analysis and an electronic nose [2], a working hypothesis is that chitosan–gelatin cryogels can retain selected coffee-derived volatile organic compounds through vapor-phase loading (fumigation). The bioactive potential of the resulting materials would subsequently be evaluated experimentally, with a view to possible applications in food packaging and preservation. A relevant example is provided by Brebu et al., who demonstrated that loading chitosan–gelatin cryogels with clove essential oil through fumigation imparted antioxidant activity to the polymeric matrix [3]. Extending these findings, a similar approach could be explored by loading chitosan–gelatin cryogels with coffee-derived volatile compounds through fumigation or other potentially sustainable impregnation methods. The retention of these compounds within the porous matrix and their contribution to the antioxidant activity of the resulting materials could then be evaluated with complementary methods. A potential application of the proposed chitosan–gelatin cryogels is their use as carriers of coffee-derived volatile compounds in active food-packaging systems.

To investigate this hypothesis, dry chitosan–gelatin cryogels would be exposed to the headspace of Panamanian Geisha and Indian Robusta coffee samples under controlled conditions. Cryogel composition, material mass and residual moisture would be evaluated alongside exposure time and temperature to investigate their influence on VOC retention. HS-SPME–GC/MS would be used to characterize the volatile profiles of the coffee samples, as seen in Figure 1, providing a basis for comparison with the compounds recovered from the loaded materials. However, further experimental studies are needed to validate the hypothesis proposed in this work about coffee and chitosan materials.

Figure 1 presents the GC–MS chromatograms of Panamanian Geisha Arabica and Indian Robusta coffee samples. For example, Panamenian Geisha coffee is reacher in furfural, while the Indian Robusta coffee is reacher in pyridine and furanemethanol acetate.

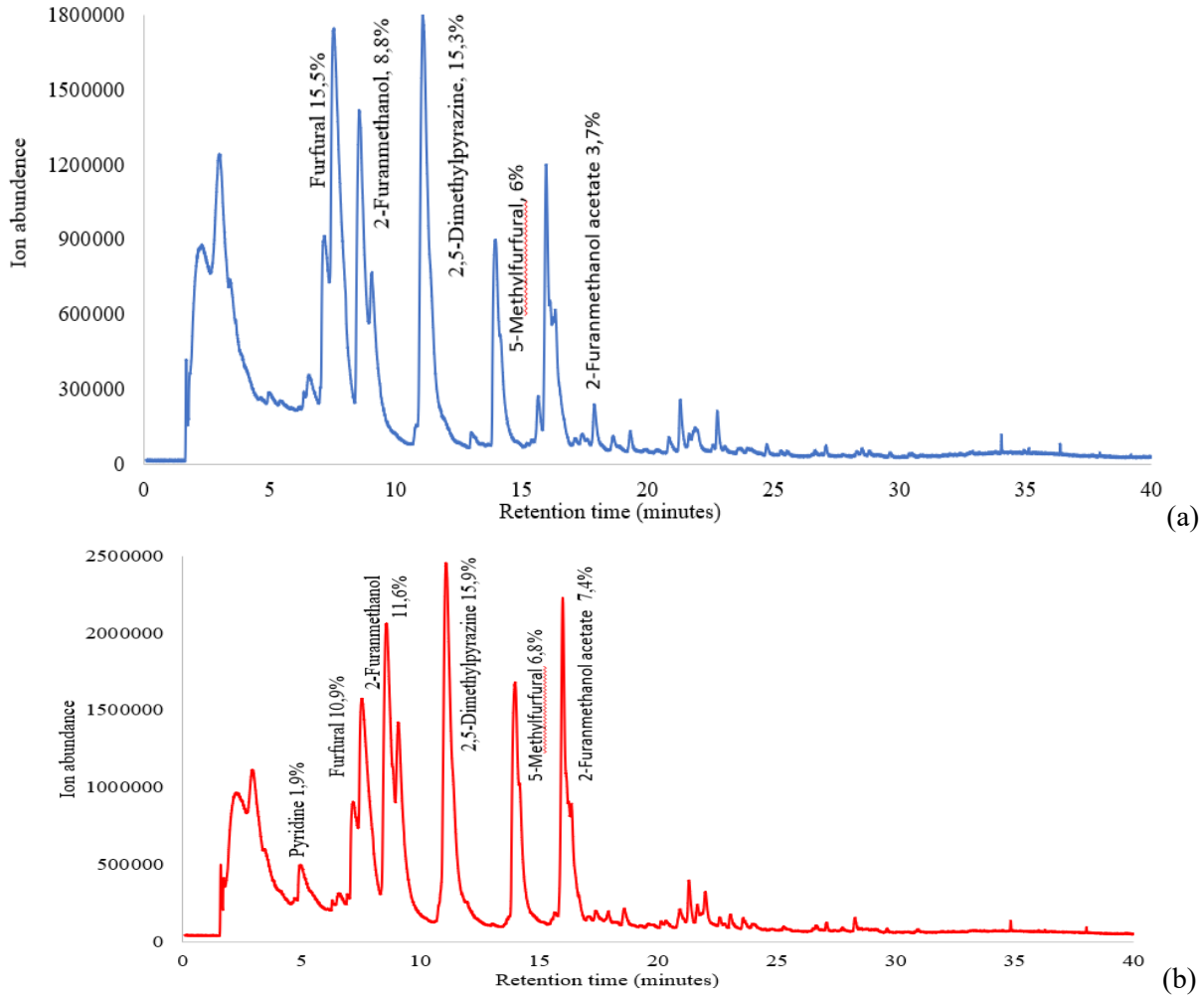


Figure 1. GC-MS chromatograms for Panamanian Geisha (a) and Indian Robusta (b) coffees.

The VOC profile of the two coffees reveal differences in the types and amount of main components. The main chemical classes of VOCs include furan derivatives, pyrazines, aldehydes, ketones and phenolic compounds. This chemical diversity provides a basis for selecting candidate compounds for future investigations of vapor-phase loading into chitosan–gelatin cryogels and their potential contribution to the antioxidant activity of the resulting materials.

References

[1] International Coffee Organization Informe del Mercado del Café (2026). Available online: http://www.ico.org/ (accessed on 29 October 2026)
[2] N. Santamaría, F. Meléndez, P. Arroyo, P. Calvo, F. Sánchez, J. Lozano, R. Sánchez, *Chemosensors* 2023, 11(11), 559.
[3] M. Brebu, R.P. Dumitriu, D. Pamfil, E. Butnaru, E. Stoleru, *Carbohydrate Polymers* 2024, 324, 121521.

Acknowledgment:

This work was supported by grants of the Ministry of Education and Research, CCCDI - UEFISCDI, project number PN-IV-P6-6.1-CoEx-2024-0056 and project number PN-IV-P2-2.1-TE-2023-1725 within PNCDI IV.

PP21. BIOACTIVE HYBRID HYDROGEL FOR CONTROLLED DELIVERY IN BIOMEDICAL APPLICATIONS

Ana Rebeca Pintilii*, Anca Mihaela Mocanu, Margareta Gabriela Ciobanu
Cristofor Simionescu Faculty of Chemical Engineering and Environmental Protection, Gheorghe Asachi Technical University of Iasi, Iasi, Romania
**ana-rebeca.pintilii@student.tuiasi.ro*

Current research in the field of biomaterials is undergoing a major paradigm shift, transitioning from inert structural implants to smart, interactive and bioactive systems capable of directly directing cellular behavior and supporting tissue regeneration processes. Advanced and multifunctional solutions capable of withstanding the dynamic and demanding biological environment are required in medical applications, particularly in dentistry and orthopedics.

Among biomedical ceramics, calcium phosphates represent one of the most thoroughly studied and promising classes of materials due to their exceptional biocompatibility, osteoconductivity and biological responsiveness. The thermodynamic stability, bioactivity and degradation kinetics of calcium phosphates are dictated by their Ca/P ratio [1, 2]. Among these phases, stoichiometric hydroxyapatite, $Ca_{10}(PO_4)_6(OH)_2$, with a characteristic Ca/P ratio of 1.67, exhibits chemical and structural similarity to the mineral phase of human bone and hard dental tissues. This structural analogy recommends hydroxyapatite for a wide spectrum of biomedical applications, being used in pure form, substituted with various biologically relevant cations (such as magnesium, strontium or zinc), or in different forms including functional surface coatings, thin films or cements [3–5].

Despite these remarkable biological advantages, standalone hydroxyapatite presents certain limitations, such as high intrinsic brittleness and a tendency toward particle agglomeration. To overcome these physical obstacles, current research focuses on the strategic integration of hydroxyapatite into three-dimensional hydrogel polymeric networks. Hydrogels are highly hydrated, porous matrices capable of absorbing large amounts of biological fluids without losing their structural integrity, thereby closely mimicking the hydrophilic microenvironment and architecture of the native extracellular matrix. Selecting an appropriate polymer matrix is crucial in designing these hybrid platforms. Natural polymers, such as chitosan, alginate, collagen and hyaluronic acid, offer native biocompatibility and enzymatic biodegradability. Conversely, synthetic polymers, including polyvinyl alcohol, polylactic acid, polycaprolactone and polyethylene glycol, provide superior mechanical strength, reproducible processability and precise control over degradation kinetics. Combining natural and synthetic polymers into blended or interpenetrating networks enables the fine-tuning of both biological response and structural durability [6, 7].

The resulting hybrid systems offer remarkable application versatility. Depending on the chemical formulation and processing methodology, they can be engineered as mucoadhesive patches for localized drug delivery at mucosal sites, injectable gels for minimally invasive defect filling, or three-dimensional porous scaffolds for bone tissue engineering. However, their practical development and translational implementation face major scientific and technological challenges.

Achieving an optimal balance between the inorganic mineral phase and the polymeric component is a delicate process; excessive hydroxyapatite loading causes matrix embrittlement, reducing swelling capacity and mucoadhesive properties, while insufficient ceramic content compromises osteoconductivity. Furthermore, controlling scaffold porosity is critical to ensure cellular infiltration and nutrient transport without compromising overall mechanical performance. Synchronizing the polymer matrix degradation rate with the natural tissue healing pace remains another complex task, as premature degradation leads to structural failure, while excessively slow resorption inhibits new tissue formation.

Thus, this work aims to develop and characterize a hybrid nanocomposite hydrogel designed for localized dental applications, based on a polymeric matrix of Carbopol and sodium alginate, reinforced with hydroxyapatite and functionalized with allantoin. Carbopol provides optimal mucoadhesive and rheological properties to ensure retention at the application site, while sodium alginate enhances long-term mechanical stability. Hydroxyapatite serves a dual role: providing bioactivity and acting as a carrier for sustained release of allantoin, a phytopharmaceutical agent that stimulates cellular proliferation and tissue healing.

The nanocomposite hydrogel was prepared by aqueous solution blending and homogenization under controlled stirring, followed by crosslinking of the polymeric matrix formed by Carbopol and sodium alginate, into which hydroxyapatite nanoparticles and allantoin were uniformly dispersed. Chemical interactions and the successful encapsulation of allantoin were evaluated using Fourier-transform infrared spectroscopy (FT-IR). Surface morphology and porous network architecture were analyzed via Scanning Electron Microscopy (SEM), while thermal stability and degradation behavior were determined by Thermogravimetric Analysis (TGA).

FT-IR spectra confirmed the structural integration of all components, while SEM analysis revealed an adequate porosity for a controlled release system. The combination of synthetic and natural polymers with the mineral phase offers a stable and mucoadhesive hybrid platform capable of preventing burst release and ensuring sustained allantoin delivery, representing a promising solution for biomedical applications.

References

[1] S.V. Dorozhkin , *Prog.Biomater.* 2016, 5(1), 9–70.
[2] X. Hou, L. Zhang, Z. Zhou, X. Luo, T. Wang, X. Zhao, B. Lu, F. Chen, L. Zheng, *J. Funct. Biomater.* 2022, 13(4), 187.
[3] R. Ghosh, S. Das, S.P. Mallick, Z. Beyene, *Mater. Today Commun.* 2022, 31, 103311.
[4] J. Jeong, J.H. Kim, J.H. Shim, N.S. Hwang, C.Y. Heo, *Biomater. Res.* 2019, 23 (1), 4.
[5] N. Eliaz, N. Metoki, *Materials* 2017, 10, 334.
[6] A.E. Segneanu, L.E. Bejenaru, C. Bejenaru, A. Blendea, G.D. Mogoşanu, A. Biţă, E.R. Boia, *Polymers* 2025, 17, 2115.
[7] A. Revete, A. Aparicio, B.A. Cisterna, J. Revete, L. Luis, E. Ibarra, E.A. Segura González, J. Molino, D. Reginensi, *Int. J. Biomater.* 2022, 2022(1), 3606765.

PP22. CHROMATOGRAPHIC IDENTIFICATION OF BIOLOGICALLY ACTIVE COMPOUNDS FROM DIFFERENT PLANT SPECIES

Raluca-Nicoleta Raileanu[1], Anna Busuioc[1], Alexandra-Mariana Ionescu[1], Costel Vinatoru[2], Geanina Negosanu[2], Andreea Veronica Botezatu[1], Bianca Furdui[1], Rodica Mihaela Dinica[1]*

[1]*Faculty of Sciences and Environment, "Dunarea de Jos" University of Galati, Galati, Romania*
[2]*Genetic and Vegetal Resources Bank (GVRB), Buzau, Romania*
**rodica.dinica@ugal.ro*

Chromatography is used for separating complex mixtures of substances belonging to different classes of compounds. It is also used for identification and quantification of these compounds found in different types of samples [1]. Chromatographic methods are used in research, in food industry, in environmental protection and the pharmaceutical industry. They help with the detection of natural compounds, pesticides, colorants, toxins and more. Some of the most used chromatographic techniques are thin-layer chromatography (TLC), gas chromatography (GC) and high-performance liquid chromatography (HPLC). High-performance thin-layer chromatography (HPTLC) is a semi-automated version of TLC, that allows a better separation of the compounds [1, 2, 3].

The purpose of this study was to extract, separate, identify, and quantify some bioactive compounds from selected plant species, as well as to characterize the chemical profile of the obtained extracts. Furthermore, the study aimed to evaluate their biological properties, including antioxidant, anti-inflammatory, antimicrobial, and other relevant bioactivities, to explore their potential applications in pharmaceutical, nutraceutical, and biomedical fields. Several plants were analysed in this study for the determination of their chemical composition. The polyphenols class was of special interest, with focus on flavonoids and phenolic acids.

First, the ultrasound-assisted extraction (UAE) was employed for obtaining the plant extracts. Each plant species was extracted individually under the same experimental conditions, as illustrated in Figure 1. to ensure the reproducibility and comparability of the results.

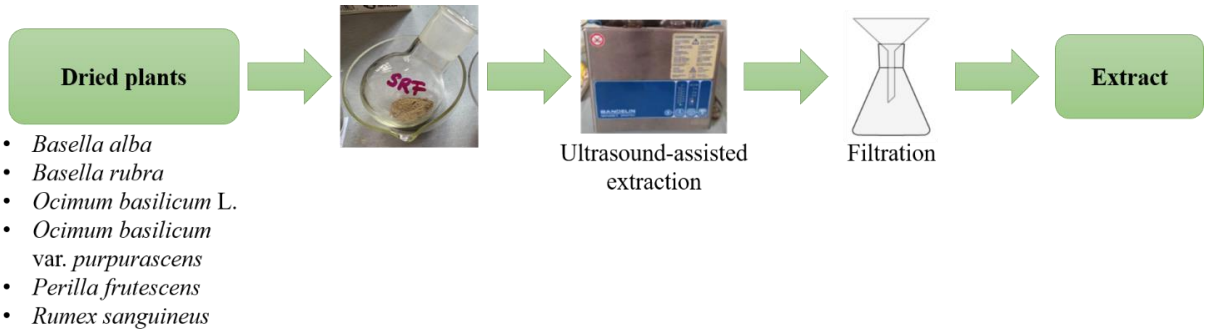


Figure 1. Extraction process.

Subsequently, various mobile phase compositions were evaluated and optimised using TLC plates. The mobile phase that provided the best separation performance was then selected and further tested on an HPTLC plate (Figure 2).



Figure 2 TLC extracts separation.

The Total Phenolic Content (TPC) was determined for the obtained extracts using the Folin-Ciocalteu assay and the Total Flavonoid Content (TFC) was determined through the spectrophotometric method which is based on the formation of the aluminium complexes. The antioxidant activity was evaluated through the DPPH method and through HPTLC-DPPH assay [4]. Several compounds, such as hesperidin, caffeic acid and rosmarinic acid, were identified in some tested extracts. Not all the separated compounds could be identificated, so further study is necessary to complete the phytochemicals identification. The results obtained for TPC and TFC show a significative content of polyphenols and flavonoids in some of the extracts, but not in all of them. Not all of the extracts analysed are rich in these classes of compounds, as determined in this study. The DPPH assay for the determination of the antioxidant activity revealed that the studied plants are different regarding their antioxidant power, with *Basella* species having the weakest content of antioxidant compounds. HPTLC-DPPH revealed the presence of certain antioxidant compounds, one of them being caffeic acid, which can be clearly seen on the plate that was previously sprayed with DPPH (2,2-diphenyl-1-picrylhydrazyl) reactive.

This study shows the importance of studying plants, as they are important sources of different classes of compound with different biologic activities. The studies need to continue to be able to establish the exact chemical composition and biologic importance of the studied plants' extracts.

References

[1] A. Pyka, Applications of Chromatographic Separation Techniques in Food and Chemistry—Second Edition. *Processes* 2026, *14*.
[2] M. Attimarad, K. K. Mueen Ahmed, B. E. Aldhubaib, S. Harsha, *Pharm. Methods* 2011, 2, 71.
[3] G. Dharmamoorthy, K. Saiteja, J. Keerthana, L. Dinesh Ajay, A. Ganesh, A. Balaji, *An Overview on High-Performance Thin-Layer Chromatography (HPTLC)*, 2023, Vol. 17.
[4] M. K. Islam, T. Sostaric, L. Y. Lim, K. Hammer, C. Locher, *Journal of Planar Chromatography - Modern TLC* 2020, 33, 301.

Acknowledgment: This work was partially supported by UDJG internal Grant" Targeted therapeutic molecules, anti-inflammatory and antitumor, isolated from exotic plants acclimatized in Romania", funding contract no. 7956/31.03.2025.

PP23. PHENANTHRIDINIUM YLIDES IN [3+2] CYCLOADDITIONS: DIPOLAROPHILE EFFECTS AND NMR CHARACTERIZATION

Claudiu Ticaleac[1]*, Costel Moldoveanu[1], Catalina Ciobanu[2], Ionel Mangalagiu[1], Gheorghita Zbancioc[1]

[1]*Faculty of Chemistry, "Alexandru Ioan Cuza" University of Iasi, Iasi, Romania*
[2]*CERNESIM Centre, "Alexandru Ioan Cuza" University of Iasi, Iasi, Romania*
**claudiu.ticaleac@chem.uaic.ro*

Introduction

The construction of fused nitrogen-containing heterocycles is an important objective in synthetic organic chemistry because small changes in ring connectivity and oxidation state can generate markedly different molecular architectures. Quaternized aza-aromatic systems are convenient precursors of azomethine ylides, which can participate in [3+2] dipolar cycloaddition reactions with electron-deficient unsaturated substrates [1,2]. In the present study, a benzo[*c*]quinolinium (phenanthridinium) platform was investigated as a source of an *in situ* generated ylide. Particular attention was paid to how the structure of the dipolarophile affects the isolated cycloadducts and to the spectroscopic evidence used for their characterization.

Experimental approach

Phenanthridine was N-alkylated with 1-bromopinacolone (1-bromo-3,3-dimethylbutan-2-one) in toluene at room temperature, affording the corresponding phenanthridinium bromide in 95% isolated yield. This salt served as the key precursor for ylide formation. Subsequent reactions were performed in 1,2-butylene oxide under reflux for at least 48 h, in the presence of three activated dipolarophiles: 1,4-naphthoquinone, acrylonitrile and ethyl acrylate (Figure 1). Following the cycloaddition step, the product mixtures were separated by silica-gel column chromatography. The isolated compounds were examined using one- and two-dimensional nuclear magnetic resonance (NMR) spectroscopy.

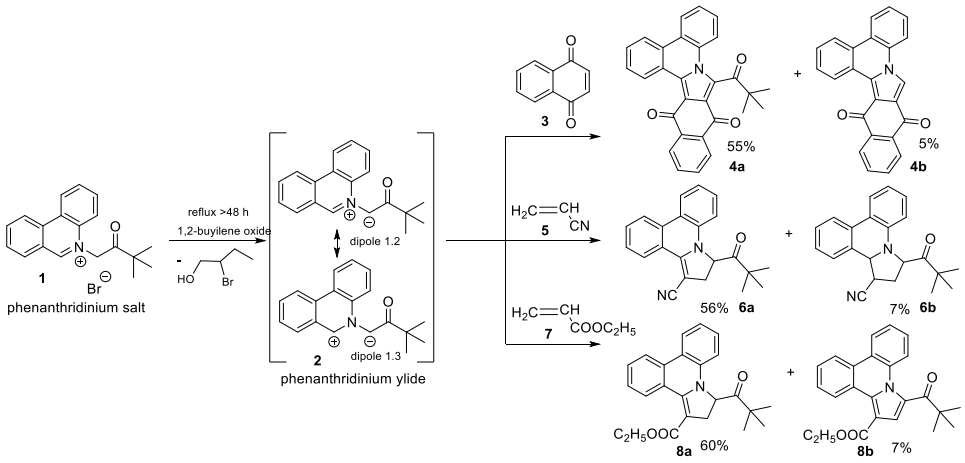


Figure 1. Preparation of the phenanthridinium salt and [3+2] cycloaddition with three activated dipolarophiles; percentages denote isolated yields.

Results and discussion

Each of the three dipolarophiles gave two chromatographically isolated cycloadducts. The product distributions were not identical: the 1,4-naphthoquinone reaction afforded products in 55% and 5% yields; acrylonitrile gave 56% and 7%; and ethyl acrylate yielded 60% and 7%, respectively (Table 1).

These results demonstrate that the ylide can be intercepted by dipolarophiles containing different electron-withdrawing groups. The product pairs also exhibit different degrees of hydrogenation or aromatization in the newly formed pyrrolic portion of the fused framework, highlighting the importance of structural analysis beyond the overall synthetic transformation.

Table 1. Isolated yields of the two products obtained with each dipolarophile.

Dipolarophile	Major product	Minor product
1,4-Naphthoquinone	55%	5%
Acrylonitrile	56%	7%
Ethyl acrylate	60%	7%

NMR characterization

The phenanthridinium salt and the major cycloadducts derived from 1,4-naphthoquinone (55%) and acrylonitrile (56%) were investigated by ^{1}H, ^{13}C and 2D NMR spectroscopy. Diagnostic ^{1}H signals of the precursor salt at δ 11.49 ppm (H-6) and δ 7.06 ppm (N–CH_2) are consistent with N-alkylation. The major naphthoquinone-derived cycloadduct exhibits predominantly aromatic ^{1}H resonances, whereas the major acrylonitrile-derived cycloadduct also displays characteristic olefinic and aliphatic signals associated with its partially saturated fused heterocyclic ring. Experimental ^{1}H–^{1}H COSY spectra support vicinal proton-coupling networks (H1–H4, H5–H8 and H12–H15 for the naphthoquinone-derived product; H5–H8 and H9–H12 for the acrylonitrile-derived product). These correlations, alongside ^{13}C and complementary 2D data, support the proposed structural assignments.

Conclusions

Phenanthridinium bromide (95% isolated yield) was employed as a precursor to *in situ* generated corresponding phenanthridinium ylides for [3+2] cycloadditions. Reactions with 1,4-naphthoquinone, acrylonitrile and ethyl acrylate afforded six isolated cycloadducts 4a/4b, 6a/6b and 8a/8b (major yields of 55–60% and minor yields of 5–7%). The dipolarophile influenced both product distribution and the hydrogenation/aromatization state of the fused pyrrolic system. Complementary ^{1}H and ^{13}C NMR spectra, supported by available 2D experiments, allowed comparison of the isolated frameworks.

References

[1] R. Huisgen, *Angew. Chem. Int. Ed.* 1963, 2, 565–598.
[2] A. Padwa, W.H. Pearson, Synthetic Applications of 1,3-Dipolar Cycloaddition Chemistry toward Heterocycles and Natural Products, Wiley, New York, 2002.

Acknowledgment: The authors acknowledge RECENT AIR (MySMIS 127324) for access to the RA04 organic synthesis laboratory and POSCCE-O 2.2.1 (SMIS-CSNR 13984-901; no. 257/28.09.2010, CERNESIM) for NMR experiments.

PP24. SENSORS FOR MELATONIN DETECTION: RECENT ADVANCES, ANALYTICAL PERFORMANCE, AND FUTURE PERSPECTIVES

Andra-Georgiana Trifan*, Andreea-Loredana Comanescu, Constantin Apetrei
Faculty of Science and Environment, "Dunarea de Jos" University of Galati, Galati, Romania
**andra.trifan@ugal.ro*

Melatonin (N-acetyl-5-methoxytryptamine) is a hormone primarily associated with the regulation of circadian rhythms and the sleep-wake cycle. In addition to its role in sleep regulation, it has been investigated for its antioxidant and neuroprotective properties, making its accurate determination relevant for both medical research and pharmaceutical analysis [1]. Detection of melatonin requires analytical methods with adequate sensitivity and selectivity. Although techniques such as high-performance liquid chromatography (HPLC), fluorometric detection or enzyme-linked immunosorbent assays (ELISAs) provide reliable results, they generally require specialized equipment and trained personnel [2]. These limitations have encouraged the development of alternative methods, particularly electrochemical sensors, which offer the possibility of rapid measurements and simple analytical procedures.

Most electrochemical methods for melatonin detection rely on its oxidation at the electrode surface. The resulting current is related to the analyte concentration and can be measured using techniques such as differential pulse voltammetry (DPV), amperometry, and square-wave voltammetry (SWV). The sensitivity and selectivity of these methods depend strongly on the electrode material, surface modification, and experimental conditions.

Carbon-based electrodes are widely investigated because of their conductivity, relatively low cost, and compatibility with surface modification. In our recent study, we compared four screen-printed electrodes modified with graphene, graphene modified with gold nanoparticles, graphene oxide, and reduced graphene oxide. Our work demonstrated how the composition of the electrode surface influences its electrochemical response to melatonin. Among the tested configurations, the graphene-modified electrode exhibited the best analytical performance, with a limit of detection (LOD) of 0.3424 μM. Graphene-based materials are particularly attractive because they can improve electron transfer and provide a suitable surface for further functionalization [3].

Lete et al. [4] developed a sensor based on sonogel-carbon material modified with gold nanoparticles, providing another example of how electrode modification can influence melatonin detection. Deng et al. [5] developed a graphene-based electrochemical flow system capable of simultaneously detection of dopamine, serotonin, and melatonin. The reported LOD for melatonin was 0.087 μM. The separation of the electrochemical signals of these compounds is particularly relevant because several electroactive molecules may be present in the same biological sample. In addition, the flow configuration offers advantages in terms of sample handling, repeatability, and potential integration into portable analytical devices.

While voltammetric sensors detect melatonin through its electrochemical oxidation, impedimetric sensors measure changes in interfacial properties, using the electrochemical impedance spectroscopy (EIS) technique.

Jin et al. [6] developed an EIS-based sensor using gold nanoparticles supported on polydopamine-modified glassy carbon electrodes. The reported LOD was 0.32 pM, indicating high analytical sensitivity under the conditions investigated. Selectivity can be further improved through the use of molecularly imprinted polymers (MIPs). These materials are prepared to contain recognition sites that are complementary to the target molecule, allowing it to be distinguished from other compounds. A study published in 2024 described a molecularly imprinted electrochemical sensor incorporating a Cu_xO/MXene nanocomposite for melatonin determination [7]. This combination brings together the electrical properties of a nanostructured material and the recognition capabilities of an imprinted polymer. Under optimal conditions, the sensor exhibited a LOD of 0.029 µM. The sensor also demonstrated good selectivity, reproducibility, and stability, and was successfully applied to melatonin determination in human urine. These results highlight the potential of combining molecular imprinting with nanocomposite-modified electrodes to improve the analytical performance of electrochemical sensors for melatonin detection.

Optical sensors provide another approach for melatonin analysis. Fluorescence-based methods detect changes in emitted light, while colorimetric sensors rely on measurable color changes. These techniques can provide relatively simple readouts, and some designs may be adapted for portable applications. Khan et al. [8] reviewed advances in electrochemical and optical sensors for melatonin and tryptophan, highlighting the contributions of nanomaterials and different sensing strategies. However, optical methods may be influenced by background signals, sample composition, and the requirements of the high quality detection equipment. Their analytical performance therefore depends on both the sensing material and the measurement conditions, as well as the characteristics of the sample being analyzed. Electrochemical sensors represent a promising approach for melatonin detection, offering good analytical performance and the potential for rapid and accessible measurements. The studies reviewed demonstrate that electrode modification with materials such as graphene, gold nanoparticles, and molecularly imprinted polymers can improve sensor sensitivity and selectivity. The reported detection limits vary considerably depending on the sensing strategy and electrode design, highlighting the importance of selecting suitable materials and optimizing experimental conditions. Further advances in sensitive, selective, and portable electrochemical sensors may expand their use in pharmaceutical analysis and medical research.

References

[1] S.B. Ahmad, A. Ali, M. Bilal, S.M. Rashid, A.B. Wani, R.R. Bhat, M.U. Rehman, *Cell. Mol. Neurobiol*. 2023, 43, 2437-2458.
[2] S. Barreiro Astray, L. Barbosa-Pereira, M.A. Lage-Yusty, J. López-Hernández, *Food Anal. Methods* 2021, 14, 734-741.
[3] A.G. Trifan, C. Apetrei, *Appl. Sci*. 2026, 16, 924.
[4] C. Lete, D. López-Iglesias, J.J. García-Guzmán, S.A. Leau, A.E. Stanciu, M. Marin, J.M. Palacios-Santander, S. Lupu, L. Cubillana-Aguilera, *Sensors* 2022, 22, 120.
[5] H. Deng, J. Zhao, S. Zhao, S. Jiang, G. Cui, *Analyst* 2022, 147, 1598-1610.
[6] X. Jin, J. Wang, X. Li, Y. Zhang, Y. Liu, *Environ. Res*. 2023, 238, 117080.
[7] X. Wang, W. Wang, M. Gao, H. Yu, M. Fu, W. Chen, *ACS Appl. Nano Mater*. 2024, 7, 22832-22842.
[8] Z.A. Khan, P.J.S. Hong, C.H. Lee, Y. Hong, *Int. J. Nanomedicine* 2021, 16, 6861-6888.

PP25. VOLATILE ORGANIC COMPOUND FROM HONEY TO INDUCE A CASEIN BAZED MATERIALS

Grigore Ungureanu[1]*, Marius Niculaua[2], Alin-Constantin Dirțu[3], Elena Stoleru[1], Mihai Brebu[1]

[1]*Petru Poni Institute of Macromolecular Chemistry, Romanian Academy, Iasi, Romania*
[2]*Center for Oenological Research - Romanian Academy, Iași, Romania*
[3]*Faculty of Chemistry, "Alexandru Ioan Cuza" University of Iași, Iași, Romania*
* *ungureanu.grigore@icmpp.ro*

Introduction

Honey constitutes a complex biological matrix, predominantly composed of carbohydrates (39% fructose, 32% glucose) and water (17-18%), but its biological value and reactivity is dictated by synergistic action of over 200-300 minor constituents. This bioactive fraction includes organic acids (with gluconic acid predominating), polyphenols (phenolic acids and flavonoids), and free amino acids. In addition to these constituents the volatile fraction includes monoterpenes (e.g. p-cymene, camphene, α-pinene), terpenic alcohols (e.g. linalool and hotrienol, aliphatic and aromatic aldehydes) that carry reactive functional groups (e.g. -OH, -CHO, -COOH) with a high functionalization capacity [1] as well as antioxidant and antimicrobial activity. Caseins are protein biopolymers characterized by high conformational flexibility (intrinsically disordered proteins), this structural feature giving them a particular sensitivity to the action of small-molecule natural ligands, allowing for the reorganization of the protein network. Based on the specialized literature [2], this study aims to use chromatographic method for identifying and selecting potential bioactive compounds in honey and evaluating their potential for conformational modulation of casein.

Extraction and preconcentration techniques of VOCs from honey

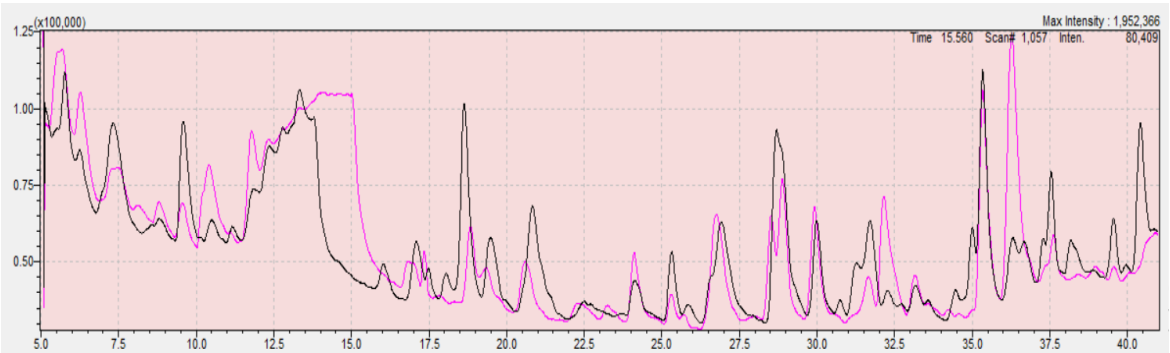


Figure 1. GC-MSD chromatograms of VOCs in polyfloral (black) and May (magenta) honey.

The extraction and preconcentration of volatile organic compounds (VOCs) from honey samples were performed using in-tube extraction coupled with headspace sampling (ITEX-HS), followed by gas chromatography–mass spectrometry (GC/MS) analysis using a polar WAX capillary column. This analytical approach enabled the characterization of the volatile chemical profile of honey and the identification of compositional differences among honey varieties, as illustrated in Figures 1 and 2 [3]. These differences provide a basis for comparing the relative abundance and distribution of volatile compounds across the analyzed samples and for identifying potential candidates for further investigation of their interactions with casein.

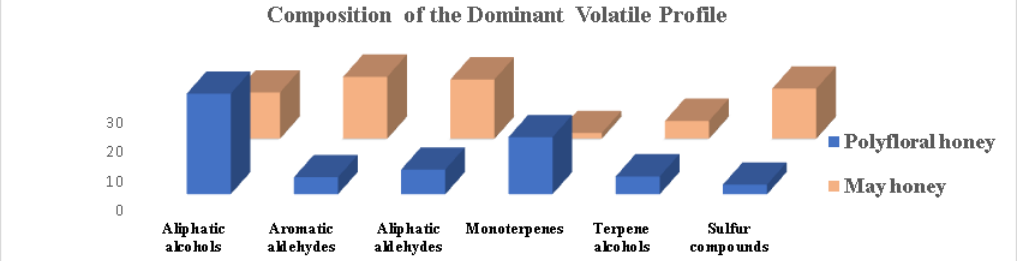


Figure 2. Global composition of main volatile compounds in polyfloral and May honey.

Hypothesized interactions between honey compounds and caseins

Chromatographically identified compounds contain functional groups, such as hydroxyl (-OH), aldehyde (-CHO), and carboxyl (-COOH), which can participate in physicochemical interactions with proteins. According to the literature, interactions between honey constituents and casein may involve electrostatic interactions, hydrogen bonding, and hydrophobic interactions.[3] Gluconic acid, the predominant organic acid in honey, may contribute to lowering the pH of the medium. As the pH approaches the isoelectric point of casein (approximately 4.6), electrostatic repulsion decreases, promoting protein aggregation. Polyphenolic compounds may interact with casein through hydrogen bonding and hydrophobic interactions, potentially influencing its stability and association behaviour [4]. Additionally, reactive carbonyl compounds, such as methylglyoxal, can react with lysine and arginine residues in proteins, leading to the formation of glycation products [2]. The extent of these reactions depends on the concentration of reactive compounds and the physicochemical conditions of the system. Overall, changes in pH and interactions between honey constituents and casein may influence the colloidal stability and aggregation behaviour of the protein system, potentially promoting casein association under suitable conditions.

Conclusion and Future Perspectives

ITEX-HS-GC/MS analysis enabled the characterization of the volatile chemical profile of honey, providing a basis for identifying and selecting compounds with potential interactions with casein. Future research will focus on applying headspace solid-phase microextraction (HS-SPME) to compare its extraction efficiency and the range of volatile compounds detected with those obtained using ITEX. In parallel, the interactions between honey constituents and casein will be experimentally investigated. Different honey varieties will also be evaluated to identify chemical profiles associated with desirable modifications in casein-based materials. Additionally, direct exposure of casein matrices to honey-derived volatile compounds will be explored as a potential approach to modify protein structure, with the long-term aim of developing biodegradable packaging films and biocompatible electrospun nanofibers.

References

[1] D. Cianciosi, T.Y. Forbes-Hernández, S. Afrin, M. Gasparrini, P. Reboredo-Rodriguez, P.P. Manna, J. Zhang, L.B. Lamas, S.M. Flórez, P.A. Toyos, J.L. Quiles, F. Giampieri, M. Battino, *Molecules* 2018, 23(9), 2322.
[2] S.K.T. Seraglio, M. Schulz, L.V. Gonzaga, R. Fett, A.C.O. Costa, *Food Chemistry* 2021, 357, 129807.
[3] N.E. Gomez Mesa, K. Vasilev, Y. Tang, *Molecules* 2025, *30(15),* 3278;
[4] Y. Arii, K. Nishizawa, *Heliyon* 2020, 6(4), e03673.

Acknowledgment:

This work was supported by grants of the Ministry of Education and Research, CCCDI - UEFISCDI, project number PN-IV-P6-6.1-CoEx-2024-0056 and project number PN-IV-P2-2.1-TE-2023-1725 within PNCDI IV.


MacroYouth 2026

Sponsors

INTEGRATED ANALYTICAL INSTRUMENTATION - PRO ANALYSIS SYSTEMS PORTFOLIO AND MICROPLASTICS DETERMINATION BY MILD PYROLISYS-GC-MS

Gheorghita Cretu*

Pro Analysis Systems, Bucharest, Romania
gheorghita.cretu@proanalysis.ro

1. Pro Analysis Systems portfolio

1.1 Analytical instrumentation for integrated workflows

Modern analytical laboratories increasingly require platforms that combine chromatographic separation, selective detection, high-resolution mass spectrometry, automated sample preparation and unified data handling. The Thermo Scientific portfolio presented by Pro Analysis Systems covers liquid chromatography (HPLC/UHPLC), ion chromatography and combustion ion chromatography, gas chromatography, single- and triple-quadrupole mass spectrometry, linear ion-trap and Orbitrap high-resolution accurate-mass systems, isotope-ratio mass spectrometry, trace elemental analysis (TEA) by ICP-OES, ICP-MS and ICP-MS/MS, CHNS-O elemental analysis, discrete photometric analysis and automated sample preparation. The portfolio is therefore structured around complete analytical workflows rather than isolated instruments. In Romania, Pro Analysis Systems reports an installed base spanning HPLC/UHPLC, LC-MS, GC, GC-MS, IC/IC-MS, IRMS, CHNS-O and accelerated solvent extraction platforms.

1.2 Chromatography and mass spectrometry

The Vanquish LC family addresses different performance requirements through Core HPLC, Flex UHPLC, Horizon UHPLC, Duo and Access configurations. The same workflow concept extends to ion chromatography, where reagent-free eluent generation and automatic suppression are complemented by combustion ion chromatography for halogen and PFAS-related applications. For mass spectrometry, the portfolio progresses from ISQ single-quadrupole instruments to TSQ triple quadrupoles, the Stellar hybrid triple-quadrupole/linear-ion-trap platform, Orbitrap Exploris and Excedion Pro systems, Tribrid instruments and Orbitrap Astral architectures. These high-resolution accurate-mass platforms support both small-molecule and biomolecular applications. GC and GC-MS workflows are represented by the TRACE 1610 GC, ISQ 7610 GC-MS, TSQ 9610 GC-MS/MS and Orbitrap Exploris GC platforms. Trace elemental analysis (TEA) is covered by ICP-OES, ICP-MS and ICP-MS/MS, with IC-ICP coupling for speciation, and is extended by the Element Series HR-ICP-MS, the Neoma MS/MS MC-ICP-MS and the Triton Plus thermal ionization mass spectrometer (TIMS) for high-resolution and isotope-ratio analysis.

1.3 Elemental and discrete photometric analysis

The FlashSmart Elemental Analyzer determines C, H, N, S and O using the dynamic flash combustion method, with TCD detection, from a few ppm up to 100%. It operates automatically, offers an alternative to the Kjeldahl method for nitrogen/protein determination and requires no sample digestion or toxic chemicals. The OxyTune function optimizes the oxygen dose, helium or argon can be used as carrier gas, and the MultiValve Control (MVC) module switches automatically between two analytical channels and changes the carrier gas during stand-by to reduce helium consumption. The Gallery automated discrete photometric analyzers automate all analytical steps and deliver reproducible results within minutes. Ready-to-use reagents cover drinking water, wastewater, surface water, seawater, groundwater, sludge and soil extracts, as well as wine, juice, milk and honey, fermentation and enzyme production processes, and user-developed applications are supported.

1.4 Sample preparation and software

Sample preparation is treated as an integral component of the analytical chain. Accelerated Solvent Extraction includes Dionex ASE 350 and the Extreva ASE platform, with automated extraction, cleanup and evaporation, parallel sample processing, barcode-based traceability and automated detection of evaporation completion. AutoTrace 280 provides automated solid-phase extraction, while Markes thermal-desorption systems extend GC-based workflows to sorbent tubes, canisters, bags and online monitoring. Chromeleon CDS provides a common software environment across chromatography and mass-spectrometry workflows, establishing the instrumental context for targeted applications such as microplastics characterization.

2. Microplastics determination by Mild Py-GC-MS

2.1 Context and workflow

Microplastics are polymeric materials smaller than 1 mm found in air, water, soil, food and biota. Following the thermo-analytical approach of SR EN ISO 24187:2023, polymers are pyrolyzed under inert conditions and characteristic degradation products are detected. In conventional high-temperature Py-GC-MS, sample preparation is complex: a small part of the filter containing microplastic particles must be isolated, cut, weighed (0.1–0.5 mg) and placed manually in a pyrolysis sample cup, each sample can be analyzed only once, and the pyrograms of mix polymer and volatile signals making results difficult to interpret. In the mild (medium-temperature) Py-GC-MS workflow, microplastics are retained on a filter, which is introduced directly into a thermal-desorption tube and analyzed using Markes UNITY-xr, ULTRA-xr or TD100-xr with Thermo Scientific ISQ 7610 GC-MS or TSQ 9610 GC-MS/MS under Chromeleon control. The method is quantitative, automatable, allows sample re-analysis and avoids plastic labware, reducing contamination risk.

2.2 Calibration and applications

Calibration uses commercial polymer reference materials (30–2000 µg) wrapped in conditioned quartz filter and degraded at 300 °C (helium 30 mL/min, trap −20 °C, trap desorption 40 °C/s), giving reproducible chromatographic fingerprints and good linearity. Polymer-specific markers allow identification, for example formic acid (m/z 46) for cotton/cellulose and acetamide (m/z 59) for wool, while acetic acid (m/z 60) may originate from both. Applications include tap, bottled and wastewater (250–5000 mL filtered on 47 mm quartz filters, then oxidized and washed to remove the organic matrix) and salt (20 g washed with 2 L of ultrapure water). In wastewater, higher suspended-solids content was associated with higher microplastics concentration. Future applications may include airborne tire particles on PM10 filters, microplastics in air and plastics in biota.

Conclusions

The Pro Analysis Systems portfolio covers complete analytical workflows, from sample preparation to separation, detection and data processing. Mild Py-GC-MS illustrates this integration as a simple, sensitive and quantitative route for microplastics determination.

References

[1] SR EN ISO 24187:2023, Principles for the analysis of microplastics present in the environment.
[4] TA Instruments, 2025, https://www.tainstruments.com/pdf/brochure/ TA-Instruments-HR-Brochure-EN.pdf

SC EKY-SAM SRL – Company Presentation 2026

History

SC EKY-SAM SRL was established in 1997 (Tax ID 9672080, Trade Register No. J1997000973223) and is one of the longest-established companies in the industry. It started road works in 2000 with earthworks, and in 2006 it purchased its first fixed asphalt plant, in Târgu Frumos. The group was later joined by SC CARIMAR SRL, which specialises in gravel and sand extraction, and ARTCON WAY SRL, which builds roads, produces cement concrete and carries out fluid network works.

Quality and Laboratory

The group companies operate an integrated management system certified to SR EN ISO 9001:2015 and SR EN ISO 14001:2015. Production at the asphalt and concrete plants is certified for Factory Production Control. Eky-Sam has a testing laboratory authorised by ISC (the State Construction Inspectorate) in accordance with SR EN ISO/IEC 1075:2018, for the GTF, AN.CF.D, D, MD, MBM and BBABP profiles.

Equipment

The group owns more than 320 vehicles and machines, most of them manufactured after 2015, including:

- 50 tractor units, 40 dump trucks, 50 tipping semi-trailers, 19 trailers and tankers;
- 13 truck mixers, 2 truck-mounted concrete pumps, 2 Liebherr truck cranes;
- 20 wheel loaders, 14 excavators, 21 compaction rollers, 6 motor graders, 2 bulldozers;
- 5 Vögele asphalt pavers, 2 Wirtgen/Gomaco concrete pavers, cold milling machines, recyclers, binder distributors and 3 emulsion sprayers;
- more than 60 vans and passenger cars;
- more than 100 snow ploughs and gritters.

Production Bases

- Târgu Frumos, Iași (13,200 m², plus 7,000 m² for winter maintenance equipment): 110 t/h OHL asphalt plant, emulsion plant, 70 m³/h Betonmec concrete plant, central laboratory, railway siding.
- Războieni, Iași (30,600 m²): 50 m³/h Skako concrete plant, precast concrete production hall.
- Oniceni, Suceava (176,000 m²), the group's main aggregate supplier: 240 t/h Benninghoven asphalt plant, 80 m³/h concrete plant, crushers and a 200 t/h screening plant. The extraction licence on the Moldova River covers 1.099 km², with 3 authorised perimeters (355,000 m²).

- At the beginning of 2026, stocks amounted to 315,000 m³ of pit-run gravel and 20,000 t of graded aggregates
- Leţcani, Iași (60,000 m², since 2023): 160 t/h Benninghoven mobile asphalt plant, 110 m³/h ELKON concrete plant, railway siding. It is the group's largest production facility.
- Pașcani, Iași (7,200 m²): 80 t/h fixed asphalt plant.

All bases hold environmental permits and are connected to utilities. In addition, the administrative headquarters in Târgu Frumos (11,150 m²) includes a 1,200 m² workshop for fleet maintenance.

Financial Data

The group's turnover increased from RON 75.1 million in 2021 to RON 253.9 million in 2025, and net profit reached RON 37.4 million in 2025. SC EKY-SAM SRL has 178 employees. Except for CARIMAR, the figures come solely from road construction works.

Experience

The group carries out, entirely in-house, earthworks, superstructure works (asphalt mixtures, road cement concrete) and drainage works. By the end of 2025, it had completed:

- more than 200 km of asphalt overlays on national roads (DRDP Iași: SDN Iași, Bacău, Câmpulung), with approximately 350,000 t of asphalt mixture laid in 2021–2024;
- the upgrade of DN 28B in Târgu Frumos (1.7 km, including the DN 28 – DN 28B roundabout);
- more than 300 km of county roads in Iași, Suceava and Botoșani counties, for example DJ 282C/282/282B Iași – Botoșani, DJ 281C, DJ 249D;
- more than 50 km of streets in Târgu Frumos, Pașcani and Iași;
- more than 500 km of commune roads in Iași, Neamț, Suceava and Botoșani counties.

The group has held winter maintenance contracts with DJADP Iași since 2008 and with DRDP Iași since 2014. All contracts were completed on time, some of them even a year ahead of schedule. With more than 25 years of experience, the EKY group has the resources, positioning and dedication required for road infrastructure works. We remain at your disposal for any further information.

ION ECHIMOV
Chairman of the Board of Directors
EKY GRUP

EKY-SAM SRL
705300 - Tg. Frumos, str. Justiției 2-5, jud. Iași | contact@ekysam.ro
CUI: RO9672080 | ORC: J22/973/1997 |Tel: 0232.710.478 | Fax: 0232.711.801
Banca Transilvania: RO59BTRL02401202449730XX | Trezoreria Iași: RO25TREZ4065069XXX014063

CARL ZEISS INSTRUMENTS

Seeing beyond

Carl Zeiss is the only one supplier which is offering the widest product portfolio to enable seeand analyse with micro to nano resolution.

From Micro to Nano – the Most Extensive Product Portfolio on the Market

Choose the best microscope for your application:
ZEISS systems provide you with information
in the micro to nano ranges.



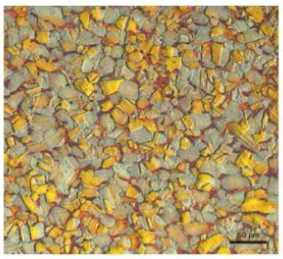
High-end inverted optical microscope AxioObserver

ZEISS Axio Observer

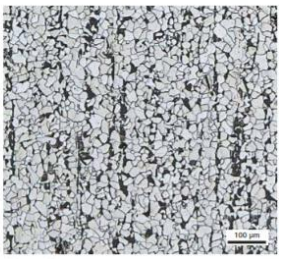
Your inverted microscope system for metallography







Brass structure
Objective: EC-Epiplan NEOFLUAR 20×/0.50, brightfield
Courtesy of: the Materials Research Institute at Aalen University



Steel, tempered structure
Objective: EC-Epiplan NEOFLUAR 50×/0.80, bright field
Courtesy of: the Materials Research Institute at Aalen University

Axio Observer, the inverse material microscope from ZEISS, provides almost unlimited sample space. That means you will save all that time and needless effort on extensive sample preparation – a big advantage.

You will get a flexible platform, perfectly adapted to the requirements of your work in metallography. Use all the contrast methods to produce brilliant images of your structures.

Axio Observer is future-proof: simply adapt the microscope to meet your changing requirements.

Configured to your requirements

Microscope
Axio Observer 3 materials (coded)
Axio Observer 5 materials (coded, partly motorized)
Axio Observer 7 materials (motorized)

Contrasting techniques
Reflected light: brightfield, darkfield, DIC, C-DIC, polarization, fluorescence
Transmitted light: brightfield, DIC, PlasDIC, polarization, phase contrast

Simpler. More Intelligent. More Integrated.

- Automated components give you reproducible results. The contrast and light managers automatically control your microscope settings.
- Take advantage of the numerous analysis options for investigating structures, grain boundaries and phases.
- Choose between three different types of stand – from manual to fully motorized.
- Navigate and control your Axio Observer in comfort by using either the operating buttons on the stand or the touch screen, or via the software.

Created for your applications

- Investigate the structure and determine grain size, distribution and phases with the aid of optional software modules.
- Examine steel for purity and identify non-metallic inclusions on the basis of color, contrast, shape and orientation.
- Measure the layer thickness and geometric properties of electrodes.
- Using polarized light, analyze anisotropic structures such as Barker-etched aluminum alloys, zinc alloys, graphite, titanium alloys.

The latest confocal generation made by Carl Zeiss **- LSM 980** with unique performance Airyscan2 detector, to enable acquisition super-resolution images and high speed also.



LSM 980 with Airyscan 2
Your Next Generation Confocal for Fast and Gentle Multiplex Imaging

Optimized for simultaneous spectral detection of multiple weak labels with highest light efficiency.

Electronic microscope made by Carl Zeiss MultiSEM – the world's fastest SEM

ZEISS MultiSEM 505/506
The World's Fastest Scanning Electron Microscopes



Carl Zeiss Instruments SRL
Dipl. Ing. Radu HOGAS
Regional Sales Manager Microscopy-Romania
www.zeiss.ro